Aus der Medizinischen Klinik mit Schwerpunkt Infektiologie und Pneumologie
der Medizinischen Fakultät Charité – Universitätsmedizin Berlin

DISSERTATION

Ventilator-induced alveolar acidification increases the susceptibility and severity to *Pseudomonas aeruginosa* pneumonia

Die beatmungsinduzierte alveoläre Übersäuerung erhöht die Suszeptibilität und den Schweregrad einer *Pseudomonas aeruginosa* Pneumonie

zur Erlangung des akademischen Grades
Doctor medicinae (Dr. med.)
vorgelegt der Medizinischen Fakultät
Charité – Universitätsmedizin Berlin

von
Chunjiang Tan

Datum der Promotion: 30.11.2023

Table of Contents

List of Abbreviations

ALF	alveolar lining fluid
ALI	acute lung injury
AM	alveolar macrophage
ARDS	acute respiratory distress syndrome
AST	aminotransferase
ATCC	American Type Culture Collection
BAL	broncho-alveolar lavage
BALF	broncho-alveolar lavage fluid
BSA	bovine serum albumin
CFU	colony forming unit
CS	cell stretch
CT	computed tomography
CXCL	C-X-C motif chemokine ligand
DAPI	4′,6-Diamidino-2-phenylindole dihydrochloride
EBC	exhaled breath condensates
EDTA	ethylenediaminetetraacetic acid
ELISA	enzyme-linked immunosorbent assay
ExoU	exotoxin U
FACS	fluorescence-activated cell sorting
FCS	fetal calf serum
GFP-PAO1	green fluorescent protein-*Pseudomonas aeruginosa*-strain1
GM-CSF	granulocyte-macrophage colony-stimulating factor

H&E	hematoxylin and eosin
HCl	hydrochloric acid
HFOV	high-frequency oscillatory ventilation
HVt	high tidal volume
I:E	inspiration-to-expiration ratio
ICU	intensive care unit
IFN	interferon
IL	interleukin
JNK	c-Jun N-terminal kinase
LVt	low tidal volume
MAP	mean airway pressure
MCP	monocyte chemoattractant protein
MDR	multidrug resistance
MIP	macrophage inflammatory protein
MOI	multiplicity of infection
MPO	myeloperoxidase
MV	mechanical ventilation
NaOH	sodium hydroxide
NCS	non-stretched
NV	non-ventilated
OD	optical density
PA	*Pseudomonas aeruginosa*
PBS	phosphate buffered saline
PEEP	positive end-expiratory pressure
PFA	Paraformaldehyde

PMN	polymorphonuclear cell
qRT-PCR	quantitative reverse transcription polymerase chain reaction
RT	room temperature
SPF	specific-pathogen free
T3SS	type 3 secretion system
TMB	3,3′,5,5′-Tetramethylbenzidine solution
TNF	tumor necrosis factor
TSB	Tryptic Soy Broth
VAP	ventilator-associated pneumonia
VILI	ventilator-induced lung injury

List of Figures and Tables

List of Figures

List of Tables

Abstract

Background: Ventilator-associated pneumonia (VAP) is one of the most common nosocomial infections acquired in the intensive care unit. *Pseudomonas aeruginosa* (PA) is a leading pathogen isolated from VAP patients and PA-VAP is associated with high mortality. It is imperative to establish an animal VAP model to study the pathogenesis and pathophysiology of VAP.

Objectives: Establish a murine VAP model that closely reflects disease onset and progression. Analyze the pathophysiological, immunological and histopathological response in the models and investigate the underlying linking mechanism between mechanical ventilation (MV) and VAP.

Methods: *In vivo*: C57BL/6J mice were intubated and subjected to either high (HVt: 34 mL/kg) or low (LVt: 9 mL/kg) tidal volume ventilation for 4 hours. Mice ventilated for 10 min using LVt ventilation settings were taken as non-ventilated (NV) control group. After MV, mice were infected with either PA103 or sterile phosphate buffered saline. Twenty-four hours post infection, mice were euthanized and physiological, immunological and histopathological parameters were determined and analyzed. *In vitro*: Human A549 cells were cultured and exposed to cell cyclic stretch followed by PAO1 infection and immunofluorescence microscopy. *Ex vivo*: A fluorescent pH indicator was applied to the lung subjected to MV to determine the pH of the alveolar lining fluid (ALF).

Results: Mice subjected to HVt ventilation developed ventilator-induced lung injury with significant lung function deterioration. Upon subsequent PA infection, substantially higher bacterial burden, as well as more severe alveolar-capillary barrier disruption and pulmonary inflammation were found in HVt-PA mice compared with LVt-PA and NV-PA mice. In addition, HVt-PA mice showed signs of extra-pulmonary bacterial dissemination

and increased levels of systemic inflammation. Furthermore, HVt and cell stretch resulted in ALF acidification and thereby promoted the pulmonary PA adhesion and growth.

Conclusion: Our results provide evidence that mechanical overventilation is a critical factor for the onset and progression of VAP, contributing to systemic inflammation and distal organ bacterial dissemination. Furthermore, *in vitro* and *ex vivo* studies provided evidence that high stretch-induced ALF acidification promotes PA adhesion and proliferation as critical factor, explaining the enhanced susceptibility to the development of PA pneumonia in overventilated mice. These findings may enable future studies to deeply investigate the pathogenesis of VAP and may promote the discovery of new treatment strategies to reduce VAP-associated mortality.

Zusammenfassung

Hintergrund: Die beatmungsassoziierte Pneumonie (VAP) ist eine der häufigsten auf der Intensivstation erworbenen, nosokomialen Infektionen. *Pseudomonas aeruginosa* (PA) ist der häufigste Erreger, der bei VAP-Patienten isoliert wird, und PA-VAP ist mit einer hohen Sterblichkeit verbunden.

Zielsetzungen: Um die Pathogenese und Pathophysiologie der VAP zu untersuchen, wurde ein murines VAP-Modell etabliert, welches den Beginn und den Verlauf der Krankheit genau widerspiegelt. Mit diesem Modell sollten immunologische und pathophysiologische Zusammenhänge zwischen mechanischer Beatmung (MV) und VAP untersucht werden.

Methoden: *In vivo*: C57BL/6J-Mäuse wurden intubiert und 4 Stunden lang entweder mit hohem (HVt: 34mL/kg) oder niedrigem (LVt: 9mL/kg) Tidalvolumen beatmet. Mäuse, die 10 Minuten lang mit LVt-Einstellungen beatmet wurden, dienten als nicht beatmete (NV) Kontrollgruppe. Nach der MV wurden die Mäuse entweder mit PA103 oder steriler Kochsalzlösung infiziert. Vierundzwanzig Stunden nach Infektion wurden die Mäuse euthanasiert und physiologische, immunologische und histopathologische Parameter bestimmt und analysiert. *In vitro*: Humane A549-Zellen wurden kultiviert und einer zyklischen Dehnung ausgesetzt, gefolgt von einer PAO1-Infektion und Immunfluoreszenzmikroskopie. *Ex vivo*: Explantierte murine Lungen wurden für 2 Stunden beatmet und anschließend ein fluoreszenzbasierter pH-Indikator appliziert, um den pH-Wert des alveolären Flüssigkeitsfilms zu bestimmen.

Ergebnisse: Mäuse, die einer HVt-MV unterzogen wurden, entwickelten eine beatmungsinduzierte Lungenschädigung mit signifikanter Verschlechterung der Lungenfunktion. Nach anschließender PA-Infektion wurden bei HVt-PA-Mäusen im Vergleich zu LVt-PA- und NV-PA-Mäusen eine wesentlich höhere Bakterienlast sowie

eine stärkere Störung der alveolar-kapillaren Barriere und Zeichen einer schweren Lungenentzündung festgestellt. Darüber hinaus zeigten HVt-PA-Mäuse Anzeichen einer extrapulmonalen bakteriellen Dissemination und erhöhte Werte systemischer Entzündung. Die *ex vivo* HVt-Beatmung und die zyklische Zelldehnung *in vitro* führten zu einer Übersäuerung des pH-Wertes des alveolären Flüssigkeitsfilms und förderten dadurch das pulmonale Wachstum und die Adhäsion von PA.

Schlussfolgerung: Die Ergebnisse belegen, dass eine Überbeatmung (HVt) ein entscheidender Faktor für den Beginn und das Fortschreiten einer VAP ist, der zur systemischen Entzündung und zur Verbreitung von Bakterien in distale Organe beiträgt. Darüber hinaus zeigten *in vitro* und *ex vivo* Untersuchungen, dass eine durch hohe Dehnung induzierte Übersäuerung des alveolären Flüssigkeitsfilms die Adhäsion und Proliferation von PA fördert und somit entscheidend für die erhöhte Anfälligkeit für die Entwicklung einer PA-Pneumonie bei überbeatmeten Mäusen ist. Diese Ergebnisse könnten künftige Studien zur Pathogenese und zu neuen Behandlungsstrategien der VAP sowie zur Senkung der VAP-assoziierten Mortalität entscheidend vorantreiben.

1. Introduction

1.1. Ventilator-associated pneumonia

1.1.1. Definition

Ventilator-associated pneumonia (VAP) is defined as a lung infection that occurs in patients who are mechanically ventilated for over 48 h [1] and is one of the most common nosocomial infections acquired in the intensive care unit (ICU) [2]. If VAP occurs within the initial 4 days of hospital admission, it is categorized as early-onset VAP, and after 5 days of hospitalization it is termed late-onset VAP [3].

1.1.2. Diagnosis of ventilator-associated pneumonia

To date, there is no single clinically sensitive and specific criterion for VAP diagnosis. Hence, it is common consensus that VAP is diagnosed using a combination of the three following criteria [3] :

- New clinical signs of infection (e.g., fever, purulent sputum or endotracheal secretions and leukocytosis or leucopenia) [1].
- Chest radiograph or computed tomography (CT) scan (Figure 1) with new or progressive pulmonary infiltrate [3].
- Noninvasive microbiological sampling with semi-quantitative cultures should be carried out to confirm VAP [4].

Figure 1: CT scan of ventilator-associated pneumonia caused by *Pseudomonas aeruginosa* in a 45-year-old female patient. A cavity (arrowhead), bronchial wall thickening (black arrow), and nodules (white arrows) are shown (adapted from Omeri et al., 2014 [5]).

1.1.3. Incidence and mortality

The reported incidence of VAP is high in Europe (18.3 VAP cases per 1,000 ventilator-days) [6] and low in the USA (1-2.5 cases per 1,000 ventilator-days) [7]. These variations may be due to geographical, diagnostic and population discrepancies [8, 9, 10]. Moreover, the incidence in lower- and middle-income nations is notably higher as compared with high-income countries (18.5, 15.2, and 9.0 per 1,000 ventilator-days, respectively, P=0.035) [11]. As one of the most common ICU-acquired pneumonia [12], results from a prospective cohort study involving 16 Canadian ICUs exhibited that 177 of 1,014 patients (17.5 %) developed VAP and had a higher morality (23.7 %) compared with patients without VAP (19.7 %) [13]. Generally, patients subjected to mechanical ventilation have an approximately 6- to 20-fold higher risk of developing pneumonia as compared with non-ventilated patients [3], While VAP mortality was particularly high in critically ill patients

(characterized by higher APACHE II score) (46.67 %) as compared to subjects with a lower APACHE II score (27.28 %) [14], and the overall attributable mortality was 9 % based on combined results from 58 randomized controlled studies [15]. Furthermore, late-onset VAP patients exhibit higher mortality compared with early-onset VAP cases (50 % versus 25 %) [14]. Interestingly, in patients with acute respiratory distress syndrome (ARDS), VAP was identified as risk factor associated with a significantly higher mortality [9].

1.2. Pathogens responsible for ventilator-associated pneumonia

Causative pathogens identified in VAP patients may vary due to different factors, including length of hospital or ICU stay, duration of mechanical ventilation, local epidemiology and timing of exposure to antimicrobials [1]. The most common Gram-negative pathogens isolated in VAP patients are *Pseudomonas aeruginosa* (PA)*, Escherichia coli,* and *Klebsiella pneumoniae*, while *Acinetobacter* species and *Staphylococcus aureus* are the most commonly isolated Gram-positive bacteria [16, 17, 18, 19, 20, 21]. There are some regional differences: *Staphylococcus aureus* is the most common VAP pathogen isolate in Spain, France, Belgium and Ireland [6], while PA is the predominant isolate in Italy and Portugal. Moreover, *Staphylococcus aureus, Streptococcus pneumoniae* and *Haemophilus influenzae/Moraxella catarrhalis* are more prevalent in the early-onset VAP [6], while *Acinetobacter* species and PA were more commonly isolated in late-onset VAP [22]. The spectrum of VAP pathogens isolated in clinical studies in recent years is shown in Table 1 below.

Table 1 Overview of clinical studies analyzing VAP pathogens

References	Microbiology		
Esperatti et al. (2010) [17]	*Pseudomonas aeruginosa* (24 %)	*Staphylococcus aureus* (23 %)	*Escherichia coli* (7 %)
Martin-Loeches et al. (2015) [23]	*Pseudomonas aeruginosa* (24 %)	*Staphylococcus aureus* (22 %)	*Klebsiella pneumoniae* (14 %)
Pulido et al. (2018) [24]	*Pseudomonas aeruginosa* (21 %)	*Acinetobacter baumannii* (21 %)	*Klebsiella pneumoniae* (15 %)
Huang et al. (2018) [21]	*Acinetobacter baumannii* (34 %)	*Klebsiella pneumoniae* (24 %)	*Pseudomonas aeruginosa* (20 %)
Ibn Saied et al. (2019) [25]	*Pseudomonas aeruginosa* (34 %)	*Enterobacteriaceae* (32 %)	*Staphylococcus aureus* (19 %)

1.2.1. *Pseudomonas aeruginosa*

Pseudomonas aeruginosa (PA) is a ubiquitous Gram-negative, encapsulated and rod-shaped bacterium that can cause acute and chronic diseases in humans. PA is a facultative anaerobe and therefore it is able to survive and proliferate in conditions with partial oxygen depletion [26]. Due to the capacity of biofilm formation of many PA strains, the bacterium is able to survive on surfaces of medical equipment (e.g., hand hygiene sink and catheters) [27], generating a common risk for nosocomial infections. PA has emerged as one of the most common isolates from VAP patients worldwide and was found in 25.9 % and 26.4 % of VAP cases in Asia and Europe, respectively [6, 22]. PA-VAP patients are more likely to develop severe complications (e.g., septic shock and multiple organ dysfunction) [28]. In addition, a sensitivity analysis using the multistate model showed that VAP patients infected with PA had higher mortality as compared to VAP patients infected with *Staphylococcus aureus* [29].

1.2.2. Antimicrobial resistance of *Pseudomonas aeruginosa*

As PA is known for its high likelihood to develop multidrug resistance (MDR) mechanisms, MDR isolates are becoming increasingly prevalent [30] and remain a great challenge in VAP treatment. PA antimicrobial resistance mechanisms can be classified in intrinsic, acquired and adaptive mechanisms [31].

Intrinsic antibiotic resistance refers to the low membrane permeability of PA. It is reported that the permeability of the outer membrane of PA is approximately 12- to 100-fold lower compared with *E. coli* [32]. Furthermore, the expression of bacterial efflux pumps can facilitate ejection of β-lactams and fluoroquinolones, which are commonly used antibiotics in hospitals [33, 34]. In addition, β-lactamase, an enzyme produced by PA, results in inactivation of β-lactam antibiotics [35].

Acquired antibiotic resistance caused by genetic mutations that may influence PA-specific porins (e.g., OprD) [36] or lead to aberrant overexpression of antibiotic efflux pumps [37], enhancing antibiotic resistance capacity.

The adaptive antimicrobial resistance of PA refers to the capacity of biofilm formation and biofilm-related phenotypic changes [31, 38], contributing to chronic and persistent PA infection. For example, in the context of lung cystic fibrosis, PA may convert to a mucoid phenotype that promotes biofilm formation and contributes to antimicrobial resistance [39].

1.2.3. Virulence factors *of Pseudomonas aeruginosa*

PA has several virulence factors that contribute to its pathogenicity. Figure 2 below illustrates the major virulence factors of PA. The Type 3 secretion system (T3SS) enables PA to directly inject toxins into host cells [40], which is of relevance in acute PA infection [41] and is associated with poor clinical outcomes [42]. ExoU, the most potent exotoxin secreted by T3SS, is responsible for rapid loss of the plasma membrane integrity and the death of host eukaryotic cells [43]. Furthermore, PA ExoU is highly cytotoxic and can induce lung

epithelial barrier injury in animal models [44]. Pyocyanin, a blue-green pigment and exotoxin of PA, is able to kill alveolar epithelial cells [45] and cause apoptosis of neutrophils [46]. Moreover, secretion of PA protease IV by PA can lead to degradation of host surfactant proteins A and D, thereby impeding macrophage phagocytosis and contributing to PA survival, colonization and disease severity [47]. The enzyme PA elastase can directly impair lung epithelial barrier integrity [48] and cleave the host surfactant proteins A and D, resulting in increased susceptibility to subsequent PA infection [49]. In addition, the PA flagellum enables the bacteria to adhere to the airway epithelial cells [50].

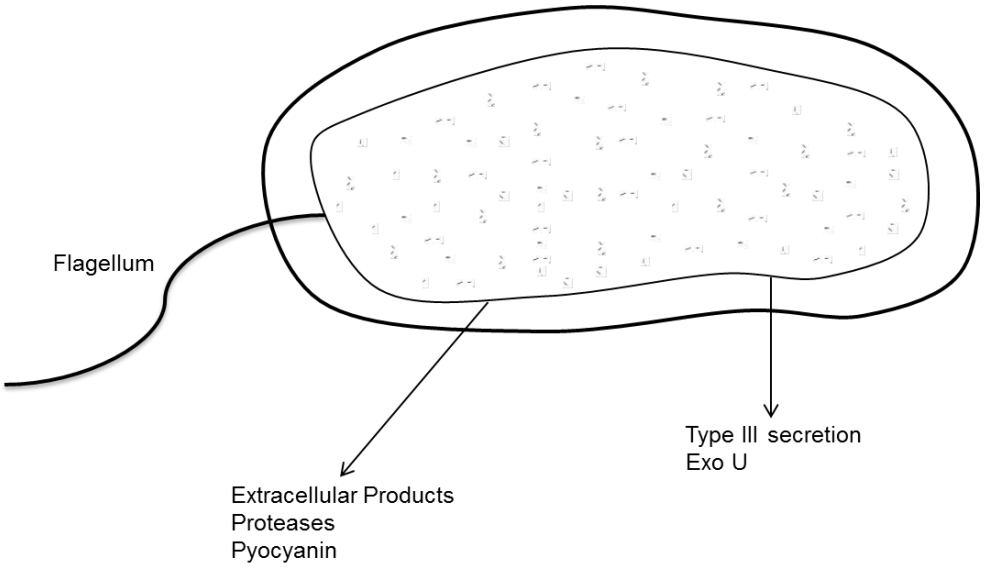

Figure 2: *P. aeruginosa* with critical virulence factors (extracellular secretion products, flagellum, Pyocyanin, Type III secretion system, Exotoxin U (Exo U) (adapted from Sadikot et al. 2005 [51]).

1.3. Risk factors of ventilator-associated pneumonia

Various risk factors are associated with the onset of VAP. Previous studies revealed that increased duration of mechanical ventilation enhances the risk of VAP onset [52, 53, 54]. A comparative study reported that reintubation is another major risk factor of VAP [55]. Furthermore, microaspiration of gastric contents is correlated with the occurrence of VAP [56] and reported as a major risk factor for pneumonia in critically ill patients who received

mechanical ventilation [57]. In addition, disorders of consciousness, burns, and comorbidities (e.g., diabetes) are risk factors for VAP [58, 59, 60]. Interestingly, a randomized controlled trial revealed that patients with severe acute respiratory distress syndrome exhibited a high incidence of VAP (28.9 %) [9], complementing results of a multicenter study where an increased risk of VAP was noted in patients with acute respiratory distress syndrome [61]. Hence, acute respiratory distress syndrome appears to be a critical factor for the onset of VAP, while the specific underlying pathomechanisms are not known yet.

1.4. Acute respiratory distress syndrome

Acute respiratory distress syndrome (ARDS) is a severe respiratory complication, characterized by acute onset of hypoxemia and bilateral lung infiltrates, that are not due to cardiac pathogenesis (left atrial hypertension) [62]. According to the 2012 Berlin definition, the onset of ARDS must be considered to be within a week of a known clinical insult or new or worsening respiratory symptoms [63]. Symptoms of ARDS include severe dyspnea, tachypnea, and cyanosis [64]. In addition, bilateral opacities in chest imaging that cannot be fully explained by pleural effusions, lung atelectasis and left ventricular failure are necessary criteria for ARDS diagnosis [63]. The severity of ARDS can be categorized into three degrees based on the ratio of arterial oxygen partial pressure to fractional inspired oxygen (PaO_2:FiO_2 ratio) (mild: PaO_2:FiO_2, 201 to 300 mmHg; moderate: PaO_2:FiO_2, 101 to 200 mmHg; severe: PaO_2:FiO_2, ≤100 mmHg) [63]. Additionally, a positive end-expiratory pressure (PEEP) of 5 cmH_2O or more is needed for accurate consideration of the PaO_2:FiO_2 ratio [63]. Criteria for the Berlin definition of ARDS are summarized in Table 2 below.

Table 2 Berlin definition of ARDS

Onset	Within 1 week after a known clinical insult or new or worsening respiratory symptoms
Infiltrates on chest radiograph or CT	Bilateral opacities that cannot be fully explained by effusions, lobar/lung collapse or nodules
Categorization of severity:	
Mild	PaO_2:FiO_2, 201 to 300 mmHg
Moderate	PaO_2:FiO_2, 101 to 200 mmHg
Severe	PaO_2:FiO_2, ⩽100 mmHg
Heart failure	Left ventricular failure that cannot be simply explained by clinical state
Specificity for diffuse alveolar damage	Autopsy: 45 % [65] Biopsy: 58 % [66]

Pneumonia, aspiration of gastric contents, and pulmonary contusion are major direct risk factors of ARDS. Non-pulmonary sepsis, non-thoracic trauma or hemorrhagic shock, pancreatitis and burn injury are the major indirect risk factors for the development of ARDS [67]. The incidence of ARDS varies, with 34 cases/100,000 patients per year in the USA [68] and around 5-8 cases/100,000 inhabitants in Europe [69]. An observational study conducted in 50 countries reported that ARDS was observed in 10.4 % of total ICU patients and 23.4 % of severely ill patients who needed mechanical ventilation [70].

While an overall ARDS mortality in ICU and hospital of 42.7 % and 47.8 %, respectively [71], has been reported from large multicenter studies, an additional 22 % of patients died within one year after hospital discharge [72]. ARDS is characterized by the severe impairment of the alveolar-capillary barrier, subsequent lung edema formation and recruitment of innate (mostly granulocytes) and adaptive immune cells [73], worsening lung inflammation and tissue injury. Furthermore, the occurrence of endothelial damage can

cause vasomotor tone alteration and microthrombi formation [73]. The inflammatory exudate can lead to dysfunction of the alveolar surfactant and impair its production, contributing to hyaline membrane formation and pulmonary compliance decrease, further impairing gas exchange [73]. According to the “baby lung” concept, the volume of aerated lung regions with functional gas change is largely reduced in ARDS patients [74, 75]. In consequence, despite a lung protective ventilation strategy, regional lung hyperinflation may occur, worsening the preexisting lung injury; and is a condition that is simulated for research in experimental animal models by applying high tidal volume to previously healthy lungs [76, 77, 78].

1.5. Ventilator-induced lung injury

MV is a life-saving medical intervention for patients with acute respiratory distress syndrome. Nevertheless, an inappropriate MV strategy can cause lung injury in healthy lungs or worsen pre-existing lung injury, a process termed ventilator-induced lung injury (VILI). The following mechanisms account for the pathogenesis of VILI:

VILI induced by overventilation by high lung volumes is termed volutrauma [79]. Due to regional over-distention in the aerated lung adjacent to atelectasis areas, even protective tidal volume ventilation may result in alveolar-capillary barrier dysfunction, pulmonary edema and air leaks [79]. Importantly, the impaired lung barrier may contribute to the translocation of intra-alveolar substances (e.g., inflammatory mediators and lipopolysaccharides) to the systemic circulation and thereby cause multiple organ dysfunction and death [79].

The term atelectrauma refers to the process of cyclic opening and closing of atelectatic but recruitable airways and alveoli [80, 81], leading to surfactant dysfunction [82] and regional

hypoxia [79]. The atelectrauma may be particularly amplified in lungs of ARDS patients due to the high tissue inhomogeneity [79].

Lung stress is the internal force per unit area caused by mechanical ventilation [83]. The term lung strain refers to the change of lung volume in response to the applied factor (e.g., tidal volume) [84]. Both stress and strain are mechanical determinants of VILI [85]. In the context of atelectrauma, high stress and strain are produced at the margins between aerated and collapsed airways during alveolar recruitment [81, 83, 86]. In severe ARDS, injurious levels of stress and strain in the lung can be generated as a consequence of the strongly reduced aerated lung volume [87].

The term biotrauma summarizes the biological translation of the mechanical stress signal by ventilation into a biological response including the release of inflammatory mediators and recruitment of innate immune cells [77, 79, 83], also possibly affecting adjacent, previously healthy lung sections [83]. These mediators may directly damage lung tissue or act as chemoattractants, further promoting the recruitment of inflammatory cells (e.g., neutrophils) to the lung [79]. Increased IL-1β in VILI was shown to contribute to alveolar barrier dysfunction and promote neutrophil recruitment [88]. Furthermore, increased levels of neutrophil chemoattractants MCP-1, CXCL-1 and MIP-2 were found in experimental VILI models [77, 78]. The increased number of recruited neutrophils can further exacerbate lung injury through the release of reactive oxygen species, elastase and neutrophil extracellular traps [89, 90, 91]. In addition, activation of alveolar macrophages and recruitment of Gr-1 (high) monocytes was reported in the context of VILI [92, 93].

When considering VILI as a major contributor for the onset and progression of ARDS [73, 94, 95], the term “lung protective ventilation” describes the attempt to set ventilator settings to minimize VILI while optimizing gas exchange, which has improved remarkably during the last decades through many clinical and experimental studies. First, since a landmark

study in 2000 [94], the concept of protective low tidal volume ventilation (6 mL/kg) and high PEEP values (>5 cmH_2O) has been accepted worldwide, contributing to a decrease of mortality in patients with ARDS [96, 97]. A combination of low tidal volume ventilation and PEEP titration has been shown to limit overinflation of inhomogeneous lung areas and to reduce the atelectrauma [79]. Compared with lung protective ventilation strategy, abdominal surgery patients ventilated with non-lung protective ventilation strategy (tidal volume of 10–12 mL/kg and PEEP of 0) had more complications (e.g., pneumonia and sepsis) and longer hospital stay [98].

When patients are mechanically ventilated in supine position (lying on their backs), the inflated lung area is more inhomogeneously distributed, particularly in patients with ARDS [99], while temporal prone positioning (lying on the abdomen) was found to promote a more homogeneous lung inflation and redistribution of lung densities from dorsal to ventral lung regions [100, 101]. In 2013, a clinical trial demonstrated that early application of prone positioning significantly decreased the mortality of patients with severe ARDS [102]. Possible mechanisms for the advantages of prone position may include increased end-expiratory lung volume, improved regional ventilation and better matching of ventilation and perfusion [79]. Pharmacologic interventions to limit VILI have often been successful in experimental studies [103, 104], but have failed in clinical translation [105, 106]. Only recently, the administration of neuromuscular blocking agents was shown to improve the patient-ventilator synchrony and thereby the 90-day survival of severe ARDS patients in a clinical trial [107].

1.6. Experimental models of ventilator-associated pneumonia

Animal models are crucial to bridge between *in vitro* experiments and clinical studies, enabling researchers to precisely understand cellular and molecular mechanisms in the

pathophysiology of diseases. The aim of establishing animal VAP models is to imitate the pathophysiologic and phenotypic characteristics of human VAP in a more controlled setting [108]. Compared with human VAP subjects, experimental models provide pure pneumonia models without interference factors, such as comorbidities, previous infection and prior use of antibiotics [109]. Furthermore, experimental models render the possibility to precisely investigate the role of the immune response including local and systemic inflammation. In addition, sampling limitations that are usually encountered with human cases can be prevented [108], and the experimental process can be strictly controlled based on the accurate timing of ventilation, infection and endpoints, so that natural variables in the course of human VAP can be minimized [108, 109].

In the last few decades, different animal models have been used to study the pathophysiology and therapy of VAP *in vivo*. In the 1980s, baboon models were established for bacteriological analysis of VAP [110, 111, 112]. In a porcine model, prolonged mechanical ventilation (up to 4 days) led to the development of a spontaneous pneumonia (mainly caused by common airway colonization microorganisms, e.g., *Pasteurella multocida* and *Streptococcus suis*) [113]. Furthermore, in another porcine model, it was shown that mechanical ventilation following PA infection exacerbated pulmonary bacterial growth and histopathological signs of pneumonia [114].

Due to the high homology of genomes between rodents and humans, murine models have been becoming a preferred choice for translational pulmonary research [108]. Prior studies aimed to establish experimental murine VAP-like models [115, 116, 117] to study the pathogenesis of VAP. In contrary to the pathophysiological sequence in humans, in these studies, pneumonia was induced by bacterial inoculation followed by mechanical ventilation. Verbrugge and colleagues proved that the use of PEEP (10 cmH_2O) could reduce pneumonia severity in rats [115]. In a murine pneumonia model with *Staphylococcus*

aureus and *E. coli*, higher numbers of recruited neutrophils, increased levels of inflammatory mediators (e.g., IL-6, TNF-α and CXCL-1) and increased alveolar-capillary permeability were observed compared with animals subjected to bacterial infection alone without MV [116]. Tsay and colleagues showed that PA infection prior to MV increased the level of VILI via the c-Jun N-terminal kinase (JNK) signaling pathway in the lung [117]. Furthermore, PA infection carried out with an acidic inoculation medium led to increased neutrophil recruitment and release of inflammatory mediators, resulting in more severe lung damage and increased bacterial load [118]. However, in turn the neutrophil infiltration *per se* may also decrease the pH of the microenvironment and thereby amplify the inflammatory response [119], contributing to disease progression.

To examine the molecular effects in detail, mechanical ventilation can be modeled *in vitro* by exposing cells to cyclic cell stretch [120, 121, 122]. Pugin and collaborators showed that cyclic stretch could lead to the acidification of the extracellular milieu via activation of the Na^+/K^+-ATPase in alveolar epithelial cells and the resulting increased proton release may favor the growth of various VAP pathogens (e.g., PA, *Escherichia coli* and *Klebsiella pneumoniae*) [123].

1.7. Hypothesis

As described above, VAP is one of the most common ICU-acquired infections associated with long hospital stay and high mortality. Prolonged mechanical ventilation is a major risk factor responsible for the development of VAP [52]. During mechanical ventilation, particularly in ARDS patients, VILI can occur despite the use of lung protective ventilation. Interestingly, mechanically ventilated patients with ARDS were shown to have substantially lower airway pH measured in exhaled breath condensates (EBC) compared to non ARDS patients [124, 125], and several *in vivo* and *in vitro* studies indicated a possible

association of an acidic environment and VAP pathogen proliferation [118, 123]. Hence, we hypothesized that VILI-induced alveolar lining fluid acidification may be associated with the pathogenesis of VAP and may contribute to the disease onset and progression. The present study aimed to establish a murine VAP model by instilling bacteria via the endotracheal tube after mechanical ventilation. Using this novel approach that more realistically mimics human pathologic sequence, the influence of MV on the onset and progression of VAP was evaluated *in vivo*. Furthermore, additional *ex vivo* and *in vitro* experiments were performed to characterize whether MV-induced acidification of alveolar lining fluid may affect pneumonia severity.

2. Materials and Methods

2.1. Materials

2.1.1. Instruments

Table 3 Instruments used in the course of experiments

Instrument	Manufacturer	Company location
Air flow bench	Thermo Scientific	USA
AMBIO Nikon Upright Spinning Disk Confocal S2 microscope	Nikon	Japan
Autoclave	Systec	Germany
Centrifuge	Thermo Scientific	USA
CFX96 real-time PCR detection system	BIO-RAD	USA
FACS Canto-II	BD Bioscience	USA
Fiber Optic Laryngoscope System	Welch Allyn	USA
FX-5000™ Tension System	Flexcell International	USA
High pressure syringe (Model No.FMJ-250)	Penn-Century	USA
Homeothermic Blanket System	Harvard Apparatus	USA
Incubator	Heraeus	Germany
Incubator hood	Edmund Bühler	Germany
Multiphoton Microscope LSM 780	Carl-Zeiss	Germany
Multiskan™ FC Microplate Photometer	Thermo Scientific	USA
pH Electrode	Mettler-Toledo	USA
pH meter 340	WTW	Germany
Small animal ventilator (FlexiVent)	SCIREQ	Canada
Thermal cycler	Biometra	Germany

Transmitted light brightfield microscope	Carl-Zeiss	Germany
Vet ABC ™Hematology Analyzer	scil	Germany
Water bath	Julabo	Germany

2.1.2. Consumables

Table 4 Consumables used in the course of experiments

Supplies	**Manufacturer**	**Company location**
µ-Slide 8 Well	ibidi	Germany
20G IV cannula	B. Braun	Germany
Cassettes for histology	Carl Roth	Germany
Cell culture flask, T-75	SARSDEDT	Germany
Cell culture plates	Corning	USA
Cell strainers (70µm)	Greiner Bio-One	Germany
Columbia agar plate + 5% sheep blood	BD	USA
Conical tubes (15ml, 50ml)	Corning	USA
Cuvettes	SARSDEDT	Germany
Eppendorf tubes	SARSDEDT	Germany
FACS tubes	Corning	USA
GentleMACS M Tubes	Miltenyi Biotec	Germany
Inoculation loop	SARSDEDT	Germany
K2EDTA tubes	SARSDEDT	Germany
Micro test plate, 96 well	SARSDEDT	Germany
Pipette tips	Clearline/SARSDEDT	France/ Germany
Sterican needles	B. Braun	Germany
Syringes (1ml, 5ml, 10ml)	B. Braun/BD	Germany/USA

Type IV collagen coated 6-well BioFlex plate	Dunn Labortechnik	Germany

2.1.3. Reagents and chemicals

Table 5 Reagents and chemicals used in the course of experiments

Reagents	**Manufacturer**	**Company location**
3,3′,5,5′-Tetramethylbenzidine solution	Thermo Scientific	USA
4% paraformaldehyde	neoFroxx	Germany
4′,6-Diamidino-2-phenylindole dihydrochloride	Merck KGaA	Germany
Bovine Serum Albumin	Sigma-Aldrich	USA
Collagenase	Biochrom	Germany
CountBright™ Absolute Counting Beads	Thermo Scientific	USA
Dimethyl sulfoxide	PanReac AppliChem	Germany
DNAse	PanReac AppliChem	Germany
Ethanol	Carl Roth	Germany
Fentanyl	Hexal AG	Germany
Flumazenil	hameln pharma	Germany
Glycerol		
Hanks' Balanced Salt Solution	Thermo Scientific	USA
HCl	PanReac AppliChem	Germany
Heparin	Ratiopharm	Germany
Hydrogen peroxide	Sigma-Aldrich	USA
Ketamine	Cp-pharma	Germany
Medetomidine	Cp-pharma	Germany
Midazolam	Hexal AG	Germany

NaOH	Carl Roth	Germany
PBS	Gibco	UK
pHrodo™ Red Dextran (10.000 MW)	Thermo Scientific	USA
Protease Inhibitor Cocktail	Roche Diagnostics	Germany
Revertor	Cp-pharma	Germany
Saline	B. Braun	Germany
Triton X-100	Sigma-Aldrich	USA
TRIzol	Thermo Scientific	USA
Tryptic Soy Broth	BD	USA
Tween-20	Fisher Bioreagents	Germany
Xylazine	Cp-pharma	Germany

2.1.4. Kits

Table 6 Kits used in the course of experiments

Kit	**Manufacturer**	**Company location**
DC protein assay	BIO-RAD	USA
High-Capacity cDNA Reverse Transcription Kit	Thermo Fisher Scientific	USA
LEGENDplex™ Mouse Inflammation Panel	BioLegend	USA
LEGENDplex™ Mouse Proinflammatory Chemokine Panel	BioLegend	USA
Luminaris Color HiGreen Mastermix	Thermo Fisher Scientific	USA
Mouse Albumin ELISA Quantitation	Biomol	Germany
RNA mini prep kit	Zymo Research	USA

2.1.5. Media and solutions

Table 7 Media and solutions used in the course of experiments

Reagent	Manufacturer	Company location
Fetal bovine serum	Capricorn scientific	Germany
Penicillin/Streptomycin	Gibco	UK
RPMI-1640	Gibco	UK

2.1.6. Antibodies for immunofluorescence

Table 8 Antibodies used for immunofluorescence experiments

Antibody	Manufacturer	Company location
Anti-Alexa Fluor 546 Phalloidin	Thermo Fisher Scientific	USA
Anti-GFP Polyclonal Antibody Alexa Fluor 488	Thermo Fisher Scientific	USA

2.2. Methods

2.2.1. *In vivo* experiments

2.2.1.1. Ethical statement

All animal experiments were ethically approved by the governmental animal welfare authorities (Landesamt für Gesundheit und Soziales Berlin, application number: G0291/16).

2.2.1.2. *Pseudomonas aeruginosa* storage, culture and preparation

In vivo:

The *Pseudomonas aeruginosa* strain 103 (PA103) (American Type Culture Collection (ATCC), #29260) was frozen in Tryptic Soy Broth (TSB) medium (BD Biosciences; USA) containing 20 % glycerol at -80 °C for long-term storage. Prior to use, the bacteria were

inoculated on Columbia agar plates containing 5 % sheep blood (BD Bioscience; USA) and incubated at 37 °C and 5 % CO_2 overnight. The next day, 2-3 single colonies were sterilely inoculated into the TSB and allowed to grow at 37 °C for 2 h with shaking until the optical density (OD_{600}) of bacterial suspension reached 1.0-1.5. The PA103 suspension was then centrifuged at 800 g for 15 min at room temperature (RT). After centrifugation, the supernatant was discarded, followed by bacterial pellet resuspension using sterile phosphate buffered saline (PBS) (Gibco; UK), followed by centrifugation (800 g, 15 min, RT). Subsequently, the supernatant was discarded, and the PA pellet was resuspended in sterile PBS for further serial dilution. For calculating the bacterial concentration, OD_{600} = 1 corresponds to 5.62×10^8 colony forming units (CFUs) per mL. Bacteria were serially diluted with sterile PBS to reach the required concentration for infection.

In vitro:

The green fluorescent protein-*Pseudomonas aeruginosa* PAO1 (GFP-PAO1), purchased from Prof. Susanne Häußler (TWINCORE; Germany), was used for *in vitro* infection. GFP-PAO1 was stored, cultured and prepared as described above for PA103. For calculation of bacterial concentration, OD_{600} = 1 corresponds to 1.0×10^9 CFUs per mL.

2.2.1.3. Mice

For the *in vivo* experiments, female specific-pathogen-free (SPF) C57BL/6J mice (8-11 weeks; 18-20 g; Charles River; Germany) were used. Mice were kept in sterile cages with food and water *ad libitum*. For acclimation, mice were housed in the animal facility (12/12 h light dark cycle, 20-23 °C and 40-60 % humidity) for more than 1.5 weeks. All handling and sampling operations were carried out under sterile conditions.

2.2.1.4. Mechanical ventilation

The mechanical ventilation applied to mice was performed as previously described [77]. In brief, mice were anaesthetized intraperitoneally with fentanyl (75 µg/kg), midazolam (1.5 mg/kg), and medetomidine (0.75 mg/kg). Mice were then endotracheally intubated with a 20G IV cannula (B. Braun; Germany) and connected to a small animal ventilator (FlexiVent; Scireq; Canada). During MV, fentanyl (16 µg/kg), midazolam (0.33 mg/kg) and medetomidine (0.16 mg/kg) were applied through an intraperitoneal catheter to maintain sedation when required. Body temperature was retained at 37 °C by using a homeothermic blanket system (Harvard Apparatus; USA) and a urinary catheterization was performed to collect urine and avoid urinary retention. After connecting intubated mice to the ventilator, the airway pressure was increased to 27 cmH_2O for 6 seconds to carry out the initial recruitment maneuver. Mice were mechanically ventilated using the following ventilation settings:

- High tidal volume (HVt) ventilation

  In this group, mice were ventilated for 4 h with a tidal volume of 34 mL/kg, respiratory rate of 69 per min, inspiration-to-expiration ratio (I:E) of 1:1, FiO_2 of 50 % and PEEP of 2 cmH_2O.

- Low tidal volume (LVt) ventilation

  In this group, mice were ventilated for 4 h with a tidal volume of 9 mL/kg, respiratory rate of 160 per min, IE ratio of 1:1, FiO_2 of 50 % and PEEP of 2 cmH_2O. In order to avoid atelectasis, deep inflation (27 cmH_2O for 1 second) was carried out every 5 min.

- Non-ventilated (NV) control

  In this group, after the initial recruitment maneuver, mice were attached for 10 min only using the settings of the LVt group to generate a baseline control.

2.2.1.5. Infection

After MV, mice were weaned from the ventilator, and subsequently 20 μL PA103 suspension (5×10^4 CFUs/mouse) was instilled through the endotracheal cannula. Sham-infected groups were treated with 20 μL sterile PBS in the same manner as the PA-infected mice. After infection, sedation was antagonized by intraperitoneal injection of flumazenil (0.5 mg/kg) and antipamezol (5 mg/kg). Mice were then extubated and allowed to breath spontaneously for 24 h. The endpoint of this experiment was 24 h post infection. Clinical symptoms (body temperature and weight) were monitored every 12 h until the endpoint of this experiment.

2.2.1.6. Lung function measurement

Lung compliance is calculated as the change in lung volume in relation to the change in pressure ($\Delta V/\Delta P$) [83], a parameter indicating the flexibility of lung tissue during physiological stretch in respiration. As the reciprocal of compliance, lung elastance ($\Delta P/\Delta V$) represents the stiffness of the lung [83]. Characteristically, ARDS patients exhibit a pathological decrease in lung compliance [126]. Inspiratory capacity is the maximum volume of air that can be inhaled into the lungs after the end of normal expiration and indicates the limit of lung expansion [127].

During MV, dynamic lung elastance and resistance were measured and recorded every 5 min by using forced oscillation techniques. The initial recruitment maneuver was performed immediately after mice were connected to the ventilator and the terminal recruitment maneuver was carried out 5 min before the end of MV. During the initial and final recruitment maneuvers, static lung compliance and inspiratory capacity were measured and recorded. Experimental design of the *in vivo* experiments is shown below.

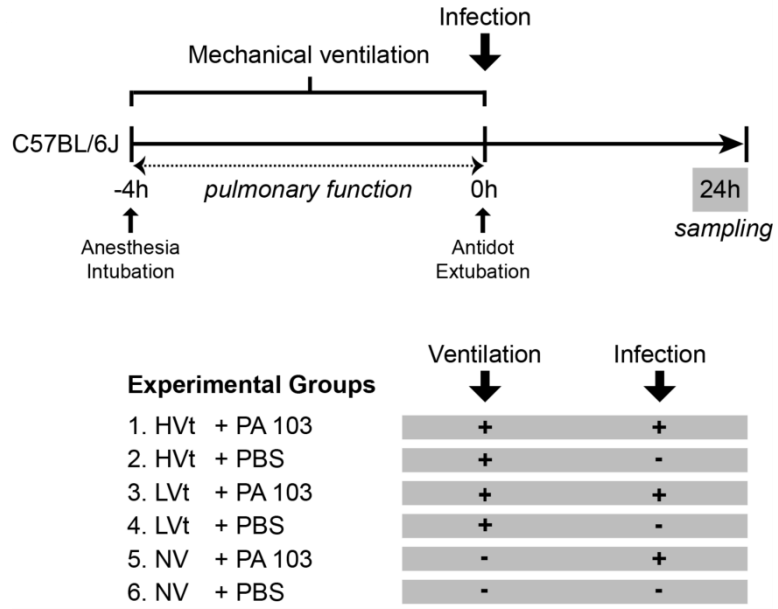

Figure 3: Experimental design of the in vivo experiment. Mice were anaesthetized, intubated and mechanically ventilated with HVt (34 mL/kg), LVt (9 mL/kg) for 4 h or ventilated for 10 min (LVt) as NV control. Pulmonary function parameters were measured during MV. After MV, either PA103 or sterile PBS was instilled intratracheally and mice were extubated and left breathing spontaneously for 24 h. Mice were euthanized and sampling was performed 24 h post infection.

2.2.1.7. Mice plasma preparation and blood leukocyte quantification

Twenty-four hours post infection, mice were anaesthetized intraperitoneally with 80 mg/kg ketamine and 25 mg/kg xylazine. Blood was drawn from the *vena cava* using heparin coated syringes and kept in ethylenediaminetetraacetic acid (EDTA) tubes to prevent coagulation. Blood was then centrifuged at 1050 g for 10 min at 4 °C and the supernatant (plasma) was collected and frozen at -80 °C for further analysis. A scil Vet abc™ hematology analyzer (scil animal care company GmbH; Germany) was used to differentiate and quantify blood leukocytes.

2.2.1.8. Broncho-alveolar lavage and lung preparation

Mice were anaesthetized 24 h post infection. Tracheotomy was carried out and the trachea was cannulated with an 18-gauge needle. Broncho-alveolar lavage (BAL) was performed once with chilled 800 µL sterile PBS containing protease inhibitors (1 tablet/10 mL; complete Mini; Roche diagnostics GmbH; Germany). The BAL was then centrifuged at 1000 g for 10 min at 4 °C and supernatant (BAL fluid, BALF) was collected and stored at -80 °C for further experiments. Cell pellets were resuspended in sterile PBS for cell cytometry. An 18-gauge needle was inserted into the right atrium of the mouse heart and lungs were flushed by injecting 500 µL chilled saline (B. Braun; Germany) to wash out residual blood in the pulmonary vascular system. The left lung was then harvested and stored at -80 °C for the quantitative reverse transcription polymerase chain reaction (qRT-PCR) and protein quantification. Right lung lobes were divided into two parts - one part was homogenized for bacterial load determination, and the other part was used for cell cytometry.

2.2.1.9. Bacterial load determination

Mice were sacrificed 24 hours after infection. BAL and blood were prepared as previously described. Half of the right lung, liver (one lobe) and spleen were harvested and homogenized in sterile PBS through a cell strainer (70 µm, Greiner Bio-One; Germany). Subsequently, serial dilutions of these samples were carried out, each plated on Columbia agar plates containing 5 % sheep blood (BD Bioscience; USA) and incubated overnight at 37 °C and 5 % CO_2. CFUs were counted and calculated the following day.

2.2.1.10. Mouse albumin ELISA

To assess the impact of VILI and subsequent PA pneumonia on the alveolar-capillary permeability, albumin concentrations in BALF and plasma were determined using the

mouse albumin ELISA kit (Bethyl; Germany) according to the manufacturer's instructions. BALF and plasma were prepared as previously described. Briefly, a 96-well flat-bottom plate was coated with affinity purified antibody (1:100 dilution) overnight. After incubation, the liquid was discarded and the plate was washed five times with wash buffer. After washing, blocking solution was added and the plate was blocked for 30 min at RT. To ensure that the OD values of each sample were detectable and within the linear range of the standard curve, different sample dilutions were performed depending on the sample type (detailed dilution information is provided in Table 9). After preparation of the standards and samples, each was loaded onto the plate and incubated at RT for 60 min. The plate was then washed five times with wash buffer again and incubated with streptavidin-horseradish peroxidase conjugated detection antibody (1:75,000 dilution) for 1 h at RT in darkness. After incubation, the plate was washed and the TMB substrate solution was loaded for 10 min incubation in darkness. Finally, the stop solution (H_2SO_4) was added and OD_{450} values of each sample were measured using the Multiskan™ FC Microplate Photometer (Thermo Scientific; USA). The standard curve was used to quantify the OD of each sample and the albumin concentration was calculated and expressed as ng/mL. The albumin BALF/plasma ratio was used to evaluate alveolar-capillary permeability.

Table 9 Dilution information for mouse albumin ELISA

experimental groups	**infection**	**sample**	**dilution factor**
HVt	PA103	BALF	1:20,000
LVt	PA103	BALF	1:20,000
NV	PA103	BALF	1:20,000
HVt	PBS	BALF	1:5,000
LVt	PBS	BALF	1:1,000

NV	PBS	BALF	1:1,000

The plasma dilution factor was 1:500,000.

2.2.1.11. Cytokine and chemokine quantification

BALF and plasma were prepared as described above. The concentrations of inflammatory cytokines (IL-6, IL-10, IL-1α, IL-1β, IFN-γ and GM-CSF) and chemokines (MCP-1, CXCL-1, CXCL-5, MIP-1α, MIP-1β and eotaxin) in BALF and plasma were quantified by a multiplex bead-based immunoassay technique (LEGENDplex™; BioLegend; Germany) according to the manufacturer's instructions. Briefly, standards were diluted (1:4 dilution) with assay buffer from the highest concentration (10,000 pg/mL) to the lowest concentration (2.4 pg/mL). Plasma was diluted (1:2 dilution) with assay buffer. Subsequently, assay buffer was added onto a V-bottom plate followed by the standards and sample loading. For the measurement of inflammatory mediators in plasma, the Matrix C solution and assay buffer were added to the standard wells and sample wells, respectively, and then the standards and plasma samples were loaded. After this step, customized-mixed beads were loaded and the plates were shaken at 800 rpm at 4 °C overnight. The next day, the plates were washed twice with wash buffer and incubated with biotinylated detection antibodies for 1 h at RT with shaking. Subsequently, the Streptavidin-phycoerythrin fluorochrome was added and the plates were incubated for 30 min at RT on a shaker (IKA-Werke; Germany). Thirty minutes later, the plates were washed twice and the results were read with the fluorescence-activated cell sorting (FACS) Canto II (BD Bioscience; Germany). Data were further analyzed with LEGENDplex data analysis software (BioLegend; Germany).

2.2.1.12. Flow cytometry

Flow cytometry was used to differentiate and quantify leukocytes in BAL and lung as previously described [147]. Cell pellets from BAL were prepared as previously described and resuspended in 100 µL sterile PBS for flow cytometry. Lungs were flushed as described above and half of the right lung was carefully harvested. Lungs were incubated with plain RPMI-1640 medium containing DNase I (0.33 mg/mL, AppliChem GmbH; Germany) and collagenase (1 mg/mL, Biochrom GmbH; Germany) at 37 °C for 30 min. After digestion, lungs were homogenized in pre-heated plain RPMI-1640 medium through a cell-strainer (70 µm, Greiner Bio-One; Germany) to prepare a single cell suspension followed by centrifugation (480 g, 5 min, 4 °C). Cell pellets were then resuspended in sterile PBS for flow cytometry. Prior to staining, surface blocking antibody (shown in Table 10) was added and samples were incubated on ice for 3 min. Subsequently, cell surface staining antibody mix (shown in Table 11) was added and samples were incubated for 20 min at 4 °C in darkness. Samples were washed (centrifugation: 480 g, 5 min, 4 °C) and the supernatant was discarded. 1 % paraformaldehyde (PFA) was added for fixation and cells were incubated at 4 °C overnight. Afterwards, cells were washed again and resuspended in 100 µL FACS buffer (0.5 % bovine serum albumin (BSA) in PBS). Counting beads (CountBright™ Absolute Counting Beads, Thermo Fisher Scientific; USA) were added to quantify the absolute numbers of leukocytes. Results were acquired using the FACS Canto II (BD Bioscience; Germany). Data were further analyzed with FlowJo software (Ashland; USA).

Table 10 Surface blocking antibody

antibody	**company**	**amount in 100 µL staining volume (µL)**
anti-CD16/32 (Fc block)	BD Bioscience	1

Table 11 Mixture of cell surface staining antibodies

antibody	color	company	amount in 100 µL staining volume (µL)
anti-CD11c (N418)	APC (Cy5)	BD	0.4
anti-CD11b (M1/70)	PE-Cy7	eBioscience	0.5
anti-F4/80 (BM8)	PE	eBioscience	0.8
anti-CD45 (30-F11)	FITC	BD	0.25
anti-Ly6G (1A8)	PerCP-Cy5.5	BD	0.5
anti-Ly6C (HK1.4)	BV510	BioLegend	0.5
anti-MHCII (M6/114.15.2)	AF700	eBioscience	0.15
anti-SiglecF (1RNM44N)	BV421 (V450)	eBioscience	0.8
FACS buffer			16.1

2.2.1.13. Total RNA isolation

Total RNA of lung was extracted using a RNA mini prep kit (Zymo Research; Germany) according to the manufacturer's instructions. Briefly, lungs were flushed as previously described. Half of the flushed left lungs was suspended in TRIzol (Thermo Fisher Scientific; USA) and homogenized using a gentleMACS Dissociator (Miltenyi Biotech GmbH; Germany). The suspension was transferred into RNase-free Eppendorf tubes and centrifuged at 13000 g for 1 min at RT. After centrifugation, supernatants were carefully transferred into RNase-free Eppendorf tubes and thoroughly mixed with 100 % ethanol. The mixture was then transferred into Zymo-spin columns followed by centrifugation (13000 g, 30 seconds, RT). To remove residual DNA, DNA was digested with DNase I at RT. After 15 min of incubation, columns were washed twice with RNA pre wash solution and then washed once with RNA wash buffer. Thirty microliters of DNase/RNase-free water was then added to the column matrix and centrifuged at 13000 g for 1 min at RT

for eluting RNA. Extracted RNA samples were stored at -80 °C for further use. The purity and concentration of RNA was determined using NanoDrop2000 (Thermo Fisher Scientific; USA).

2.2.1.14. cDNA transcription

cDNA was synthesized using a High-Capacity cDNA Reverse Transcription Kit (Thermo Fisher Scientific; USA) by following the manufacturer's instructions. Firstly, cDNA reverse transcription master mix (Thermo Fisher Scientific; USA) was prepared (details are given in Table 12) and 10 µL of master mix was added to 10 µL RNA (after normalization). Reverse transcription was performed in a thermal cycler (Biometra; Germany) using the following program: 10 min at 25 °C, 120 min at 37 °C and 5 min at 85 °C. Subsequently, cDNA samples were diluted with DNase/RNase-free water (1:10 dilution) and stored at -20 °C for further use. All steps were carried out on ice.

Table 12 cDNA reverse transcription master mix

component	**volume (µL)**
reverse transcription buffer (10X)	2.0
dNTP mix (25X)	0.8
reverse transcription random primers (10X)	2.0
reverse transcriptase	1.0
nuclease-free water	4.2

2.2.1.15. Quantitative reverse transcription polymerase chain reaction (qRT-PCR)

In brief, all cDNA samples were thawed on ice. For each gene, 4 µL of cDNA was added to 5 µL SYBR green and 1 µL respective primer to prepare the qRT-PCR master mix (total reaction volume: 10 µL). The prepared master mix was then loaded onto 96-well plates

and qRT-PCR was carried out on a CFX96 real-time PCR detection system (BIO-RAD; Germany). The reaction conditions are shown in Table 13. To normalize data, the expression of GAPDH was used as endogenous control. The relative mRNA expression levels of inflammatory cytokines (IL-1α, IL-1β, IL-6, IL-10 and TNF-α) and chemokines (MCP-1 and CXCL-5) of experimental groups were calculated as fold change to the NV-PBS control group (ΔΔct) using the $2^{-\Delta\Delta ct}$ method.

Table 13 qRT-PCR condition

name	**temperature (°C)**	**duration**	**number of cycles**
UDG pre-treatment	50	2 min	1
initial denaturation	95	10 min	1
denaturation	95	15 sec	40
annealing	60	1 min	40
extension	60	1 min	40

2.2.1.16. Histopathology

Twenty-four hours post infection, mice were anaesthetized and euthanized by exsanguination via the *vena cava*. To avoid collapse of the alveoli, the trachea was ligated and the whole lung with trachea was carefully harvested and fixed in 4 % PFA solution (pH 7.0). The thymus, heart, liver, spleen, stomach, intestines, right kidney with adrenal gland and brain were harvested and fixed in 4 % PFA for a maximum of 48 h. After fixation, lungs and other organs were embedded in paraffin and cut into 2-µm-thick sections. The working steps of embedding, cutting, dewaxing, hematoxylin and eosin (H&E) staining, representative image acquisition and histopathologic severity evaluation were performed by Dr. Theresa Firsching (Institute of Veterinary Pathology, Freie Universität Berlin, Berlin, Germany), who was blinded to the experimental groups. All scoring parameters (total lung inflammation, polymorphonuclear cell infiltration, hemorrhage severity, perivascular

edema severity, alveolar wall damage severity, alveolar edema severity, macrophages infiltration and necrosis severity) were rated as 0: nonexistent, 1: minimal, 2: mild, 3: moderate, 4: severe.

2.2.2. *In vitro* experiments

2.2.2.1. Cell culture

Human A549 cells (ATCC #CCL-185) were cultured in RPMI-1640 medium (Gibco; UK) supplemented with 10 % fetal calf serum (FCS) (Capricorn Scientific GmbH; Germany) and 1 % Penicillin / Streptomycin (P/S) (Gibco; UK). Cells were grown in a humidified incubator at 37 °C with 5 % CO_2. Cell splitting was performed when cell confluence reached 90 %. Cells at passage 8 were used for further experiments.

2.2.2.2. A549 cell cryopreservation

After removal of culture medium, cells (at passage 5) were washed with sterile PBS and trypsinized at 37 °C and 5 % CO_2 for 5 min. Cells were then centrifuged at 300 g for 5 min at RT. After discarding the supernatant, cell pellets were resuspended in cryopreservation medium with 30 % FCS and 10 % Dimethyl Sulfoxide to a concentration of 1×10^6/mL. Subsequently, 1 mL cell suspension was added into the stock vials and the vials were placed into the freezing container with isopropyl to guarantee gentle freezing of the cells. The next day, the stock vials were stored at -80 °C for long-term use. Cell counting was performed using the Neubauer chamber. All steps were carried out under strict sterile conditions.

2.2.2.3. Cell thawing

The frozen stock vial was thawed in a 37 °C water bath. The cell suspension was transferred into a centrifuge tube containing pre-warmed complete culture medium and cells were then centrifuged at 300 g for 5 min at RT. Subsequently, the supernatant was removed and cell pellets were resuspended in pre-warmed medium. The cell suspension was then added to culture flasks for further experiments.

2.2.2.4. Cell cyclic stretch

The cell stretch (CS) was carried out using the FX-5000™ Tension System (Flexcell International; USA). Before CS, 5 x 10^5 cells were seeded onto type IV collagen coated 6-well BioFlex plates (Dunn Labortechnik; Germany). Cells were maintained in complete culture medium and incubated at 37°C and 5 % CO_2 for 24 h until a single cell monolayer was formed. Subsequently, the cell culture medium was replaced with 1 mL fresh antibiotic-deprived culture medium and the plates were transferred into a customized incubator (37 °C, 5% CO_2) containing the CS system. CS was performed using the following settings: elongation of 18 %, frequency of 20 cycles/min, duration of 24 h and stretch/relaxation ratio of 1:1. The non-stretched (NCS) control plates were kept in static condition in the same incubator. After CS, cell-free supernatant from each condition was collected, respectively, for further experiments. The pH of the supernatant was determined with a fine pH-electrode (Mettler Toledo InLab Semi-Micro; USA). The collected supernatant was used as either CS medium or NCS medium for subsequent infection experiments. Thereafter, cells on the BioFlex plates were trypsinized, resuspended in medium, counted and collected for infection.

2.2.2.5. Green fluorescent protein-*Pseudomonas aeruginosa* PAO1 preparation and infection

The GFP-PAO1 was cultured and prepared as described earlier (see 2.2.1.2). After CS, cells were seeded onto 8 well ibidi µ-slides ($1x10^5$ cells/well; ibidi GmbH; Germany), combined with the previously harvested cell-free supernatant ($1x10^5$ cells per well) and allocated into the following groups: stretched cells with stretched acidified medium, stretched cells with non-stretched medium, non-stretched cells with stretched acidified medium and non-stretched cells with non-stretched medium (detailed experimental design is shown in Figure 4). Cells were then allowed to attach for 2 h and infected with 20 µL GFP-PAO1 suspension at the multiplicity of infection (MOI) of 10 for 4 h. After infection, media were discarded and cells were washed with sterile PBS three times for immunofluorescence staining.

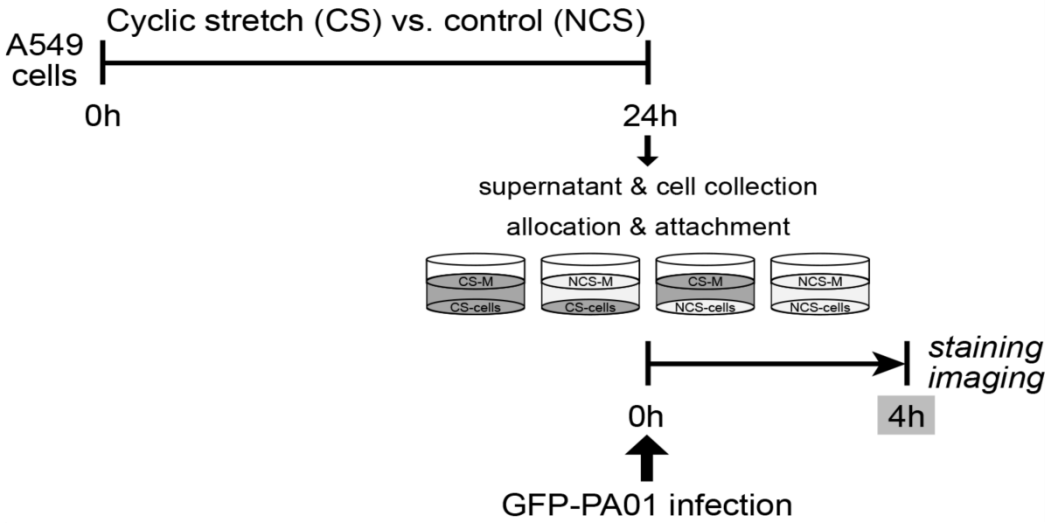

Figure 4: Experimental design of the in vitro experiment. A549 cells were exposed to either cyclic stretch (CS) or non-stretched (NCS) conditions. A549 cells were then infected with GFP-PAO1 in stretched or non-stretched medium (M) (epithelial lining fluid) for 4 h, washed and cells/adhering bacteria were stained with Phalloidin, DAPI and anti-GFP for immunofluorescence.

2.2.2.6. Immunofluorescence microscopy

After washing, cells were fixed with 3 % PFA for 20 min at RT followed by three times of washing and permeabilization (1 % Triton X-100 (Sigma-Aldrich; USA), 15 min). Cells

were then washed once with PBS and blocked with 5 % rabbit serum (MerckKGaA; Germany) for 30 min. Subsequently, cells were stained with Alexa Fluor 546 Phalloidin (1:50 dilution, Thermo Fisher Scientific; Germany) overnight and then stained with secondary antibody (GFP Polyclonal Antibody, Alexa Fluor 488, 1:500 dilution, Thermo Fisher Scientific; Germany) overnight. The next day, cell nuclei were stained with 4′,6-Diamidino-2-phenylindole dihydrochloride (DAPI) (1: 10,000, Merck KGaA; Germany) for 10 min and maintained in sterile PBS at 4 °C until microscopic analysis. The Multiphoton Microscope LSM 780 (Carl Zeiss Microscopy GmbH; Germany) was used for microscopy. At least ten (3x3) tile scans were taken from each well to calculate the bacteria to cell ratio. Images were taken at 63x magnification.

2.2.2.7. Green fluorescent protein-*Pseudomonas aeruginosa* PAO1 growth experiments

To prepare acidified or alkalized media, hydrochloric acid (HCl) or sodium hydroxide (NaOH) was instilled into pre-warmed RPMI-1640 medium supplemented with 10 % FCS. Untreated medium served as control. The pH of media was measured as previously described. Prior to the experiment, PAO1 was inoculated and cultured as described earlier. The next day, two bacterial single colonies were inoculated into acidified, untreated and alkalized media, respectively, and bacteria were allowed to grow for 5 h at 37 °C with shaking. During shaking, the OD_{600} of bacterial suspension was measured every 30 min for the growth curve. For further experiments, 20 µL PAO1 suspension (described earlier) was added into acidified, untreated and alkalized media, respectively, at the MOI of 0.1, 1, 5 and 10, and incubated in a humidified incubator at 37 °C with 5 % CO_2 for 24 h. After incubation, serial dilution of each sample was performed. Thereafter, all diluted samples were plated on Columbia agar plates with 5 % sheep blood (BD

Bioscience; USA) and incubated at 37 °C and 5 % CO_2 overnight. CFUs were counted and calculated on the following day.

2.2.3. *Ex vivo* experiment

2.2.3.1. Isolated perfused mouse lung ventilation and imaging

Male SPF C57BL/6J mice (28-30 weeks; 29-31 g; Janvier; France) were intraperitoneally euthanized with ketamine (80 mg/kg) and xylazine (25 mg/kg). Subsequently, mice were subjected to tracheotomy, MV, sternotomy and cannulation of the pulmonary artery and left atrium. Mice were mechanically ventilated with the following ventilation settings:

- HVt ventilation

  Mice were ventilated for 2 h with a tidal volume of 20 mL/kg, respiratory rate of 90 per min, I:E of 1:2, FiO_2 of 21 % and PEEP of 0 cmH_2O.

- LVt ventilation

  Mice were ventilated for 2 h with a tidal volume of 9 mL/kg, respiratory rate of 150 per min, I:E of 1:2, FiO_2 of 21 % and PEEP of 0 cmH_2O.

During MV, lungs were constantly perfused with pre-warmed Hanks' balanced salts solution supplemented with 4 % BSA through the pulmonary artery catheter. After 2 hours, lungs with trachea were carefully extracted from the thorax. Subsequently, 50 µL of pH-sensitive indicator with red fluorescence (0.2 µg/µL, 1:5 dilution, Molecular Probes™ pHrodo™ Red Dextran, Thermo Fisher; Germany) was applied via the tracheotomy cannula using a high pressure syringe (model No.FMJ-250, Penn-Century; USA). Subsequently, lungs were carefully transferred to a microscope stage, inflated with the gas mixture (N_2 75 %, O_2 20 %, CO_2 5 %) and prepared for microscopy under constant pressure (18 mmHg). A Nikon upright spinning disk confocal S2 microscope and NIS-Elements AR V.5.21.02 software (Nikon; Japan) were used to capture images. At least 9

images from three independent experiments were analyzed. Images were taken at a magnification of 25x. Alveolar brightness was assessed with Fiji software (ImageJ; USA). Data were normalized in relation to the brightest alveolus of each scan and alveolar brightness was calculated. The numbers of alveoli for each intensity (0.1 to 1.0) were quantified.

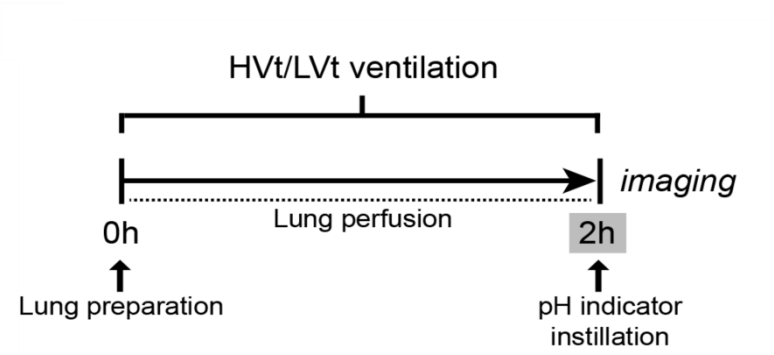

Figure 5: Experimental design of the ex vivo experiment. Mice lungs were isolated, perfused and mechanically ventilated for 2 h with high tidal volume (HVt 20 mL/kg) or low tidal volume (LVt 9 mL/kg). At the end of MV, a pH-sensitive indicator with red fluorescence (0.2 µg/µl, Molecular Probes™ pHrodo™ Red Dextran, Thermo Fisher, Berlin, Germany) was applied into the lungs using a micro-sprayer. Lungs were prepared for microscopy and alveolar brightness was calculated for evaluation of pH alterations.

2.2.4. Data analysis

Statistical analysis was performed using GraphPad Prism 8.00 (San Diego, CA, USA). Data are presented as mean with SEM or box-and-whisker plots depicting median, quartiles and range excluding outliers (open circles). Wilcoxon matched-pairs signed rank test or Mann-Whitney U test were used for comparison between two groups. Two-way ANOVA with Sidak's multiple comparisons test or multiple Mann-Whitney U tests followed by Bonferroni-Holm correction were applied for multiple comparisons. CFU data were logarithmized and one-way ANOVA with Sidak's multiple comparisons test was applied for data comparison. P-values of $P<0.05$ were considered statistically significant with $*P<0.05$, $**P<0.01$, $***P<0.001$.

3. Results

3.1. High tidal volume ventilation resulted in deterioration of pulmonary function

To assess whether VILI was successfully induced by HVt MV, we analyzed lung function at the beginning and termination of MV. During MV, lung function parameters (mean airway pressure (MAP)), static lung compliance, dynamic lung elastance and inspiratory capacity) were measured. HVt mice showed a constant and gradual increase of MAP, whereas the MAP of LVt mice remained stable (Figure 6 A). At the end of 4 h MV, mice subjected to HVt exhibited a significant increase in dynamic lung elastance and inspiratory capacity as well as a substantial decrease in static lung compliance compared with LVt mice. All lung function parameters of LVt mice were improved after MV (Figure 6 B-D).

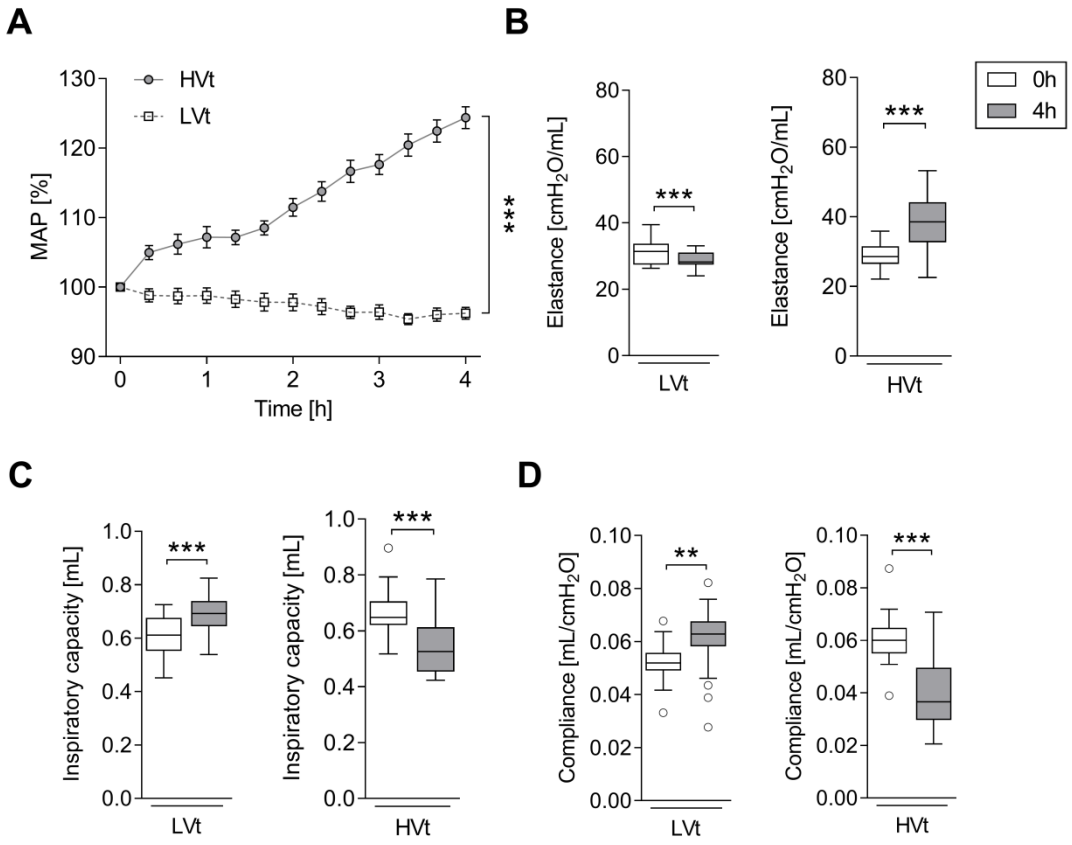

Figure 6: High tidal volume ventilation resulted in deterioration of pulmonary function. Mice were mechanically ventilated for 4 h with either high tidal volume (HVt 34 mL/kg), low tidal volume (LVt 9 mL/kg), or ventilated for 10 min using LVt ventilation settings (non-ventilated control group, NV). (**A**) Mean airway pressure (MAP) was constantly measured during MV. (**B**) Dynamic lung elastance, (**C**) inspiratory capacity and (**D**) static compliance were measured by recruitment maneuvers at the beginning (0 h) and end of ventilation (4 h). Data are expressed as either mean and SEM (**A**) or represented as boxplots (**B**-**D**) showing median, quartiles and ranges excluding outliers (open circles); n = 19 each group. (**A**), ***p<0.001 (two-way repeated measures ANOVA). (**B-D**), **p<0.01, ***p<0.001 (Wilcoxon matched-pairs signed rank test). *HVt,* high tidal volume; *LVt,* low tidal volume; *MAP,* mean airway pressure.

3.2. High tidal volume ventilation caused lower body temperature in subsequent *Pseudomonas aeruginosa* pneumonia

Next, this study investigated whether VILI induced by HVt MV could increase susceptibility to the onset and development of subsequent PA pneumonia. Twenty-four hours post infection, the body temperature of HVt-PA mice was significantly decreased compared to all other groups (Figure 7).

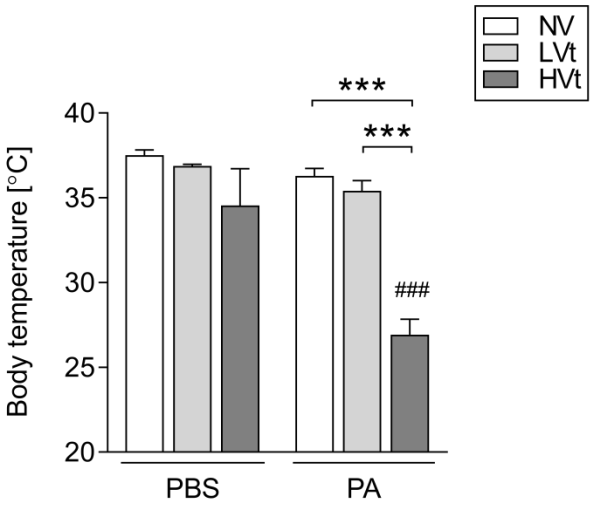

Figure 7: High tidal volume ventilation caused lower body temperature in subsequent Pseudomonas aeruginosa pneumonia. Mice were mechanically ventilated for 4 h with either high tidal volume (HVt 34 mL/kg), low tidal volume (LVt 9 mL/kg), or ventilated for 10min using LVt ventilation settings (non-ventilated control group, NV). After mechanical ventilation, mice were weaned from the ventilator and then infected with either PA103 or sterile PBS. After infection, mice were extubated and left spontaneously breathing until the endpoint. Body temperature was measured before MV and 24 h post infection. n = 5 (NV-PBS), n = 5 (LVt-PBS), n = 5 (HVt-PBS), n = 10 (NV-PA), n = 14 (LVt-PA), n = 10 (HVt-PA). Data are expressed as mean and SEM. ***p<0.001 between indicated groups, $^{###}p$<0.001 compared with HVt-PBS group (two-way ANOVA and Sidak's multiple comparisons test). *HVt,* high tidal volume; *LVt,* low tidal volume; *NV*, non-ventilated; *PA*, *Pseudomonas aeruginosa*; *PBS*, phosphate buffered saline.

3.3. High tidal volume ventilation led to more severe lung barrier disruption in subsequent *Pseudomonas aeruginosa* pneumonia

To evaluate the permeability of the lung barrier after MV and subsequent PA infection, the mouse albumin BALF/plasma ratio and total protein concentration in BALF were determined and analyzed. The results showed that the albumin BALF/plasma ratio was strongly increased in HVt-PA mice 24 h post infection as compared to all other groups (Figure 8). Notably, 24 h post infection, mice that were subjected to MV and subsequent PBS sham-infection did not show any significant changes of lung permeability (Figure 8).

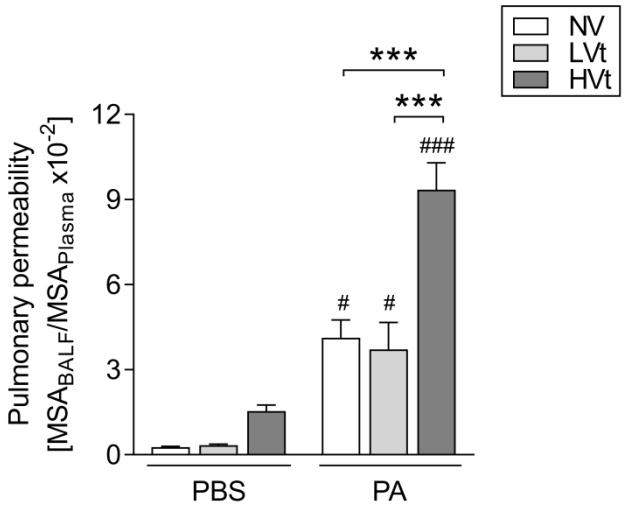

Figure 8: High tidal volume ventilation led to more severe lung barrier disruption in subsequent Pseudomonas aeruginosa pneumonia. Mice were mechanically ventilated for 4 h with either high tidal volume (HVt 34 mL/kg), low tidal volume (LVt 9 mL/kg), or ventilated for 10 min using LVt ventilation settings (non-ventilated control group, NV). After mechanical ventilation, mice were weaned from the ventilator and then infected with either PA103 or sterile PBS. After infection, mice were extubated and left spontaneously breathing until 24 h post infection. Albumin concentrations in BALF and plasma were determined by ELISA and the albumin BALF/plasma ratio was calculated. n = 6 (NV-PBS), n = 5 (LVt-PBS), n = 6 (HVt-PBS), n = 5 (NV-PA), n = 8 (LVt-PA), n = 6 (HVt-PA). Data are expressed as mean and SEM. ***p<0.001 between indicated groups, $^{\#}p$<0.05, $^{\#\#\#}p$<0.001 compared with respective PBS sham-infected group (two-way ANOVA and Sidak's multiple comparisons test). *BALF*, broncho-alveolar lavage fluid; *HVt,* high tidal volume; *LVt,* low tidal volume; *MSA*, mouse serum albumin; *NV*, non-ventilated; *PA*, *Pseudomonas aeruginosa*; *PBS*, phosphate buffered saline.

3.4. High tidal volume ventilation resulted in higher pulmonary bacterial load in subsequent *Pseudomonas aeruginosa* pneumonia

To quantify pulmonary bacterial growth, CFUs in BAL and lung homogenates were quantified and analyzed. Twenty-four hours post infection, HVt-PA mice showed significantly higher pulmonary CFU counts as compared to all other groups (Figure 9 A-B).

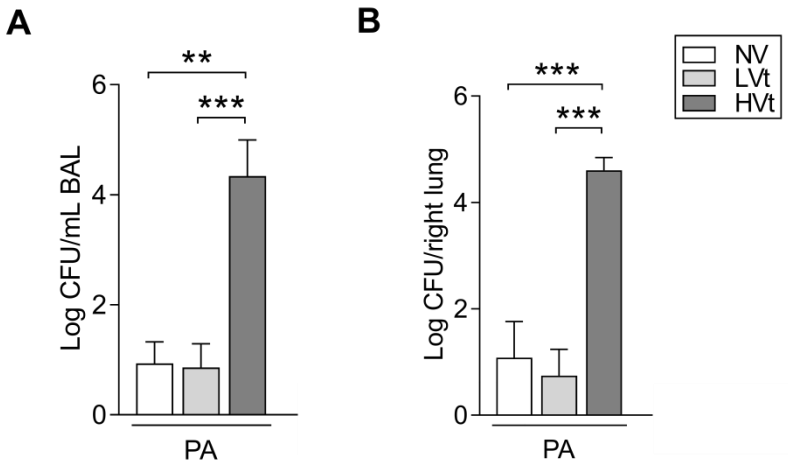

Figure 9: High tidal volume ventilation resulted in higher pulmonary bacterial load in subsequent Pseudomonas aeruginosa pneumonia. Mice were mechanically ventilated for 4 h with either high tidal volume (HVt 34 mL/kg), low tidal volume (LVt 9 mL/kg), or ventilated for 10 min using LVt ventilation settings (non-ventilated control group, NV). After mechanical ventilation, mice were weaned from the ventilator and then infected with either PA103 or sterile PBS. After infection, mice were extubated and left spontaneously breathing until the endpoint. CFUs in BAL (**A**) and lung homogenates (**B**) were determined and logarithmized. n = 5 (NV-PA), n = 9 (LVt-PA), n = 6 (HVt-PA). Data are expressed as mean and SEM. ***p*<0.01, ****p*<0.001 between indicated groups (one-way ANOVA and Sidak's multiple comparisons test). *BAL*, broncho-alveolar lavage; *CFU*, colony forming units; *HVt,* high tidal volume; *LVt,* low tidal volume; *NV*, non-ventilated; *PA*, *Pseudomonas aeruginosa*; *PBS*, phosphate buffered saline.

3.5. High tidal volume ventilation contributed to the increase in pulmonary cytokine and chemokine levels in subsequent *Pseudomonas aeruginosa* pneumonia

To characterize the pulmonary inflammation caused by MV and subsequent PA infection, concentrations of inflammatory cytokines (Figure 10 A) and chemokines (Figure 10 B) in BALF were determined and analyzed. Twenty-four hours post infection, a significant increase in cytokines (IL-6, IL-1β, IL-10 and IL-1α) and chemokines (CXCL-1, MCP-1, MIP-1α, MIP-1β, eotaxin and CXCL-5) was detected only in HVt-PA mice (Figure 10 A-

B). The levels of IFN-γ and GM-CSF in BALF were not changed (Figure 10 A). In PBS sham-infection groups, MV did not result in any significant release of pulmonary inflammatory cytokines and chemokines (Figure 10 A-B).

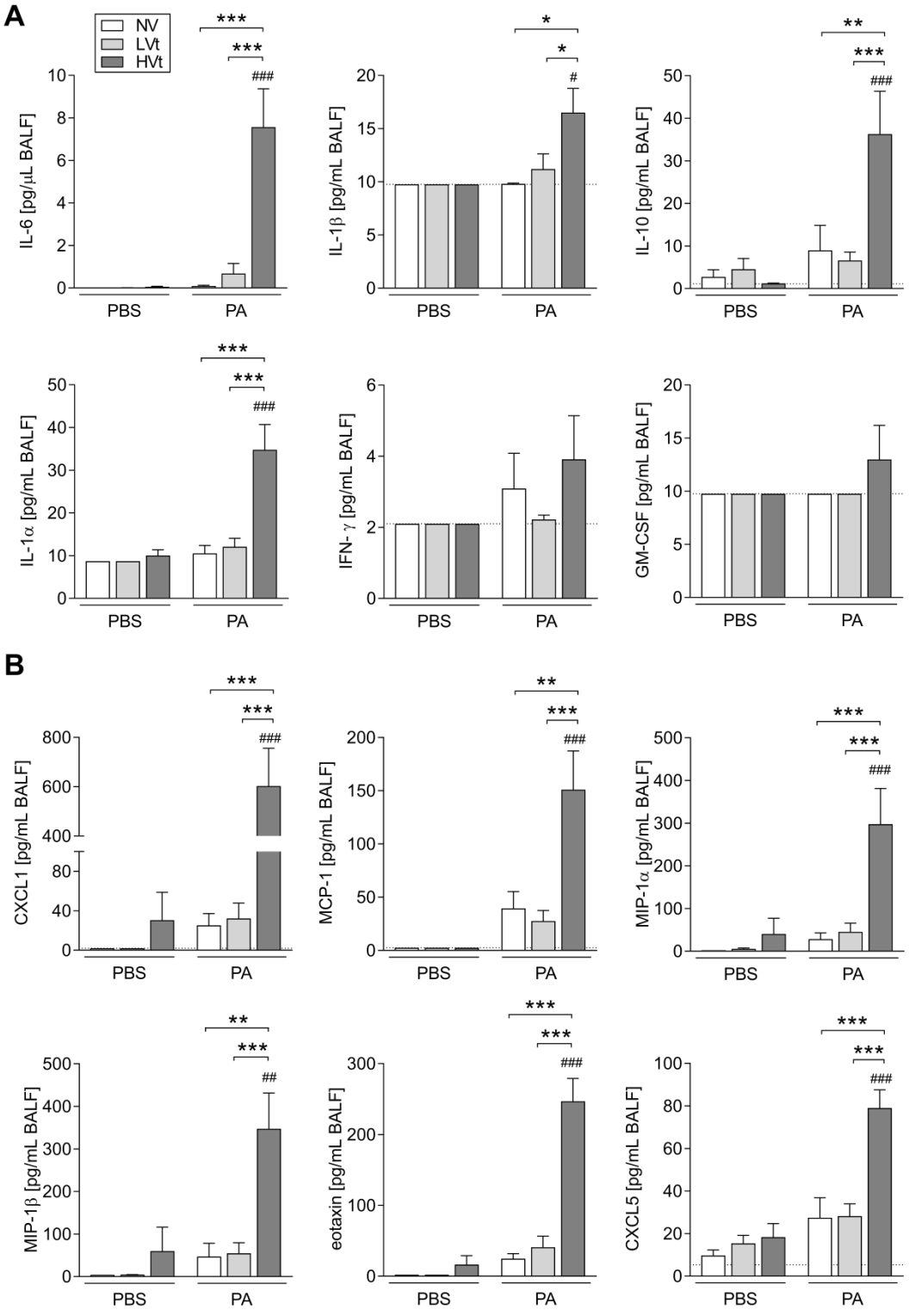

Figure 10: High tidal volume ventilation contributed to the increase in pulmonary cytokine and chemokine levels in subsequent Pseudomonas aeruginosa pneumonia. Mice were mechanically ventilated for 4 h with either high tidal volume (HVt 34 mL/kg), low tidal volume (LVt 9 mL/kg), or ventilated for 10 min using LVt ventilation settings (non-ventilated control group, NV). After mechanical ventilation, mice were weaned from the ventilator and then infected with either PA103 or sterile PBS. After infection, mice were extubated and left spontaneously breathing until the endpoint. Inflammatory cytokines (**A**) and chemokines (**B**) in BALF were measured using the multiplex bead-based immunoassay technique. n = 6 (NV-PBS), n = 5 (LVt-PBS), n = 6 (HVt-PBS), n = 5 (NV-PA), n = 9 (LVt-PA), n = 6 (HVt-PA). Data are expressed as mean and SEM. **p*<0.05, ***p*<0.01, ****p*<0.001 between indicated groups, $^{\#}p$<0.05, $^{\#\#}p$<0.01, $^{\#\#\#}p$<0.001 compared with respective PBS sham-infected group (two-way ANOVA and Sidak's multiple comparisons test). *BALF*, broncho-alveolar lavage fluid; *CXCL*, C-X-C motif chemokine ligand; *GM-CSF*, granulocyte-macrophage colony-stimulating factor*; HVt,* high tidal volume; *IFN*, interferon; *IL*, interleukin; *LVt,* low tidal volume*; MCP,* monocyte chemoattractant protein*; MIP,* macrophage inflammatory protein*; NV,* non-ventilated*; PA, Pseudomonas aeruginosa; PBS,* phosphate buffered saline.

3.6. High tidal volume ventilation led to increased pulmonary gene expression of inflammatory mediators in subsequent *Pseudomonas aeruginosa* pneumonia

To assess gene expression of inflammatory mediators caused by MV and subsequent PA infection, relative mRNA levels of inflammatory cytokines and chemokines were calculated and analyzed. Twenty-four hours post infection, mRNA expression of IL-6 and IL-1α was significantly elevated in HVt-PA mice and a trend towards increasing levels of MCP-1, IL-10, IL-1β and CXCL-5 was observed in the HVt-PA group (Figure 11).

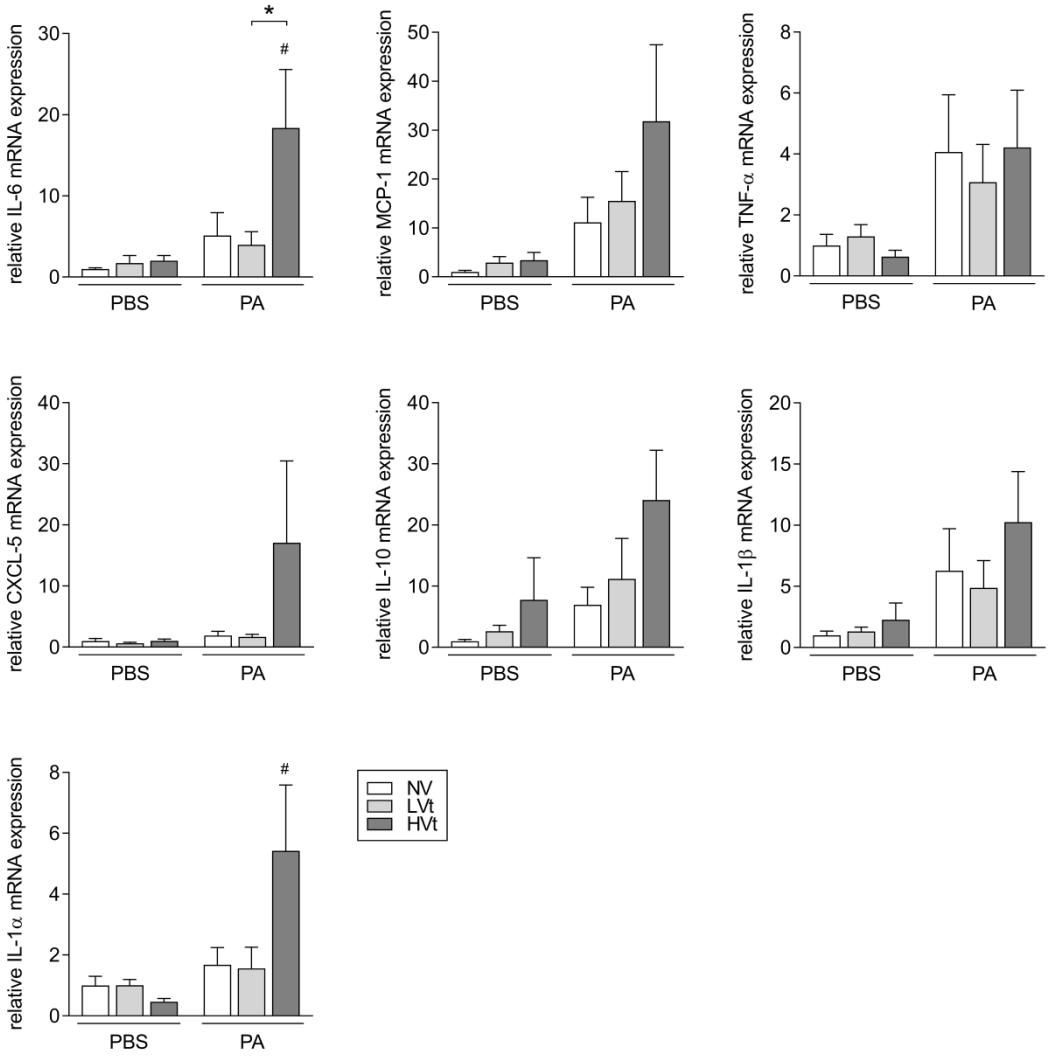

Figure 11: High tidal volume ventilation led to increased pulmonary gene expression of inflammatory mediators in subsequent Pseudomonas aeruginosa pneumonia. Mice were mechanically ventilated for 4 h with either high tidal volume (HVt 34 mL/kg), low tidal volume (LVt 9 mL/kg), or ventilated for 10 min using LVt ventilation settings (non-ventilated control group, NV). After mechanical ventilation, mice were weaned from the ventilator and then infected with either PA103 or sterile PBS. After infection, mice were extubated and left spontaneously breathing until the endpoint. Lungs were isolated for mRNA expression analyses by quantitative RT-PCR. Relative quantification of mRNA was performed using the comparative Ct method. n = 4 - 6 (NV-PBS), n = 5 (LVt-PBS), n = 6 (HVt-PBS), n = 4 (NV-PA), n = 7 - 8 (LVt-PA), n = 5 (HVt-PA). Data are expressed as mean and SEM. *p<0.05 between indicated groups; $^{\#}p$<0.05, compared with respective PBS sham-infected group (two-way ANOVA and Sidak's multiple comparisons test). *CXCL,* C-X-C motif chemokine Ligand*; HVt,* high tidal volume; *IL*, interleukin*; LVt,* low tidal volume; *MCP,* monocyte chemoattractant protein*; NV*, non-ventilated; *PA*, *Pseudomonas aeruginosa*; *PBS*, phosphate buffered saline; *TNF,* tumor necrosis factor.

3.7. Mechanical ventilation and subsequent *Pseudomonas aeruginosa* infection led to increased pulmonary polymorphonuclear cell recruitment

To characterize the innate immune response evoked by MV and subsequent infection, numbers of polymorphonuclear cells (PMNs) and alveolar macrophages in BAL and lung homogenates were differentiated and quantified using flow cytometry. Compared to HVt-PBS sham-infected mice, significant higher PMNs counts were detected in HVt-PA mice in both BAL and lung homogenates (Figure 12).

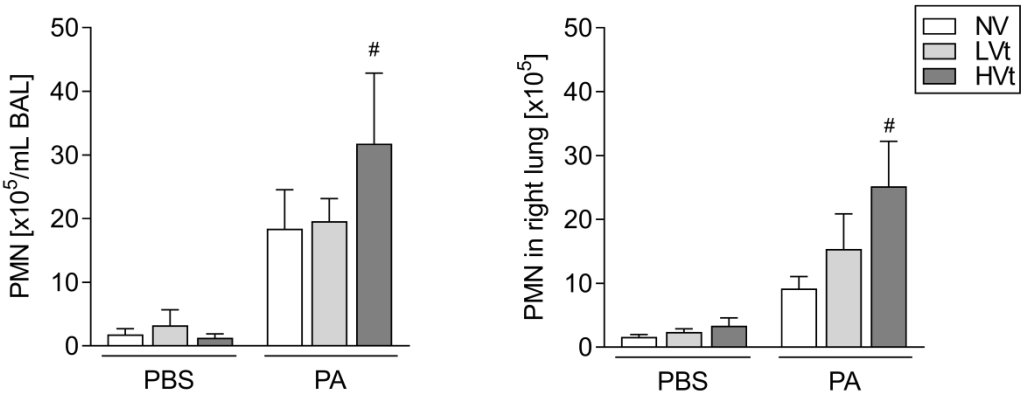

Figure 12: Mechanical ventilation and subsequent Pseudomonas aeruginosa infection led to increased pulmonary polymorphonuclear cell recruitment. Mice were mechanically ventilated for 4 h with either high tidal volume (HVt 34 mL/kg), low tidal volume (LVt 9 mL/kg), or ventilated for 10 min using LVt ventilation settings (non-ventilated control group, NV). After mechanical ventilation, mice were weaned from the ventilator and then infected with either PA103 or sterile PBS. After infection, mice were extubated and left spontaneously breathing until the endpoint. Numbers of polymorphonuclear cells in BAL and lung homogenates were differentiated and quantified by flow cytometry. n = 6 (NV-PBS), n = 5 (LVt-PBS), n = 5 (HVt-PBS), n = 5 (NV-PA), n = 9 (LVt-PA), n = 6 (HVt-PA). Data are expressed as mean and SEM. $^{\#}p<0.05$, compared with respective PBS sham-infected group (two-way ANOVA and Sidak's multiple comparisons test). *BAL*, broncho-alveolar lavage*; HVt,* high tidal volume; *LVt,* low tidal volume; *NV*, non-ventilated; *PA*, *Pseudomonas aeruginosa*; *PBS*, phosphate buffered saline*; PMN*, polymorphonuclear cells.

3.8. High tidal volume ventilation led to increased histopathologic signs of lung injury in subsequent *Pseudomonas aeruginosa* pneumonia

To evaluate the severity of PA VAP on the tissue level, lung sections were stained with hematoxylin and eosin. Histological examination of whole lung sections showed a more severe lung injury in HVt-PA mice (representative images are shown in Figure 13 A). In addition, HVt-PA mice presented a significantly higher percentage of lung area affected by infection, which was associated with an increased lung inflammation score (Figure 13 B). Specifically, significantly higher score values for neutrophil infiltration, hemorrhage, perivascular edema, alveolar wall damage and alveolar edema were observed in the HVt-PA group compared to all other groups (Figure 13 C). In addition, both the HVt-PA and LVt-PA groups had increased severity of alveolar edema (Figure 13 C). Within the three infected groups, no difference was observed regarding macrophage infiltration (Figure 13 C). Representative images from HVt-PA and LVt-PA mice presenting histopathologic signs of lung injury are shown in Figure 13 D.

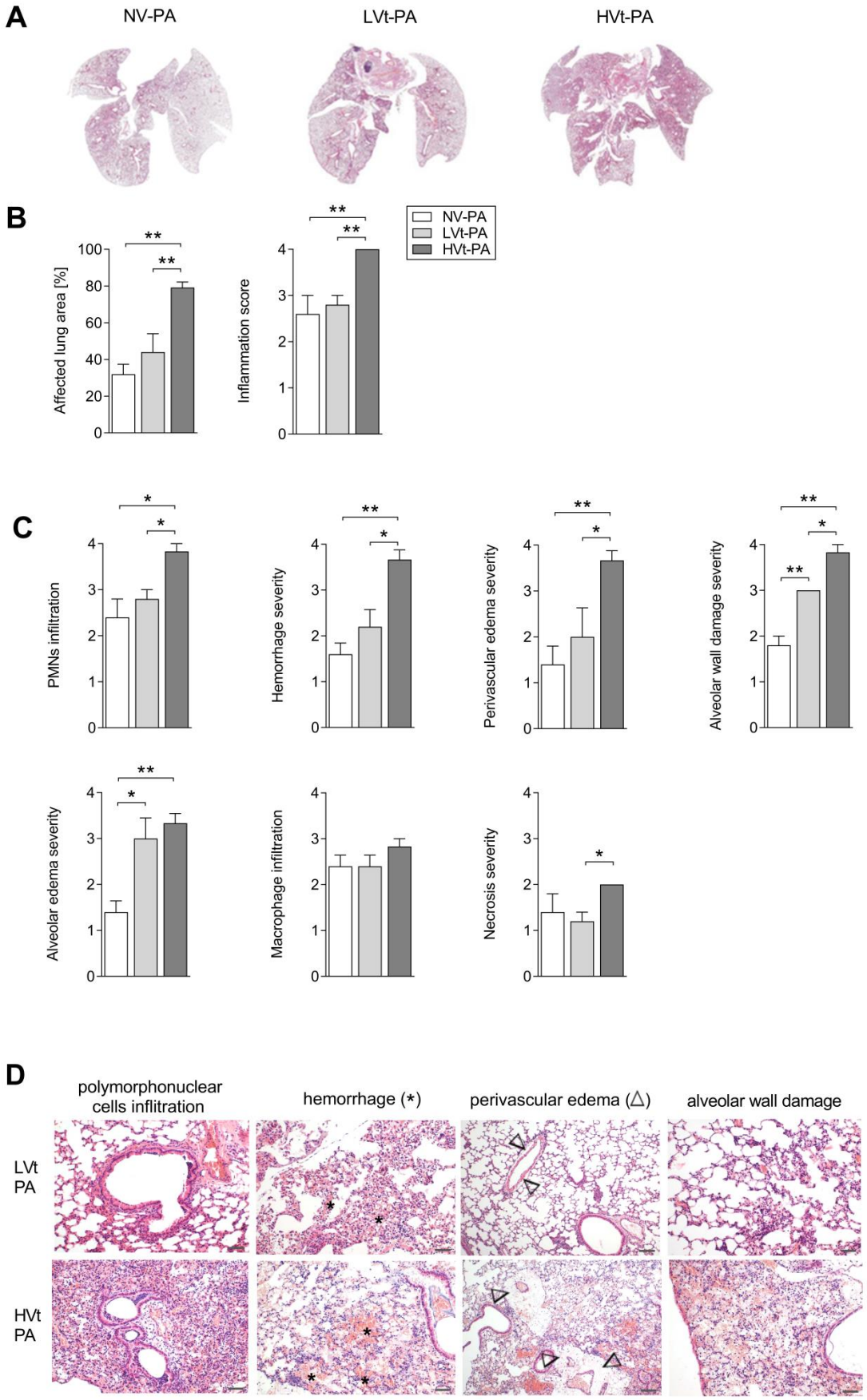
A
NV-PA
LVt-PA
HVt-PA
B
NV-PA
LVt-PA
HVt-PA
Affected lung area [%]
Inflammation score
C
PMNs infiltration
Hemorrhage severity
Perivascular edema severity
Alveolar wall damage severity
Alveolar edema severity
Macrophage infiltration
Necrosis severity
D
polymorphonuclear cells inflitration
hemorrhage (*)
perivascular edema (△)
alveolar wall damage
LVt PA
HVt PA

Figure 13: High tidal volume ventilation led to increased histopathologic signs of lung injury in subsequent Pseudomonas aeruginosa pneumonia. Mice were mechanically ventilated for 4 h with either high tidal volume (HVt 34 mL/kg), low tidal volume (LVt 9 mL/kg), or ventilated for 10 min using LVt ventilation settings (non-ventilated control group, NV). After mechanical ventilation, mice were weaned from the ventilator and then infected with either PA103 or sterile PBS. After infection, mice were extubated and left spontaneously breathing until the endpoint. Paraffin-embedded lung sections were stained with hematoxylin and eosin. (**A**) Representative images of whole lung sections of the respective infected group. (**B**) The percentage of affected lung area and total lung inflammation scores were determined. (**C**) Lung injury assessment by scoring of polymorphonuclear cell infiltration, hemorrhage, perivascular edema, alveolar wall damage, alveolar edema, macrophages infiltration and necrosis severity. All scoring parameters were rated as 0: nonexistent, 1: minimal, 2: mild, 3: moderate, 4: severe. In (**B**) and (**C**), n = 5 (NV-PA), n = 5 (LVt-PA), n = 6 (HVt-PA). **p*<0.05, ***p*<0.01 (multiple Mann-Whitney U tests with Bonferroni-Holm correction for multiple comparisons). *HVt,* high tidal volume; *LVt,* low tidal volume; *NV*, non-ventilated; *PA*, *Pseudomonas aeruginosa*; *PBS*, phosphate buffered saline*; PMN,* polymorphonuclear cells*.*

3.9. High tidal volume ventilation resulted in plasma cytokine and chemokine elevation in subsequent *Pseudomonas aeruginosa* pneumonia

To quantify the systemic inflammatory response resulting from MV and subsequent PA infection, inflammatory cytokines and chemokines in plasma were measured and analyzed. Twenty-four hours post infection, HVt-PA mice had significantly higher plasma levels of IL-6, TNF-α, MCP-1 and CXCL-1 compared with all other groups (Figure 14 A-B). No differences in the protein expression of IL-10 and IL-1β between the groups were detected. In addition, MV and subsequent PBS sham-infection did not cause any statistically relevant release of plasma inflammatory cytokines and chemokines at the endpoint (Figure 14 A-B).

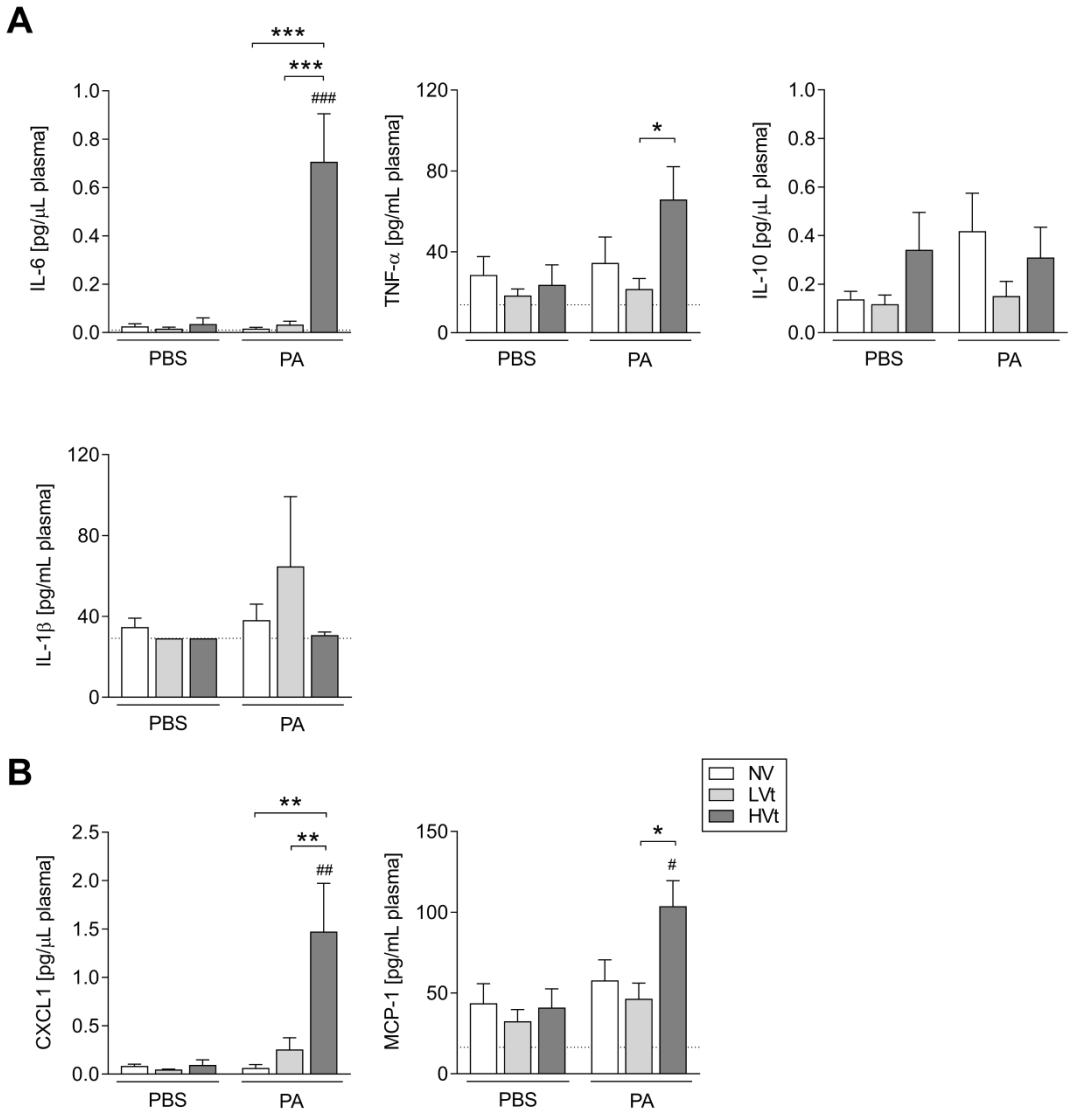

Figure 14: High tidal volume ventilation resulted in plasma cytokine and chemokine elevation in subsequent Pseudomonas aeruginosa pneumonia. Mice were mechanically ventilated for 4 h with either high tidal volume (HVt 34 mL/kg), low tidal volume (LVt 9 mL/kg), or ventilated for 10 min using LVt ventilation settings (non-ventilated control group, NV). After mechanical ventilation, mice were weaned from the ventilator and then infected with either PA103 or sterile PBS. After infection, mice were extubated and left spontaneously breathing until the endpoint. Inflammatory cytokines (**A**) and chemokines (**B**) in plasma were determined with multiplex bead-based immunoassay technique. Data are expressed as mean and SEM. n = 6 (NV-PBS), n = 5 (LVt-PBS), n = 6 (HVt-PBS), n = 5 (NV-PA), n = 9 (LVt-PA), n = 7 (HVt-PA). *p<0.05, **p<0.01, ***p<0.001 between indicated groups, $^{\#}p$<0.05, $^{\#\#}p$<0.01, $^{\#\#\#}p$<0.001 compared with respective PBS sham-infected group (two-way ANOVA and Sidak's multiple comparisons test). *CXCL,* C-X-C motif chemokine ligand*; HVt,* high tidal volume*; IL,* interleukin*; LVt,* low tidal volume*; MCP,* monocyte chemoattractant protein; *NV*, non-ventilated; *PA*, *Pseudomonas aeruginosa*; *PBS*, phosphate buffered saline; *TNF*, tumor necrosis factor.

3.10. High tidal volume ventilation caused an increase of blood polymorphonuclear cells in subsequent *Pseudomonas aeruginosa* pneumonia

Quantification of the cellular inflammatory response in blood revealed a significant number of neutrophils in the blood of HVt-PA mice compared with all other groups (Figure 15 A). No differences were observed in blood monocyte and lymphocyte counts upon MV and subsequent infection (Figure 15 B-C). Additionally, MV and subsequent PBS sham-infection did not lead to any significant changes in blood leukocyte counts (Figure 15 A-C).

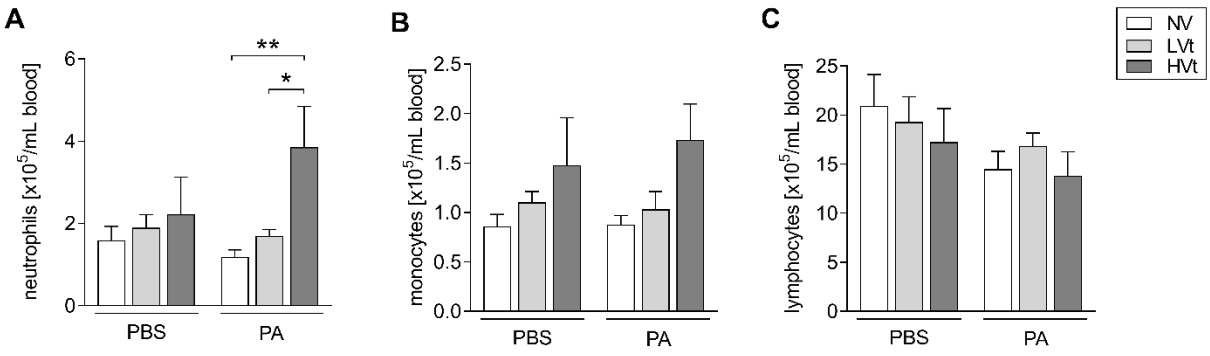

Figure 15: High tidal volume ventilation caused an increase in blood neutrophils in subsequent Pseudomonas aeruginosa pneumonia. Mice were mechanically ventilated for 4 h with either high tidal volume (HVt 34 mL/kg), low tidal volume (LVt 9 mL/kg), or ventilated for 10 min using LVt ventilation settings (non-ventilated control group, NV). After mechanical ventilation, mice were weaned from the ventilator and then infected with either PA103 or sterile PBS. After infection, mice were extubated and left spontaneously breathing until the endpoint. Neutrophils (**A**), monocytes (**B**) and lymphocytes (**C**) were differentiated and quantified using a scil Vet abc hematology analyzer. Data are expressed as mean and SEM. n = 6 (NV-PBS), n = 5 (LVt-PBS), n = 4 (HVt-PBS), n = 9 (NV-PA), n = 7 (LVt-PA), n = 5 (HVt-PA). *p<0.05, **p<0.01 between indicated groups (two-way ANOVA and Sidak's multiple comparisons test). *HVt,* high tidal volume; *LVt,* low tidal volume; *NV*, non-ventilated; *PA*, *Pseudomonas aeruginosa*; *PBS*, phosphate buffered saline.

3.11. High tidal volume ventilation caused systemic bacterial dissemination in subsequent *Pseudomonas aeruginosa* pneumonia

To assess whether MV may favor bacterial dissemination in subsequent PA pneumonia, CFUs in blood (Figure 16 A), liver homogenates (Figure 16 B) and spleen homogenates (Figure 16 C) were counted and analyzed. Surprisingly, 24 h post infection, systemic dissemination of PA was only detected in HVt-PA mice (Figure 16 A-C).

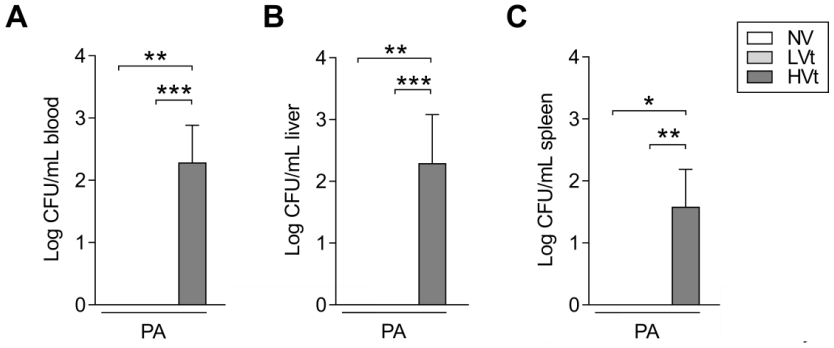

Figure 16: High tidal volume ventilation caused systemic bacterial dissemination in subsequent Pseudomonas aeruginosa pneumonia. Mice were mechanically ventilated for 4 h with either high tidal volume (HVt 34 mL/kg), low tidal volume (LVt 9 mL/kg), or ventilated for 10 min using LVt ventilation settings (non-ventilated control group, NV). After mechanical ventilation, mice were weaned from the ventilator and then infected with either PA103 or sterile PBS. After infection, mice were extubated and left spontaneously breathing until the endpoint. CFUs in blood (**A**), liver (**B**) and spleen (**C**) were determined and logarithmized. Data are expressed as mean and SEM. n = 5 (NV-PA), n = 9 (LVt-PA), n = 7 (HVt-PA). **p*<0.05, ***p*<0.01, ****p*<0.001 between indicated groups (one-way ANOVA and Sidak's multiple comparisons test). *CFU*, colony forming unit; *HVt,* high tidal volume; *LVt,* low tidal volume; *NV*, non-ventilated; *PA*, *Pseudomonas aeruginosa*; *PBS*, phosphate buffered saline.

3.12. High tidal volume ventilation contributed to the onset of extra-pulmonary organ dysfunction in subsequent *Pseudomonas aeruginosa* pneumonia

The systemic dissemination of bacteria and inflammatory mediators may lead to extra-pulmonary organ injury. To quantify liver and kidney dysfunction, plasma levels of aspartate aminotransferase (AST), total bilirubin, urea, triglyceride and albumin were determined. Twenty-four hours post infection, substantially increased plasma levels of AST, total bilirubin, urea and triglyceride were detected in HVt-PA mice compared to all other groups (Figure 17). Plasma albumin levels did not differ substantially within experimental groups (Figure 17).

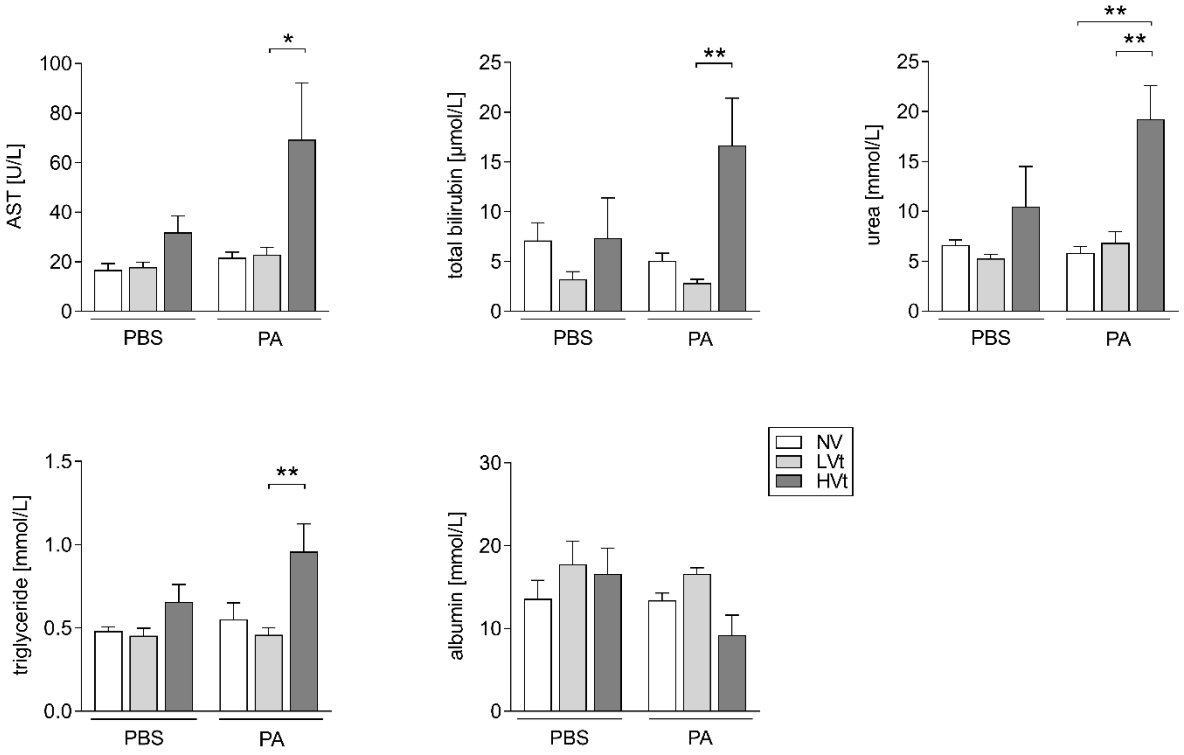

Figure 17: High tidal volume ventilation contributed to the onset of extra-pulmonary organ dysfunction in subsequent Pseudomonas aeruginosa pneumonia. Mice were mechanically ventilated for 4 h with either high tidal volume (HVt 34 mL/kg), low tidal volume (LVt 9 mL/kg), or ventilated for 10 min using LVt ventilation settings (non-ventilated control group, NV). After mechanical ventilation, mice were weaned from the ventilator and then infected with either PA103 or sterile PBS. After infection, mice were extubated and left spontaneously breathing until the endpoint. Plasma levels of AST, total bilirubin, urea, triglyceride and albumin were determined as parameters for liver and kidney function. Data are expressed as mean and SEM. n = 6 (NV-PBS), n = 5 (LVt-PBS), n = 6 (HVt-PBS), n = 5 (NV-PA), n = 9 (LVt-PA), n = 7 (HVt-PA). *p<0.05, **p<0.01 between indicated groups (two-way ANOVA

and Sidak's multiple comparisons test). *AST*, aspartate transaminase; *HVt,* high tidal volume; *LVt,* low tidal volume; *NV*, non-ventilated; *PA*, *Pseudomonas aeruginosa*; *PBS*, phosphate buffered saline.

3.13. Cyclic stretch led to alveolar lining fluid acidification and facilitated *Pseudomonas aeruginosa* adhesion

The CS model was employed to imitate the mechanical ventilation *in vitro* in order to assess acidification of the cell culture medium and investigate the relationship between ALF acidification and bacterial adhesion. A549 cells were subjected to CS for 24 h and compared to NCS controls. After CS, cells and supernatant from CS and NCS were collected respectively and then allocated into different groups for PAO1 infection (see experimental design Figure 4). Upon measurement, the pH of CS and NCS medium was 7.62 ± 0.09 and 7.30 ± 0.01, respectively (Figure 18 A). Four hours post PAO1 infection, a significantly increased bacteria/cell ratio was found only in cells cultured in CS medium (Figure 18 B), regardless of whether the cells were stretched or not (CS or NCS). Contrastingly, cells adapted in the NCS medium showed a lower bacteria/cell ratio (Figure 18 B). Representative images of CS cells adapted to CS medium (Figure 18 C) and NCS cells adapted to NCS medium (Figure 18 D) are shown.

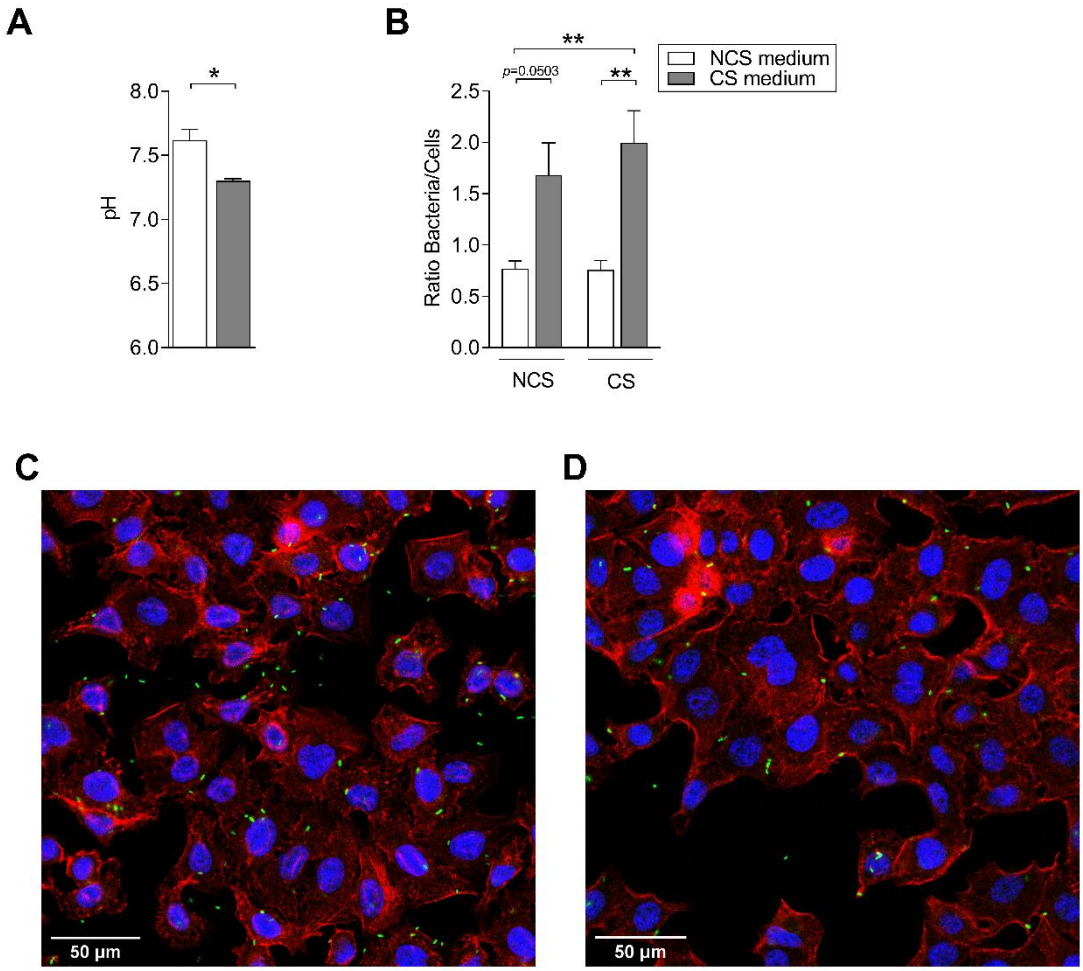

Figure 18: Cyclic stretch led to airway surface liquid acidification and facilitated Pseudomonas aeruginosa adhesion. A549 cells were subjected to cell stretch for 24 h. After CS, cells and cell-free supernatant were collected, respectively, and then allocated into different conditions for 4 h PAO1 infection. (**A**) pH of CS and NCS medium. (**B**) Data were analyzed from three independent experiments. Evaluation of n = 10 (3x3) tile scans for each condition for bacteria/cell ratio calculation. (**C**) Representative image of CS cells cultured in CS medium. (**D**) Representative image of NCS cells cultured in NCS medium. Data are expressed as mean and SEM. In (**A**), Mann-Whitney U test was used. In (**B**), two-way ANOVA and Sidak's multiple comparisons test were applied. *p<0.05, **p<0.01. *CS*, cell stretch; *NCS*, non-stretched.

3.14. High tidal ventilation led to a pH decrease of alveolar lining fluid in *ex vivo* mice lungs

It is well known that lower pH facilitates the growth of Gram-negative bacteria[123]. Next, we aimed to investigate in our model whether MV-induced acidification of ALF could be a possible cause for the increased severity of VAP. To asses ALF acidification *ex vivo*, a pH-sensitive indicator (pHrodo™ Red Dextran, Thermo Fisher, Germany) was applied intrapulmonary after 2h of mechanical ventilation (HVt or LVt) and fluorescence microscopy was used to observe pH alterations. In the HVt group, a pH decrease in the ALF led to an increase of red fluorescence and thus amplified the alveolar brightness. As shown in Figure 19 A, lungs subjected to HVt had increased numbers of alveoli with a higher relative brightness (from 0.4 to 0.9) as compared with LVt ventilated lungs, indicating that HVt led to a strong pH decrease in the ALF. Representative images of HVt and LVt lungs stained with pH indicator are shown in Figure 19 B.

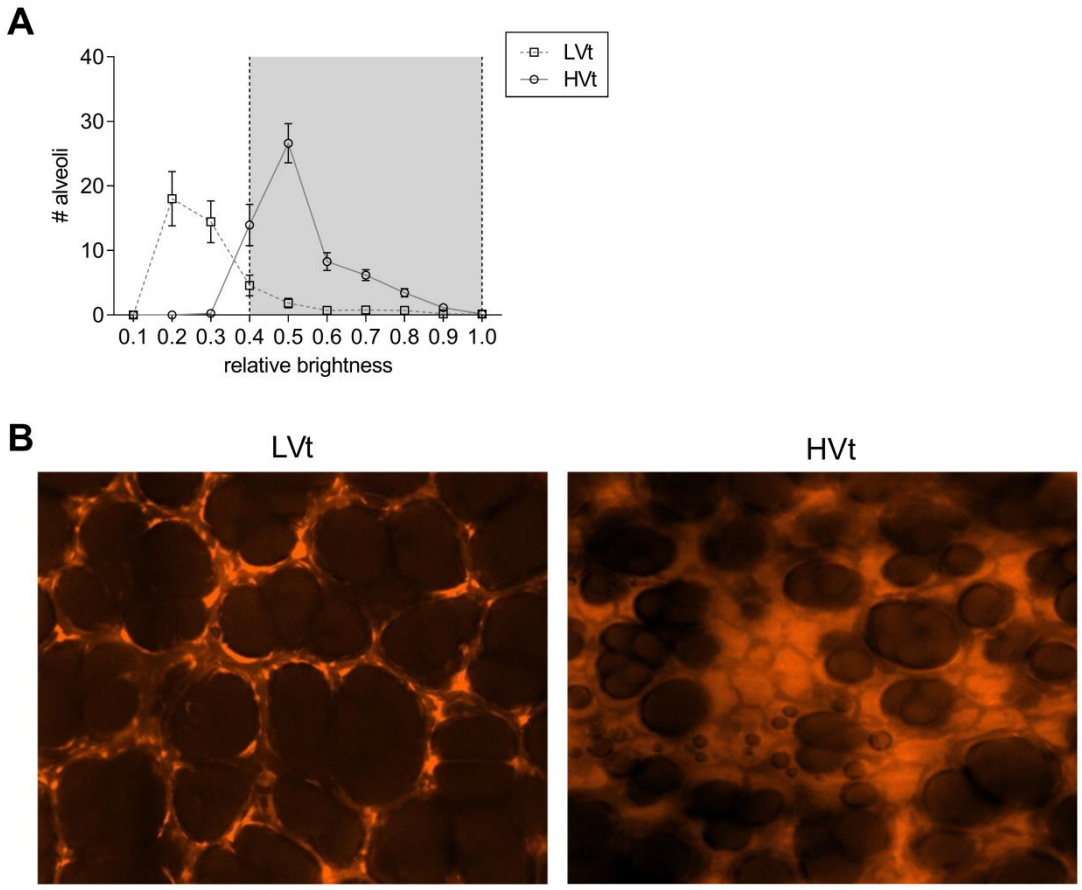

Figure 19: High tidal volume ventilation led to a pH decrease of alveolar lining fluid in ex vivo mice lungs. Ex vivo mice lungs were perfused and mechanically ventilated for 2 h with either high tidal volume (HVt 20 mL/kg) or low tidal volume (LVt 9 mL/kg). At the termination of MV, a pH-sensitive indicator with red fluorescence (Molecular Probes™ pHrodo™ Red Dextran, Thermo Fisher, Berlin, Germany) was applied into lungs using a micro-sprayer and the pH alterations of alveolar lining fluid were observed under the microscopy at constant pressure (18 mmHg). (**A**) Alveolar brightness was determined and normalized in relation to the brightest alveolus of each scan and the numbers of alveoli for each intensity were calculated. Evaluation of relative alveolar brightness was performed from tile scans (3x3) from three independent experiments. (**B**) Representative images of pH indicator stained lungs that were subjected to LVt and HVt ventilation, respectively. *HVt*, high tidal volume; *LVt*, low tidal volume.

3.15. Medium acidification promoted growth of *Pseudomonas aeruginosa*

To investigate the effects of pH decrease or acidification of the culture medium on bacterial growth, the medium was either artificially acidified with HCl or alkalized with

NaOH. The pH of the acidified, untreated and alkalized medium was 6.92 ± 0.05, 7.41 ± 0.03 and 7.96 ± 0.03, respectively (Figure 20 A). Twenty-four hours post incubation, substantially higher OD values were detected in acidified medium compared with PA incubated in alkalinized and untreated medium at all MOIs (Figure 20 B). In addition, bacterial growth experiments in liquid culture showed that PA incubated in acidified medium presented faster growth (Figure 20 C).

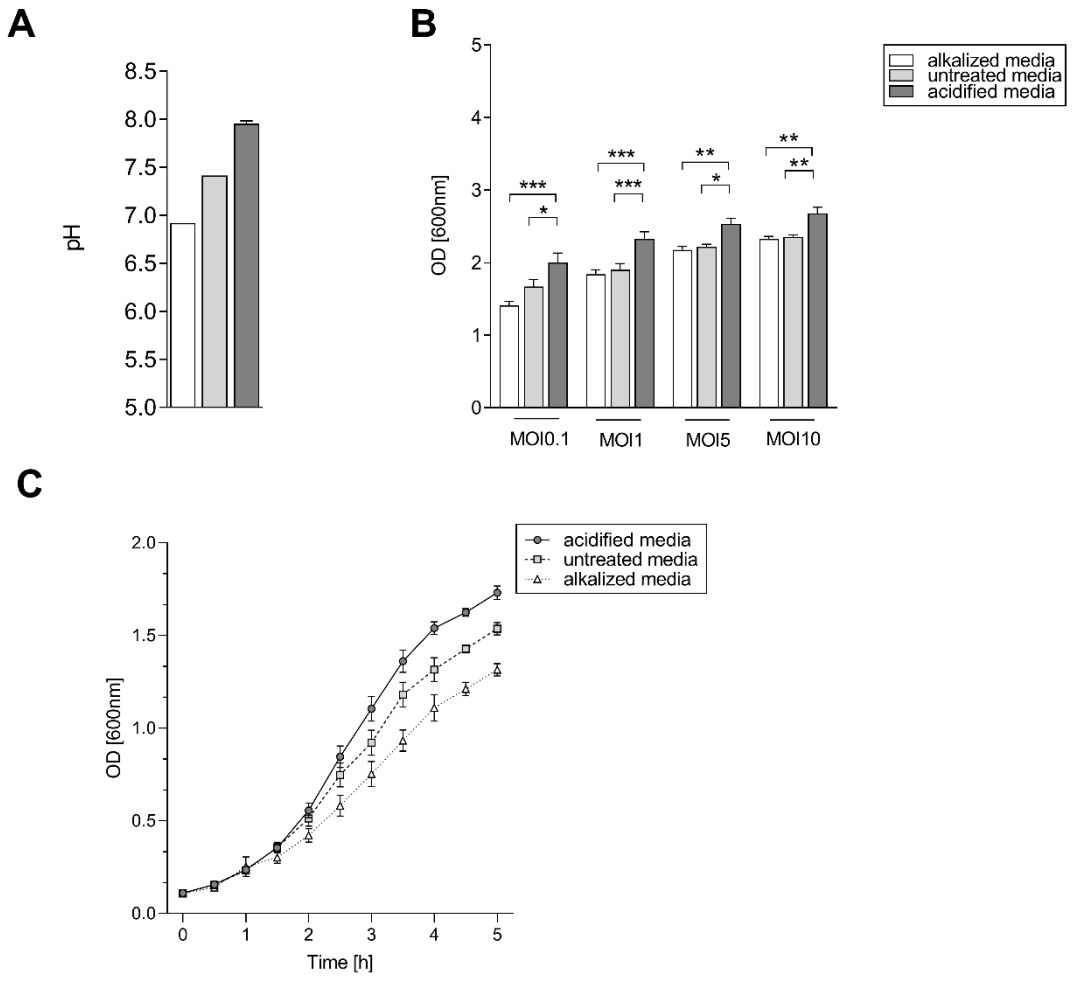

Figure 20: Medium acidification promoted growth of Pseudomonas aeruginosa. For the GFP-PAO1 growth experiments, HCl and NaOH were used to prepare acidified and alkalized medium. (**A**) pH of treated medium and untreated medium. (**B**) Twenty-four hours post PAO1 incubation at different MOIs, ODs of treated and untreated media were measured. ODs were measured from six independent experiments. (**C**) Growth curves of GFP-PAO1 in RPMI-1640 medium with different pHs. Dynamic growth curves measurement was from six independent experiments. Data are expressed as mean

and SEM. *p<0.01, **p<0.01, ***p<0.001 between indicated groups (two-way ANOVA and Sidak's multiple comparisons test). *OD*, optical density.

4. Discussion

Lung infections are one of the most common diseases worldwide and insufficient attention has been paid to this public health problem. Among them, VAP is the most common hospital-acquired lung infection in the ICU [128] and characterized by high incidence and mortality in ICU patients and particularly in subjects with ARDS [9, 13, 14].

As one of the complications of mechanical ventilation (MV), VILI is a major contributor for the onset of ARDS [73, 95]. Nevertheless, few studies have examined pathophysiological and immunological associations between VILI and subsequent pneumonia, and possible mechanistic connections between VILI and VAP are poorly understood. By establishing a new murine VAP model that mimics human pathology, this study aimed to examine how MV contributes to the onset and progression of VAP. Exposing mice to short-term HVt ventilation, a procedure widely used to induce VILI and mimic ARDS in healthy laboratory animals [129, 130, 77], it was shown that mechanical overventilation-induced VILI enhances the susceptibility and severity to subsequent PA pneumonia, including extra-pulmonary bacterial dissemination. Using additional *in vitro* and *ex vivo* models, it was shown that VILI-induced alveolar lining fluid acidification is a critical factor in our model, leading to increased proliferation of pulmonary bacteria.

4.1. High tidal volume ventilation led to the onset of ventilation-induced lung injury

As an important driver of VILI, mechanical overventilation can increase lung stress and strain, leading to pulmonary edema, alveolar rupture and alveolar-capillary barrier

disruption [79]. VILI is characterized by increased alveolar-capillary permeability and resulting changes in lung function (e.g., lung elastance) can indicate the development of VILI [79, 131, 132]. In the present work, mice subjected to 4 h HVt ventilation exhibited a significant increase in dynamic lung elastance compared with the LVt group, in line with our previous murine VILI models [77] and comparable with results from Cressoni et al. in porcine VILI models [133]. Similar to prior findings from our lab [77], the decrease in lung compliance was proportional to the severity of VILI upon HVt ventilation. Furthermore, the lung injury in the employed model met the American Thoracic Society criteria on acute lung injury (ALI) in animals [132], including the evidence of alveolar barrier function impairment and pulmonary function deterioration. Taken together, the results show that VILI was successfully induced in our model of orotracheal intubation and HVt ventilation. In contrast to previous studies that found increased neutrophil influx and activation during VILI [77, 134, 135], in the model examined in our study, alveolar-capillary barrier permeability and levels of pulmonary inflammation (inflammatory mediators release and PMN recruitment) did not differ between mice subjected to MV and NV controls 24 h post MV. These discrepancies may be explained by different sampling times, as in the studies mentioned above, the sampling was carried out immediately after MV. PMNs [136, 137] and inflammatory mediators [138, 139, 140, 141] are expected to be lower 24 h after MV [142] because of their short half-life, and alveolar-capillary barrier leakage decreases as lung injury resolution progresses.

4.2. High tidal volume ventilation contributed to increased susceptibility and severity in subsequent *Pseudomonas aeruginosa* pneumonia

It is widely recognized that hypothermia is a typical symptom of severe disease in murine pneumonia models [143, 144]. In the current study, mice subjected to HVt and subsequent PA infection had a significantly lower body temperature than all other groups, indicating enhanced pneumonia severity.

It is well known that pneumonia is one of the common causes of ALI or ARDS [145], which are characterized by increased alveolar-capillary permeability [146]. Similarly to the findings of Tsay and colleagues [117], a substantial increase in alveolar-capillary permeability was found in HVt-PA mice 24 h post infection. In LVt-PA and NV-PA groups, only a mild increase in alveolar-capillary permeability was detected, accounting for the fact that bacterial infection *per se* can partially impair the integrity of the alveolar-capillary barrier [147]. Works by Azghani et al. pointed out that PA elastase and exotoxin A may disrupt tight junctions between epithelial cells and lead to an increase in lung epithelial permeability [148, 48]. We thus deduced that both factors (injurious ventilation and PA infection) contribute to the aggravation of alveolar-capillary permeability and thereby pneumonia severity.

4.3. High tidal volume ventilation promoted increased pulmonary inflammation and lung injury in subsequent *Pseudomonas aeruginosa* pneumonia

A strong elevation of pulmonary inflammatory cytokines (IL-6, IL-1β, IL-10 and IL-1α) and chemokines (CXCL-1, MCP-1, CXCL-5, MIP-1α and MIP-1β) was observed in the HVt-

PA mice. Similarly, in lung homogenates, an increasing trend in the gene expression of the respective proteins was found. Clinical studies have shown that the inflammatory cytokines IL-6 and IL-1β are strongly increased in VAP patients and could be potentially used as biomarkers to detect early VAP [149, 150]. Elevated MCP-1 levels, as detected in our model, are consistent with results from other models of murine PA pneumonia [151]. Moreover, despite the anti-inflammatory properties of IL-10 during pneumonia [152, 153], increased levels of IL-10 are also detected during acute inflammation and found useful for early detection of VAP [154]. In addition, this acute “cytokine storm”, particularly involving IL-6 and IL-10, is associated with higher mortality of pneumonia patients [155]. In summary, the substantial increase in inflammatory mediators in our model is in line with the findings of the above-mentioned clinical and experimental studies, showing the presence of pulmonary inflammation, particularly in mice infected with PA and subjected to HVt ventilation.

Interestingly, it has been shown that PA proliferation can be favored by IL-6 in a concentration-dependent manner [156]. Thus, the increased levels of pulmonary IL-6 detected in our model might have had an additional effect on PA growth. Accordingly, a substantially higher pulmonary bacterial load was detected in HVt-PA mice.

Consistent with our observations, HVt-PA mice were found to have a higher histopathological lung inflammation score, a higher percentage of lung area affected, and more signs of severe lung injury confirming histological characteristics like neutrophil infiltration and alveolar edema from other experimental VAP models [117, 116].

Taken together, HVt MV led to aggravation of subsequent pneumonia with increased pulmonary release of inflammatory mediators, higher pulmonary bacterial burden and histopathologic signs of lung injury.

4.4. High tidal volume ventilation contributed to pulmonary neutrophil recruitment in subsequent *Pseudomonas aeruginosa* pneumonia

Clinically and experimentally, one of the characteristic features of VAP is pulmonary neutrophil infiltration [117, 116, 157]. In the present work, increased numbers of neutrophils were found in both BAL and lung of all infection groups when compared to the respective PBS control groups, which is in line with the increased chemoattractant levels of CXCL-1, CXCL-5 and MIP-1, which have been shown to attract neutrophils during infection [158, 159, 160]. An impaired neutrophil function leads to decreased bacterial clearance capacity and increased mortality in pneumonia [161, 162]. Even instillation of a very low dose (10 to 100 CFU/mouse) of PA can result in fatal lung infection in neutropenic mice [163] .

Although neutrophil recruitment is indispensable for bacterial clearance, activated neutrophils may also aggravate disease severity by releasing neutrophil proteases and extracellular traps which are also found in VAP [164, 165]. Mikacenic and colleagues demonstrated that enhanced presence of neutrophil extracellular traps in BAL is correlated with higher pulmonary bacterial load and increased levels of alveolar inflammation [165]. In summary, although neutrophil recruitment is an indicator of bacterial infection and essential for bacterial clearance in our model, the deleterious effects of neutrophil activation may further aggravate lung injury.

4.5. High tidal volume ventilation promoted systemic inflammation and extra-pulmonary bacterial dissemination

In clinical studies, increased systemic levels of proinflammatory cytokines (IL-6 and TNF-α) were observed in VAP patients [149, 166]. Moreover, an elevated MCP-1 concentration in the circulation was found to be positively correlated with disease severity in VAP patients [167]. Similar to these observations, in the murine VAP model examined here, a systemic inflammatory reaction with a higher plasma concentration of IL-6, TNF-α, MCP-1 and CXCL-1 in the HVt-PA group was observed. In accordance with elevated plasma concentrations of the neutrophil chemoattractants MCP-1 and CXCL-1, elevated blood neutrophil counts in blood of HVt-PA mice were detected.

Furthermore, in line with the systemic inflammatory reaction, a systemic spread of bacteria was detected only in HVt PA mice. The increased alveolar-capillary permeability, resulting from HVt ventilation [79] and subsequent PA infection [48], may have contributed to bacterial translocation from the lung to extra-pulmonary organs. In addition, increased levels of IL-6 in blood may favor PA proliferation in the circulation and thereby contribute to extra-pulmonary PA dissemination.

As observed in experimental and clinical studies of VAP [116, 168], parameters of liver and kidney function deteriorated significantly in HVt-PA mice, suggesting that HVt MV led to increased disease severity including increased systemic inflammation, bacterial dissemination and extra-pulmonary organ dysfunction in subsequent PA pneumonia.

4.6. Ventilator-induced lung injury promoted subsequent *Pseudomonas aeruginosa* pneumonia by alveolar acidification

Mainly generated by alveolar epithelial cells [169], the ALF is an important contributor to pulmonary host defense against pathogen invasion [170]. A pH reduction of airway surface liquid may attenuate lung antimicrobial activity and thus impair the capacity of bacterial clearance as well as airway host defense [171, 172]. Interestingly, in patients with chronic inflammatory airway diseases colonized by PA, a lower pH was detected in their breath condensate [173]. While the study did not investigate whether the observed acidification was due to chronic inflammation or a preexisting condition promoting the following bacterial colonization, Torres and colleagues showed experimentally that the artificial acidification of the respiratory milieu via acid installation significantly contributed to increased acute PA pneumonia severity in mice [118]. Interestingly, examining EBC in a cohort of ALI and ARDS patients (subjected to mechanical ventilation), Gessner et al. provided evidence that these patients had a substantially lower pH compared to healthy volunteers [124], but again, studies examining whether this is an effect or more likely a predisposing factor for infection are lacking. Using cell cyclic stretch to imitate mechanical ventilation *in vitro*, Pugin and collaborators revealed the tripartite relationship between the cell stretch of airway epithelial cells, pH decrease and the growth of the Gram-negative bacterium *Escherichia coli* [123]. Although this observation showed that PA growth was favored by artificial medium acidification, it was unclear whether mechanical overventilation would lead to airway acidification that would promote bacterial proliferation and result in aggravation of VAP *in vivo*. Thus, using the established murine VAP model, the present study aimed to investigate whether the increased VAP severity *in vivo* was due to the promoted PA proliferation induced by airway acidification due to MV.

According with our hypothesis, a strong pH reduction of ALF was observed in mice subjected to HVt ventilation by using the *ex vivo* model to visualize pH changes of ALF induced by VILI. By exposing A549 cells to CS for 24 h, a significant acidification of the medium of stretched airway epithelial cells was observed, which agrees well with the observation *in vivo*. Moreover, a higher bacteria/cell ratio was found in cells cultured in stretch-acidified medium, regardless of whether the cells were stretched or not. Additional experiments proved that bacteria proliferated faster when inoculated in artificial acidified medium, demonstrating that the acidic milieu *per se* can favor bacterial proliferation. Considering all the results, the present study demonstrated that ALF acidification induced by mechanical overventilation can promote pulmonary bacterial growth, thereby increasing the susceptibility to, and severity of VAP. The aforementioned infection experiments with artificially acidified inoculation medium replicate similar characteristics in the severity of PA pneumonia, including pulmonary CFUs, neutrophils recruitment and cytokine release [118], which complements our results well. Interestingly, previous studies indicated that an acidic milieu increased the virulence and antibiotic tolerance of PA, emphasizing the critical importance of our findings for VAP patients [174, 175].

This study has some limitations. First, in contrast to the lung-protective ventilation strategy commonly used in the clinic, a higher tidal volume (34 mL/kg) was applied to establish lung overventilation in healthy animals, as has been performed in other studies. Second, VAP patients are continuously ventilated in the clinic as pneumonia progresses, whereas a short duration of ventilation was carried out in the animals because of the experimental conditions. Therefore, the long-term effects on immune functions, disease progression, as well as morbidity and mortality cannot be fully derived from our mouse model. Third,

the acidification induced by cell stretching is moderate compared with the artificially conditioned media for bacterial growth experiments. However, pH values were measured in the cell culture supernatant, suggesting that the actual acidification in the thin alveolar lining fluid may be more drastic *in situ*. Regardless, the present new model exhibits important clinical features of PA-VAP and allows researchers to investigate the complex mechanisms of MV-induced PA susceptibility and VAP onset.

5. Conclusion

In this study, mechanical overventilation was shown to be a critical factor in the onset and aggravation of VAP in a murine model, leading to systemic inflammation and dissemination of pulmonary bacteria to extra-pulmonary organs. Furthermore, it was demonstrated that the ALF acidification induced by mechanical overventilation enhanced pulmonary PA adhesion and growth. These results provide evidence that overventilation is a critical factor in the susceptibility of mice to subsequent PA pneumonia. The established murine VAP model may enable future studies to further investigate the molecular mechanisms of VAP pathogenesis and promote the development of novel therapeutics to reduce the incidence and severity of VAP in ICU patients.

6. Bibliography

1. Papazian L, Klompas M, Luyt CE. Ventilator-associated pneumonia in adults: a narrative review. *Intensive* Care Medicine. 2020 May;46(5):888-906. doi: 10.1007/s00134-020-05980-0.
2. van Vught LA, Klein Klouwenberg PM, Spitoni C, Scicluna BP, Wiewel MA, Horn J, Schultz MJ, Nürnberg P, Bonten MJ, Cremer OL, van der Poll T; MARS Consortium. Incidence, risk factors, and attributable mortality of secondary infections in the intensive care unit after admission for sepsis. JAMA. 2016 Apr 12;315(14):1469-79. doi: 10.1001/jama.2016.2691.
3. American Thoracic Society; Infectious Diseases Society of America. Guidelines for the management of adults with hospital-acquired, ventilator-associated, and healthcare-associated pneumonia. Am J Respir Crit Care Med. 2005 Feb 15;171(4):388-416. doi: 10.1164/rccm.200405-644ST.
4. Kalil AC, Metersky ML, Klompas M, Muscedere J, Sweeney DA, Palmer LB, Napolitano LM, O'Grady NP, Bartlett JG, Carratalà J, El Solh AA, Ewig S, Fey PD, File TM Jr, Restrepo MI, Roberts JA, Waterer GW, Cruse P, Knight SL, Brozek JL. Management of Adults With Hospital-acquired and Ventilator-associated Pneumonia: 2016 Clinical Practice Guidelines by the Infectious Diseases Society of America and the American Thoracic Society. Clin Infect Dis. 2016 Sep 1;63(5):e61-e111. doi: 10.1093/cid/ciw353.
5. Omeri AK, Okada F, Takata S, Ono A, Nakayama T, Ando Y, Sato H, Hiramatsu K, Mori H. Comparison of high-resolution computed tomography findings between Pseudomonas aeruginosa pneumonia and Cytomegalovirus pneumonia. Eur Radiol. 2014 Dec;24(12):3251-9. doi: 10.1007/s00330-014-3326-3.
6. Koulenti D, Tsigou E, Rello J. Nosocomial pneumonia in 27 ICUs in Europe: perspectives from the EU-VAP/CAP study. Eur J Clin Microbiol Infect Dis. 2017 Nov;36(11):1999-2006. doi: 10.1007/s10096-016-2703-z.
7. Dudeck MA, Horan TC, Peterson KD, Allen-Bridson K, Morrell G, Anttila A, Pollock DA, Edwards JR. National Healthcare Safety Network report, data summary for 2011, device-associated module. Am J Infect Control. 2013 Apr;41(4):286-300. doi: 10.1016/j.ajic.2013.01.002.
8. Vallecoccia MS, Dominedò C, Cutuli SL, Martin-Loeches I, Torres A, De Pascale G. Is ventilated hospital-acquired pneumonia a worse entity than ventilator-associated pneumonia? Eur Respir Rev. 2020 Aug 4;29(157):200023. doi: 10.1183/16000617.0023-2020.
9. Forel JM, Voillet F, Pulina D, Gacouin A, Perrin G, Barrau K, Jaber S, Arnal JM, Fathallah M, Auquier P, Roch A, Azoulay E, Papazian L. Ventilator-associated pneumonia and ICU mortality in severe ARDS patients ventilated according to a lung-protective strategy. Crit Care. 2012 Dec 12;16(2):R65. doi: 10.1186/cc11312.
10. Douglas, I. S. Pulmonary infections in critical/intensive care - Rapid diagnosis and optimizing antimicrobial usage. Curr Opin Pulm Med. 2017 May;23(3):198-203. doi: 10.1097/MCP.0000000000000366.

11. Bonell A, Azarrafiy R, Huong VTL, Viet TL, Phu VD, Dat VQ, Wertheim H, van Doorn HR, Lewycka S, Nadjm B. A Systematic Review and Meta-analysis of Ventilator-associated Pneumonia in Adults in Asia: An Analysis of National Income Level on Incidence and Etiology. Clin Infect Dis. 2019 Jan 18;68(3):511-518. doi: 10.1093/cid/ciy543.

12. Spalding MC, Cripps MW, Minshall CT. Ventilator-Associated Pneumonia: New Definitions. Crit Care Clin. 2017 Apr;33(2):277-292. doi: 10.1016/j.ccc.2016.12.009.

13. Cook DJ, Walter SD, Cook RJ, Griffith LE, Guyatt GH, Leasa D, Jaeschke RZ, Brun-Buisson C. Incidence of and risk factors for ventilator-associated pneumonia in critically ill patients. Ann Intern Med. 1998 Sep 15;129(6):433-40. doi: 10.7326/0003-4819-129-6-199809150-00002.

14. Gupta A, Agrawal A, Mehrotra S, Singh A, Malik S, Khanna A. Incidence, risk stratification, antibiogram of pathogens isolated and clinical outcome of ventilator associated pneumonia. Incidence, risk stratification, antibiogram of pathogens isolated and clinical outcome of ventilator associated pneumonia. Indian J Crit Care Med. 2011 Apr;15(2):96-101. doi: 10.4103/0972-5229.83015.

15. Melsen WG, Rovers MM, Koeman M, Bonten MJ. Estimating the attributable mortality of ventilator-associated pneumonia from randomized prevention studies. Crit Care Med. 2011 Dec;39(12):2736-42. doi: 10.1097/CCM.0b013e3182281f33.

16. Di Pasquale M, Ferrer M, Esperatti M, Crisafulli E, Giunta V, Li Bassi G, Rinaudo M, Blasi F, Niederman M, Torres A. Assessment of severity of ICU-acquired pneumonia and association with etiology. Crit Care Med. 2014 Feb;42(2):303-12. doi: 10.1097/CCM.0b013e3182a272a2.

17. Esperatti M, Ferrer M, Theessen A, Liapikou A, Valencia M, Saucedo LM, Zavala E, Welte T, Torres A. Nosocomial pneumonia in the intensive care unit acquired by mechanically ventilated versus nonventilated patients. Am J Respir Crit Care Med. 2010 Dec 15;182(12):1533-9. doi: 10.1164/rccm.201001-0094OC.

18. Rello J, Ollendorf DA, Oster G, Vera-Llonch M, Bellm L, Redman R, Kollef MH; VAP Outcomes Scientific Advisory Group. Epidemiology and outcomes of ventilator-associated pneumonia in a large US database. Chest. 2002 Dec;122(6):2115-21. doi: 10.1378/chest.122.6.2115.

19. Bailey KL, Kalil AC. Ventilator-Associated Pneumonia (VAP) with Multidrug-Resistant (MDR) Pathogens: Optimal Treatment? Curr Infect Dis Rep. 2015 Aug;17(8):494. doi: 10.1007/s11908-015-0494-5.

20. Luyt CE, Hékimian G, Koulenti D, Chastre J. Microbial cause of ICU-acquired pneumonia: Hospital-acquired pneumonia versus ventilator-associated pneumonia. Curr Opin Crit Care. 2018 Oct;24(5):332-338. doi: 10.1097/MCC.0000000000000526.

21. Huang Y, Jiao Y, Zhang J, Xu J, Cheng Q, Li Y, Liang S, Li H, Gong J, Zhu Y, Song L, Rong Z, Liu B, Jie Z, Sun S, Li P, Wang G, Qu J. Microbial Etiology and Prognostic Factors of Ventilator-associated Pneumonia: A Multicenter Retrospective Study in Shanghai. Clin Infect Dis. 2018 Nov 13;67(suppl_2):S146-S152. doi: 10.1093/cid/ciy686.

22. Chung DR, Song JH, Kim SH, Thamlikitkul V, Huang SG, Wang H, So TM, Yasin RM, Hsueh PR, Carlos CC, Hsu LY, Buntaran L, Lalitha MK, Kim MJ, Choi JY, Kim SI, Ko KS, Kang CI, Peck KR; Asian Network for Surveillance of Resistant Pathogens Study Group. High prevalence of multidrug-resistant nonfermenters in hospital-acquired pneumonia in Asia. Am J Respir Crit Care Med. 2011 Dec 15;184(12):1409-17. doi: 10.1164/rccm.201102-0349OC.

23. Martin-Loeches I, Povoa P, Rodríguez A, Curcio D, Suarez D, Mira JP, Cordero ML, Lepecq R, Girault C, Candeias C, Seguin P, Paulino C, Messika J, Castro AG, Valles J, Coelho L, Rabello L, Lisboa T, Collins D, Torres A, Salluh J, Nseir S; TAVeM study. Incidence and prognosis of ventilator-associated tracheobronchitis (TAVeM): A multicentre, prospective, observational study. Lancet Respir Med. 2015 Nov;3(11):859-68. doi: 10.1016/S2213-2600(15)00326-4.

24. Pulido MR, Moreno-Martínez P, González-Galán V, Fernández Cuenca F, Pascual Á, Garnacho-Montero J, Antonelli M, Dimopoulos G, Lepe JA, McConnell MJ, Cisneros JM; MagicBullet Working Group. Application of BioFire FilmArray Blood Culture Identification panel for rapid identification of the causative agents of ventilator-associated pneumonia. Clin Microbiol Infect. 2018 Nov;24(11):1213.e1-1213.e4. doi: 10.1016/j.cmi.2018.06.001.

25. Ibn Saied W, Mourvillier B, Cohen Y, Ruckly S, Reignier J, Marcotte G, Siami S, Bouadma L, Darmon M, de Montmollin E, Argaud L, Kallel H, Garrouste-Orgeas M, Soufir L, Schwebel C, Souweine B, Glodgran-Toledano D, Papazian L, Timsit JF; OUTCOMEREA Study Group. A Comparison of the Mortality Risk Associated with Ventilator-Acquired Bacterial Pneumonia and Nonventilator ICU-Acquired Bacterial Pneumonia. Crit Care Med. 2019 Mar;47(3):345-352. doi: 10.1097/CCM.0000000000003553.

26. Alvarez-Ortega C, Harwood CS. Responses of Pseudomonas aeruginosa to low oxygen indicate that growth in the cystic fibrosis lung is by aerobic respiration. Mol Microbiol. 2007 Jul;65(1):153-65. doi: 10.1111/j.1365-2958.2007.05772.x.

27. Hota S, Hirji Z, Stockton K, Lemieux C, Dedier H, Wolfaardt G, Gardam MA. Outbreak of Multidrug-Resistant Pseudomonas aeruginosa Colonization and Infection Secondary to Imperfect Intensive Care Unit Room Design . Infect Control Hosp Epidemiol. 2009 Jan;30(1):25-33. doi: 10.1086/592700.

28. Bergen GA, Toney JF. Infection versus colonization in the critical care unit. Crit Care Clin. 1998 Jan;14(1):71-90. doi: 10.1016/s0749-0704(05)70382-1.

29. Nguile-Makao M, Zahar JR, Français A, Tabah A, Garrouste-Orgeas M, Allaouchiche B, Goldgran-Toledano D, Azoulay E, Adrie C, Jamali S, Clec'h C, Souweine B, Timsit JF. Attributable mortality of ventilator-associated pneumonia: Respective impact of main characteristics at ICU admission and VAP onset using conditional logistic regression and multi-state models. Intensive Care Med. 2010 May;36(5):781-9. doi: 10.1007/s00134-010-1824-6.

30. Denis JB, Lehingue S, Pauly V, Cassir N, Gainnier M, Léone M, Daviet F, Coiffard B, Baron S, Guervilly C, Forel JM, Roch A, Papazian L. Multidrug-resistant Pseudomonas aeruginosa and mortality in mechanically ventilated ICU patients. Am J Infect Control. 2019 Sep;47(9):1059-1064. doi: 10.1016/j.ajic.2019.02.030.

31. Pang Z, Raudonis R, Glick BR, Lin TJ, Cheng Z. Antibiotic resistance in Pseudomonas aeruginosa: mechanisms and alternative therapeutic strategies. Biotechnol Adv. 2019 Jan-Feb;37(1):177-192. doi: 10.1016/j.biotechadv.2018.11.013.

32. Bellido F, Martin NL, Siehnel RJ, Hancock RE. Reevaluation, using intact cells, of the exclusion limit and role of porin OprF in Pseudomonas aeruginosa outer membrane permeability. J Bacteriol. 1992 Aug;174(16):5196-203. doi: 10.1128/jb.174.16.5196-5203.1992.

33. Dupont P, Hocquet D, Jeannot K, Chavanet P, Plésiat P. Bacteriostatic and bactericidal activities of eight fluoroquinolones against Mex-AB-OprM-overproducing clinical strains of Pseudomonas aeruginosa. J Antimicrob Chemother. 2005 Apr;55(4):518-22. doi: 10.1093/jac/dki030.

34. Okamoto K, Gotoh N, Nishino T. Extrusion of penem antibiotics by multicomponent efflux systems MexAB-OprM, MexCD-OprJ, and MexXY-OprM of Pseudomonas aeruginosa. Antimicrob Agents Chemother. 2002 Aug;46(8):2696-9. doi: 10.1128/AAC.46.8.2696-2699.2002.

35. Wright, G. D. Bacterial resistance to antibiotics: Enzymatic degradation and modification. Adv Drug Deliv Rev. 2005 Jul 29;57(10):1451-70. doi: 10.1016/j.addr.2005.04.002.

36. Fang ZL, Zhang LY, Huang YM, Qing Y, Cao KY, Tian GB, Huang X. OprD mutations and inactivation in imipenem-resistant Pseudomonas aeruginosa isolates from China. Infect Genet Evol. 2014 Jan;21:124-8. doi: 10.1016/j.meegid.2013.10.027.

37. Braz VS, Furlan JP, Fernandes AF, Stehling EG. Mutations in NalC induce MexAB-OprM overexpression resulting in high level of aztreonam resistance in environmental isolates of Pseudomonas aeruginosa. FEMS Microbiol Lett. 2016 Aug;363(16):fnw166. doi: 10.1093/femsle/fnw166.

38. Drenkard, E. Antimicrobial resistance of Pseudomonas aeruginosa biofilms. Microbes Infect. 2003 Nov;5(13):1213-9. doi: 10.1016/j.micinf.2003.08.009.

39. Pritt B, O'Brien L, Winn W. Mucoid Pseudomonas in cystic fibrosis. Am J Clin Pathol. 2007 Jul;128(1):32-4. doi: 10.1309/KJRPC7DD5TR9NTDM.

40. Gellatly SL, Hancock RE. Pseudomonas aeruginosa: New insights into pathogenesis and host defenses. Pathog Dis. 2013 Apr;67(3):159-73. doi: 10.1111/2049-632X.12033.

41. Roy-Burman A, Savel RH, Racine S, Swanson BL, Revadigar NS, Fujimoto J, Sawa T, Frank DW, Wiener-Kronish JP. Type III protein secretion is associated with death in lower respiratory and systemic Pseudomonas aeruginosa infections. J Infect Dis. 2001 Jun 15;183(12):1767-74. doi: 10.1086/320737.

42. Hauser AR, Cobb E, Bodi M, Mariscal D, Vallés J, Engel JN, Rello J. Type III protein secretion is associated with poor clinical outcomes in patients with ventilator-associated pneumonia caused by Pseudomonas aeruginosa. Crit Care Med. 2002 Mar;30(3):521-8. doi: 10.1097/00003246-200203000-00005.

43. Hauser, A. R. The type III secretion system of Pseudomonas aeruginosa: Infection by injection. Nat Rev Microbiol. 2009 Sep;7(9):654-65. doi: 10.1038/nrmicro2199.

44. Finck-Barbançon V, Goranson J, Zhu L, Sawa T, Wiener-Kronish JP, Fleiszig SM, Wu C, Mende-Mueller L, Frank DW. ExoU expression by Pseudomonas aeruginosa correlates with acute cytotoxicity and epithelial injury. Mol Microbiol. 1997 Aug;25(3):547-57. doi: 10.1046/j.1365-2958.1997.4891851.x.

45. Usher LR, Lawson RA, Geary I, Taylor CJ, Bingle CD, Taylor GW, Whyte MK. Induction of Neutrophil Apoptosis by the Pseudomonas aeruginosa Exotoxin Pyocyanin: A Potential Mechanism of Persistent Infection. J Immunol. 2002 Feb 15;168(4):1861-8. doi: 10.4049/jimmunol.168.4.1861.

46. Lau GW, Ran H, Kong F, Hassett DJ, Mavrodi D. Pseudomonas aeruginosa pyocyanin is critical for lung infection in mice. Infect Immun. 2004 Jul;72(7):4275-8. doi: 10.1128/IAI.72.7.4275-4278.2004.

47. Malloy JL, Veldhuizen RA, Thibodeaux BA, O'Callaghan RJ, Wright JR. Pseudomonas aeruginosa protease IV degrades surfactant proteins and inhibits surfactant host defense and biophysical functions. Am J Physiol Lung Cell Mol Physiol. 2005 Feb;288(2):L409-18. doi: 10.1152/ajplung.00322.2004.

48. Azghani AO, Miller EJ, Peterson BT. Virulence factors from Pseudomonas aeruginosa increase lung epithelial permeability. Lung. 2000;178(5):261-9. doi: 10.1007/s004080000031.

49. Mariencheck WI, Alcorn JF, Palmer SM, Wright JR. Pseudomonas aeruginosa elastase degrades surfactant proteins A and D. Am J Respir Cell Mol Biol. 2003 Apr;28(4):528-37. doi: 10.1165/rcmb.2002-0141OC.

50. Bucior I, Pielage JF, Engel JN. Pseudomonas aeruginosa Pili and Flagella mediate distinct binding and signaling events at the apical and basolateral surface of airway epithelium. PLoS Pathog. 2012;8(4):e1002616. doi: 10.1371/journal.ppat.1002616.

51. Sadikot RT, Blackwell TS, Christman JW, Prince AS. Pathogen-host interactions in pseudomonas aeruginosa pneumonia. Am J Respir Crit Care Med. 2005 Jun 1;171(11):1209-23. doi: 10.1164/rccm.200408-1044SO.

52. Wu D, Wu C, Zhang S, Zhong Y. Risk factors of ventilator-associated pneumonia in critically III patients. Front Pharmacol. 2019 May 9;10:482. doi: 10.3389/fphar.2019.00482.

53. Liu Y, Di Y, Fu S. Risk factors for ventilator-associated pneumonia among patients undergoing major oncological surgery for head and neck cancer. Front Med. 2017 Jun;11(2):239-246. doi: 10.1007/s11684-017-0509-8.

54. Ding C, Zhang Y, Yang Z, Wang J, Jin A, Wang W, Chen R, Zhan S. Incidence, temporal trend and factors associated with ventilator-associated pneumonia in mainland China: A systematic review and meta-analysis. BMC Infect Dis. 2017 Jul 4;17(1):468. doi: 10.1186/s12879-017-2566-7.

55. Torres A, Gatell JM, Aznar E, el-Ebiary M, Puig de la Bellacasa J, González J, Ferrer M, Rodriguez-Roisin R. Re-intubation increases the risk of nosocomial pneumonia in patients needing mechanical ventilation. Am J Respir Crit Care Med. 1995 Jul;152(1):137-41. doi: 10.1164/ajrccm.152.1.7599812.

56. Rouzé A, Jaillette E, Nseir S. Relationship between microaspiration of gastric contents and ventilator-associated pneumonia. Ann Transl Med. 2018 Nov;6(21):428. doi: 10.21037/atm.2018.07.36.

57. Metheny NA, Clouse RE, Chang YH, Stewart BJ, Oliver DA, Kollef MH. Tracheobronchial aspiration of gastric contents in critically ill tube-fed patients: Frequency, outcomes, and risk factors. Crit Care Med. 2006 Apr;34(4):1007-15. doi: 10.1097/01.CCM.0000206106.65220.59.

58. Jovanovic B, Milan Z, Djuric O, Markovic-Denic L, Karamarkovic A, Gregoric P, Doklestic K, Avramovic J, Velickovic J, Bumbasirevic V. Twenty-Eight-Day Mortality of Blunt Traumatic Brain Injury and Co-Injuries Requiring Mechanical Ventilation. Med Princ Pract. 2016;25(5):435-41. doi: 10.1159/000447566.

59. Sen S, Johnston C, Greenhalgh D, Palmieri T. Ventilator-Associated Pneumonia Prevention Bundle Significantly Reduces the Risk of Ventilator-Associated Pneumonia in Critically Ill Burn Patients. J Burn Care Res. 2016 May-Jun;37(3):166-71. doi: 10.1097/BCR.0000000000000228.

60. Jiménez-Trujillo I, Jiménez-García R, de Miguel-Díez J, de Miguel-Yanes JM, Hernández-Barrera V, Méndez-Bailón M, Pérez-Farinós N, Salinero-Fort MÁ, López-de-Andrés A. Incidence, characteristic and outcomes of ventilator-associated pneumonia among type 2 diabetes patients: An observational population-based study in Spain. Eur J Intern Med. 2017 May;40:72-78. doi: 10.1016/j.ejim.2017.01.019.

61. Markowicz P, Wolff M, Djedaïni K, Cohen Y, Chastre J, Delclaux C, Merrer J, Herman B, Veber B, Fontaine A, Dreyfuss D. Multicenter prospective study of ventilator-associated pneumonia during acute respiratory distress syndrome: Incidence, prognosis, and risk factors. Am J Respir Crit Care Med. 2000 Jun;161(6):1942-8. doi: 10.1164/ajrccm.161.6.9909122.

62. Bernard GR, Artigas A, Brigham KL, Carlet J, Falke K, Hudson L, Lamy M, Legall JR, Morris A, Spragg R. The American-European Consensus Conference on ARDS: Definitions, mechanisms, relevant outcomes, and clinical trial coordination. Am J Respir Crit Care Med. 1994 Mar;149(3 Pt 1):818-24. doi: 10.1164/ajrccm.149.3.7509706.

63. ARDS Definition Task Force, Ranieri VM, Rubenfeld GD, Thompson BT, Ferguson ND, Caldwell E, Fan E, Camporota L, Slutsky AS. Acute respiratory distress syndrome: The Berlin definition. JAMA. 2012 Jun 20;307(23):2526-33. doi: 10.1001/jama.2012.5669.

64. Fan E, Brodie D, Slutsky AS. Acute respiratory distress syndrome advances in diagnosis and treatment. JAMA. 2018 Feb 20;319(7):698-710. doi: 10.1001/jama.2017.21907.

65. Thille AW, Esteban A, Fernández-Segoviano P, Rodriguez JM, Aramburu JA, Peñuelas O, Cortés-Puch I, Cardinal-Fernández P, Lorente JA, Frutos-Vivar F. Comparison of the berlin definition for acute respiratory

distress syndrome with autopsy. Am J Respir Crit Care Med. 2013 Apr 1;187(7):761-7. doi: 10.1164/rccm.201211-1981OC.

66. Guerin C, Bayle F, Leray V, Debord S, Stoian A, Yonis H, Roudaut JB, Bourdin G, Devouassoux-Shisheboran M, Bucher E, Ayzac L, Lantuejoul S, Philipponnet C, Kemeny JL, Souweine B, Richard JC. Open lung biopsy in nonresolving ARDS frequently identifies diffuse alveolar damage regardless of the severity stage and may have implications for patient management. Intensive Care Med. 2015 Feb;41(2):222-30. doi: 10.1007/s00134-014-3583-2.

67. Thompson BT, Chambers RC, Liu KD. Acute respiratory distress syndrome. N Engl J Med. 2017 Aug 10;377(6):562-572. doi: 10.1056/NEJMra1608077.

68. Rubenfeld GD, Caldwell E, Peabody E, Weaver J, Martin DP, Neff M, Stern EJ, Hudson LD. Incidence and Outcomes of Acute Lung Injury. N Engl J Med. 2005 Oct 20;353(16):1685-93. doi: 10.1056/NEJMoa050333.

69. Villar J, Sulemanji D, Kacmarek RM. The acute respiratory distress syndrome: Incidence and mortality, has it changed? Curr Opin Crit Care. 2014 Feb;20(1):3-9. doi: 10.1097/MCC.0000000000000057.

70. Bellani G, Laffey JG, Pham T, Fan E, Brochard L, Esteban A, Gattinoni L, van Haren F, Larsson A, McAuley DF, Ranieri M, Rubenfeld G, Thompson BT, Wrigge H, Slutsky AS, Pesenti A; LUNG SAFE Investigators; ESICM Trials Group. Epidemiology, patterns of care, and mortality for patients with acute respiratory distress syndrome in intensive care units in 50 countries. JAMA. 2016 Feb 23;315(8):788-800. doi: 10.1001/jama.2016.0291.

71. Villar J, Blanco J, Añón JM, Santos-Bouza A, Blanch L, Ambrós A, Gandía F, Carriedo D, Mosteiro F, Basaldúa S, Fernández RL, Kacmarek RM; ALIEN Network. The ALIEN study: Incidence and outcome of acute respiratory distress syndrome in the era of lung protective ventilation. Intensive Care Med. 2011 Dec;37(12):1932-41. doi: 10.1007/s00134-011-2380-4.

72. Wang CY, Calfee CS, Paul DW, Janz DR, May AK, Zhuo H, Bernard GR, Matthay MA, Ware LB, Kangelaris KN. One-year mortality and predictors of death among hospital survivors of acute respiratory distress syndrome. Intensive Care Med. 2014 Mar;40(3):388-96. doi: 10.1007/s00134-013-3186-3.

73. Sweeney RM, McAuley DF. Acute respiratory distress syndrome. Lancet. 2016 Nov 12;388(10058):2416-2430. doi: 10.1016/S0140-6736(16)00578-X.

74. Gattinoni L, Pesenti A. The concept of "baby lung". Intensive Care Med. 2005 Jun;31(6):776-84. doi: 10.1007/s00134-005-2627-z.

75. Gattinoni L, Marini JJ, Pesenti A, Quintel M, Mancebo J, Brochard L. The 'baby lung' became an adult. Intensive Care Med. 2016 May;42(5):663-673. doi: 10.1007/s00134-015-4200-8.

76. Wilson MR, Choudhury S, Goddard ME, O'Dea KP, Nicholson AG, Takata M. High tidal volume upregulates intrapulmonary cytokines in an in vivo mouse model of ventilator-induced lung injury. J Appl Physiol (1985). 2003 Oct;95(4):1385-93. doi: 10.1152/japplphysiol.00213.2003.

77. Müller-Redetzky HC, Felten M, Hellwig K, Wienhold SM, Naujoks J, Opitz B, Kershaw O, Gruber AD, Suttorp N, Witzenrath M. Increasing the inspiratory time and I:E ratio during mechanical ventilation aggravates ventilator-induced lung injury in mice. Crit Care. 2015 Jan 28;19(1):23. doi: 10.1186/s13054-015-0759-2.

78. Ricard JD, Dreyfuss D, Saumon G. Production of inflammatory cytokines in ventilator-induced lung injury: A reappraisal. Am J Respir Crit Care Med. 2001 Apr;163(5):1176-80. doi: 10.1164/ajrccm.163.5.2006053.

79. Slutsky AS, Ranieri VM. Ventilator-Induced Lung Injury. N Engl J Med. 2013 Nov 28;369(22):2126-36. doi: 10.1056/NEJMra1208707.

80. Slutsky, A. S. Lung Injury Caused by Mechanical Ventilation. Chest. 1999 Jul;116(1 Suppl):9S-15S. doi: 10.1378/chest.116.suppl_1.9s-a.

81. Bilek AM, Dee KC, Gaver DP 3rd. Mechanisms of surface-tension-induced epithelial cell damage in a model of pulmonary airway reopening. J Appl Physiol (1985). 2003 Feb;94(2):770-83. doi: 10.1152/japplphysiol.00764.2002.

82. Albert, R. K. The role of ventilation-induced surfactant dysfunction and atelectasis in causing acute respiratory distress syndrome. Am J Respir Crit Care Med. 2012 Apr 1;185(7):702-8. doi: 10.1164/rccm.201109-1667PP.

83. Beitler JR, Malhotra A, Thompson BT. Ventilator-induced Lung Injury. Clin Chest Med. 2016 Dec;37(4):633-646. doi: 10.1016/j.ccm.2016.07.004.

84. Nieman GF, Satalin J, Andrews P, Habashi NM, Gatto LA. Lung stress, strain, and energy load: engineering concepts to understand the mechanism of ventilator-induced lung injury (VILI). Intensive Care Med Exp. 2016 Dec;4(1):16. doi: 10.1186/s40635-016-0090-5.

85. Gattinoni L, Carlesso E, Caironi P. Stress and strain within the lung. Curr Opin Crit Care. 2012 Feb;18(1):42-7. doi: 10.1097/MCC.0b013e32834f17d9.

86. Ghadiali SN, Gaver DP. Biomechanics of liquid-epithelium interactions in pulmonary airways. Respir Physiol Neurobiol. 2008 Nov 30;163(1-3):232-43. doi: 10.1016/j.resp.2008.04.008.

87. Gattinoni L, Tonetti T, Quintel M. Regional physiology of ARDS. Crit Care. 2017 Dec 28;21(Suppl 3):312. doi: 10.1186/s13054-017-1905-9.

88. Frank JA, Pittet JF, Wray C, Matthay MA. Protection from experimental ventilator-induced acute lung injury by IL-1 receptor blockade. Thorax. 2008 Feb;63(2):147-53. doi: 10.1136/thx.2007.079608.

89. Spassov SG, Donus R, Ihle PM, Engelstaedter H, Hoetzel A, Faller S. Corrigendum to "Hydrogen Sulfide Prevents Formation of Reactive Oxygen Species through PI3K/Akt Signaling and Limits Ventilator-Induced Lung Injury". Oxid Med Cell Longev. 2017;2017:9230134. doi: 10.1155/2017/9230134.

90. Kim DH, Chung JH, Son BS, Kim YJ, Lee SG. Effect of a neutrophil elastase inhibitor on ventilator-induced lung injury in rats. J Thorac Dis. 2014 Dec;6(12):1681-9. doi: 10.3978/j.issn.2072-1439.2014.11.10.

91. Li H, Pan P, Su X, Liu S, Zhang L, Wu D, Li H, Dai M, Li Y, Hu C, Chen J. Neutrophil extracellular traps are pathogenic in ventilator-induced lung injury and partially dependent on TLR4. Biomed Res Int. 2017;2017:8272504. doi: 10.1155/2017/8272504.

92. Imanaka H, Shimaoka M, Matsuura N, Nishimura M, Ohta N, Kiyono H. Ventilator-Induced Lung Injury Is Associated with Neutrophil Infiltration, Macrophage Activation, and TGF-β1 mRNA Upregulation in Rat Lungs. Anesth Analg. 2001 Feb;92(2):428-36. doi: 10.1097/00000539-200102000-00029.

93. Wilson MR, O'Dea KP, Zhang D, Shearman AD, van Rooijen N, Takata M. Role of lung-marginated monocytes in an in vivo mouse model of ventilator-induced lung injury. Am J Respir Crit Care Med. 2009 May 15;179(10):914-22. doi: 10.1164/rccm.200806-877OC.

94. Acute Respiratory Distress Syndrome Network, Brower RG, Matthay MA, Morris A, Schoenfeld D, Thompson BT, Wheeler A. Ventilation with Lower Tidal Volumes as Compared with Traditional Tidal Volumes for Acute Lung Injury and the Acute Respiratory Distress Syndrome. N Engl J Med. 2000 May 4;342(18):1301-8. doi: 10.1056/NEJM200005043421801.

95. Determann RM, Royakkers A, Wolthuis EK, Vlaar AP, Choi G, Paulus F, Hofstra JJ, de Graaff MJ, Korevaar JC, Schultz MJ. Ventilation with lower tidal volumes as compared with conventional tidal volumes for patients without acute lung injury: A preventive randomized controlled trial. Crit Care. 2010;14(1):R1. doi: 10.1186/cc8230.

96. Villar J, Kacmarek RM, Pérez-Méndez L, Aguirre-Jaime A. A high positive end-expiratory pressure, low tidal volume ventilatory strategy improves outcome in persistent acute respiratory distress syndrome: A randomized, controlled trial. Crit Care Med. 2006 May;34(5):1311-8. doi: 10.1097/01.CCM.0000215598.84885.01.

97. Needham DM, Yang T, Dinglas VD, Mendez-Tellez PA, Shanholtz C, Sevransky JE, Brower RG, Pronovost PJ, Colantuoni E. Timing of low tidal volume ventilation and intensive care unit mortality in acute respiratory distress syndrome:A Prospective Cohort Study. Am J Respir Crit Care Med. 2015 Jan 15;191(2):177-85. doi: 10.1164/rccm.201409-1598OC.

98. Futier E, Constantin JM, Paugam-Burtz C, Pascal J, Eurin M, Neuschwander A, Marret E, Beaussier M, Gutton C, Lefrant JY, Allaouchiche B, Verzilli D, Leone M, De Jong A, Bazin JE, Pereira B, Jaber S; IMPROVE Study Group. A Trial of Intraoperative Low-Tidal-Volume Ventilation in Abdominal Surgery. N Engl J Med. 2013 Aug 1;369(5):428-37. doi: 10.1056/NEJMoa1301082.

99. Gattinoni L, Caironi P, Pelosi P, Goodman LR. What has computed tomography taught us about the acute respiratory distress syndrome? Am J Respir Crit Care Med. 2001 Nov 1;164(9):1701-11. doi: 10.1164/ajrccm.164.9.2103121.

100. Gattinoni L, Pelosi P, Vitale G, Pesenti A, D'Andrea L, Mascheroni D. Body position changes redistribute lung computed-tomographic density in patients with acute respiratory failure. Anesthesiology. 1991 Jan;74(1):15-23. doi: 10.1097/00000542-199101000-00004.

101. Gattinoni L, Pesenti A, Carlesso E. Body position changes redistribute lung computed-tomographic density in patients with acute respiratory failure: Impact and clinical fallout through the following 20 years. Intensive Care Med. 2013 Nov;39(11):1909-15. doi: 10.1007/s00134-013-3066-x.

102. Guérin C, Reignier J, Richard JC, Beuret P, Gacouin A, Boulain T, Mercier E, Badet M, Mercat A, Baudin O, Clavel M, Chatellier D, Jaber S, Rosselli S, Mancebo J, Sirodot M, Hilbert G, Bengler C, Richecoeur J, Gainnier M, Bayle F, Bourdin G, Leray V, Girard R, Baboi L, Ayzac L; PROSEVA Study Group. Prone Positioning in Severe Acute Respiratory Distress Syndrome. N Engl J Med. 2013 Jun 6;368(23):2159-68. doi: 10.1056/NEJMoa1214103.

103. Oliveira-Junior IS, Pinheiro BV, Silva ID, Salomão R, Zollner RL, Beppu OS. Pentoxifylline decreases tumor necrosis factor and interleukin-1 during high tidal volume. Braz J Med Biol Res. 2003 Oct;36(10):1349-57. doi: 10.1590/s0100-879x2003001000011.

104. Imai Y, Kawano T, Iwamoto S, Nakagawa S, Takata M, Miyasaka K. Intratracheal anti-tumor necrosis factor-α antibody attenuates ventilator-induced lung injury in rabbits. J Appl Physiol (1985). 1999 Aug;87(2):510-5. doi: 10.1152/jappl.1999.87.2.510.

105. Kor DJ, Carter RE, Park PK, Festic E, Banner-Goodspeed VM, Hinds R, Talmor D, Gajic O, Ware LB, Gong MN; US Critical Illness and Injury Trials Group: Lung Injury Prevention with Aspirin Study Group (USCIITG: LIPS-A). Effect of aspirin on development of ARDS in at-risk patients presenting to the emergency department the LIPS-a randomized clinical trial. JAMA. 2016 Jun 14;315(22):2406-14. doi: 10.1001/jama.2016.6330.

106. Xiong B, Wang C, Tan J, Cao Y, Zou Y, Yao Y, Qian J, Rong S, Huang Y, Huang J. Statins for the prevention and treatment of acute lung injury and acute respiratory distress syndrome: A systematic review and meta-analysis. Respirology. 2016 Aug;21(6):1026-33. doi: 10.1111/resp.12820.

107. Papazian L, Forel JM, Gacouin A, Penot-Ragon C, Perrin G, Loundou A, Jaber S, Arnal JM, Perez D, Seghboyan JM, Constantin JM, Courant P, Lefrant JY, Guérin C, Prat G, Morange S, Roch A; ACURASYS Study Investigators. N Engl J Med. 2010 Sep 16;363(12):1107-16. doi: 10.1056/NEJMoa1005372.

108. Bielen K, 's Jongers B, Malhotra-Kumar S, Jorens PG, Goossens H, Kumar-Singh S. Animal models of hospital-acquired pneumonia: Current practices and future perspectives. Ann Transl Med. 2017 Mar;5(6):132. doi: 10.21037/atm.2017.03.72.

109. Luna CM, Sibila O, Agusti C, Torres A. Animal models of ventilator-associated pneumonia. Eur Respir J. 2009 Jan;33(1):182-8. doi: 10.1183/09031936.00046308.

110. Campbell GD, Coalson JJ, Johanson WG Jr. The effect of bacterial superinfection on lung function after diffuse alveolar damage. Am Rev Respir Dis. 1984 Jun;129(6):974-8. doi: 10.1164/arrd.1984.129.6.974.

111. Johanson WG Jr, Seidenfeld JJ, Gomez P, de los Santos R, Coalson JJ. Bacteriologic diagnosis of nosocomial pneumonia following prolonged mechanical ventilation. Am Rev Respir Dis. 1988 Feb;137(2):259-64. doi: 10.1164/ajrccm/137.2.259.

112. Johanson WG Jr, Seidenfeld JJ, de los Santos R, Coalson JJ, Gomez P. Prevention of nosocomial pneumonia using topical and parenteral antimicrobial agents. Am Rev Respir Dis. 1988 Feb;137(2):265-72. doi: 10.1164/ajrccm/137.2.265.

113. Wermert D, Marquette CH, Copin MC, Wallet F, Fraticelli A, Ramon P, Tonnel AB. Influence of pulmonary bacteriology and histology on the yield of diagnostic procedures in ventilator-acquired pneumonia. Am J Respir Crit Care Med. 1998 Jul;158(1):139-47. doi: 10.1164/ajrccm.158.1.9710061.

114. Sibila O, Agustí C, Torres A, Baquero S, Gando S, Patrón JR, Morato JG, Goffredo DH, Bassi N, Luna CM. Experimental Pseudomonas aeruginosa pneumonia: Evaluation of the associated inflammatory response. Eur Respir J. 2007 Dec;30(6):1167-72. doi: 10.1183/09031936.00053607.

115. Verbrugge SJ, Sorm V, van 't Veen A, Mouton JW, Gommers D, Lachmann B. Lung overinflation without positive end-expiratory pressure promotes bacteremia after experimental Klebsiella pneumoniae inoculation. Intensive Care Med. 1998 Feb;24(2):172-7. doi: 10.1007/s001340050541.

116. Dhanireddy S, Altemeier WA, Matute-Bello G, O'Mahony DS, Glenny RW, Martin TR, Liles WC. Mechanical ventilation induces inflammation, lung injury, and extra-pulmonary organ dysfunction in experimental pneumonia. Lab Invest. 2006 Aug;86(8):790-9. doi: 10.1038/labinvest.3700440.

117. Tsay TB, Jiang YZ, Hsu CM, Chen LW. Pseudomonas aeruginosa colonization enhances ventilator-associated pneumonia-induced lung injury. Respir Res. 2016 Aug 9;17(1):101. doi: 10.1186/s12931-016-0417-5.

118. Torres IM, Patankar YR, Berwin B. Acidosis exacerbates in vivo IL-1-dependent inflammatory responses and neutrophil recruitment during pulmonary pseudomonas aeruginosa infection. Am J Physiol Lung Cell Mol Physiol. 2018 Feb 1;314(2):L225-L235. doi: 10.1152/ajplung.00338.2017.

119. Kostikas K, Papatheodorou G, Ganas K, Psathakis K, Panagou P, Loukides S. pH in expired breath condensate of patients with inflammatory airway diseases. Am J Respir Crit Care Med. 2002 May 15;165(10):1364-70. doi: 10.1164/rccm.200111-068OC.

120. Vlahakis NE, Schroeder MA, Limper AH, Hubmayr RD. Stretch induces cytokine release by alveolar epithelial cells in vitro. Am J Physiol. 1999 Jul;277(1):L167-73. doi: 10.1152/ajplung.1999.277.1.L167.

121. Pugin J, Dunn I, Jolliet P, Tassaux D, Magnenat JL, Nicod LP, Chevrolet JC. Activation of human macrophages by mechanical ventilation in vitro. Am J Physiol. 1998 Dec;275(6):L1040-50. doi: 10.1152/ajplung.1998.275.6.L1040.

122. Oudin S, Pugin J. Role of MAP kinase activation in interleukin-8 production by human BEAS-2B bronchial epithelial cells submitted to cyclic stretch. Am J Respir Cell Mol Biol. 2002 Jul;27(1):107-14. doi: 10.1165/ajrcmb.27.1.4766.

123. Pugin J, Dunn-Siegrist I, Dufour J, Tissières P, Charles PE, Comte R. Cyclic stretch of human lung cells induces an acidification and promotes bacterial growth. Am J Respir Cell Mol Biol. 2008 Mar;38(3):362-70. doi: 10.1165/rcmb.2007-0114OC.

124. Gessner C, Hammerschmidt S, Kuhn H, Seyfarth HJ, Sack U, Engelmann L, Schauer J, Wirtz H. Exhaled breath condensate acidification in acute lung injury. Respir Med. 2003 Nov;97(11):1188-94. doi: 10.1016/s0954-6111(03)00225-7.

125. Routsi C, Bardouniotou H, Delivoria-Ioannidou V, Kazi D, Roussos C, Zakynthinos S. Pulmonary lactate release in patients with acute lung injury is not attributable to lung tissue hypoxia. Crit Care Med. 1999 Nov;27(11):2469-73. doi: 10.1097/00003246-199911000-00024.

126. Henderson WR, Chen L, Amato MBP, Brochard LJ. Fifty years of research in ARDS: Respiratory mechanics in acute respiratory distress syndrome. Am J Respir Crit Care Med. 2017 Oct 1;196(7):822-833. doi: 10.1164/rccm.201612-2495CI.

127. Donati PA, Gogniat E, Madorno M, Guevara JM, Guillemi EC, Lavalle MDC, Scorza FP, Mayer GF, Rodriguez PO. Sizing the lung in dogs: The inspiratory capacity defines the tidal volume. Rev Bras Ter Intensiva. 2018 Apr-Jun;30(2):144-152. doi: 10.5935/0103-507X.20180028.

128. Spalding MC, Cripps MW, Minshall CT. Ventilator-Associated Pneumonia: New Definitions. Crit Care Clin. 2017 Apr;33(2):277-292. doi: 10.1016/j.ccc.2016.12.009.

129. Protti A, Cressoni M, Santini A, Langer T, Mietto C, Febres D, Chierichetti M, Coppola S, Conte G, Gatti S, Leopardi O, Masson S, Lombardi L, Lazzerini M, Rampoldi E, Cadringher P, Gattinoni L. Lung stress and strain during mechanical ventilation: Any safe threshold? Am J Respir Crit Care Med. 2011 May 15;183(10):1354-62. doi: 10.1164/rccm.201010-1757OC.

130. Martinez F, Lewis J, Copland I, Engelberts D, Kavanagh BP, Post M, Schurch S, Belik J. Mechanical ventilation effect on surfactant content, function, and lung compliance in the newborn rat. Pediatr Res. 2004 Jul;56(1):19-25. doi: 10.1203/01.PDR.0000128980.82797.29.

131. Bates JHT, Smith BJ. Ventilator-induced lung injury and lung mechanics. Ann Transl Med. 2018 Oct;6(19):378. doi: 10.21037/atm.2018.06.29.

132. Matute-Bello G, Downey G, Moore BB, Groshong SD, Matthay MA, Slutsky AS, Kuebler WM; Acute Lung Injury in Animals Study Group. An official american thoracic society workshop report: Features and measurements of experimental acute lung injury in animals. Am J Respir Cell Mol Biol. 2011 May;44(5):725-38. doi: 10.1165/rcmb.2009-0210ST.

133. Cressoni M, Gotti M, Chiurazzi C, Massari D, Algieri I, Amini M, Cammaroto A, Brioni M, Montaruli C, Nikolla K, Guanziroli M, Dondossola D, Gatti S, Valerio V, Vergani GL, Pugni P, Cadringher P, Gagliano N, Gattinoni L. Mechanical power and development of ventilator-induced lung injury. Anesthesiology. 2016 May;124(5):1100-8. doi: 10.1097/ALN.0000000000001056.

134. Hegeman MA, Hennus MP, van Meurs M, Cobelens PM, Kavelaars A, Jansen NJ, Schultz MJ, van Vught AJ, Molema G, Heijnen CJ. Angiopoietin-1 treatment reduces inflammation but does not prevent ventilator-induced lung injury. PLoS One. 2010 Dec 14;5(12):e15653. doi: 10.1371/journal.pone.0015653.

135. Choudhury S, Wilson MR, Goddard ME, O'Dea KP, Takata M. Mechanisms of early pulmonary neutrophil sequestration in ventilator-induced lung injury in mice. Am J Physiol Lung Cell Mol Physiol. 2004 Nov;287(5):L902-10. doi: 10.1152/ajplung.00187.2004.

136. Summers C, Rankin SM, Condliffe AM, Singh N, Peters AM, Chilvers ER. Neutrophil kinetics in health and disease. Trends Immunol. 2010 Aug;31(8):318-24. doi: 10.1016/j.it.2010.05.006.

137. Lord BI, Woolford LB, Molineux G. Kinetics of neutrophil production in normal and neutropenic animals during the response to filgrastim (r-metHu G-CSF) or filgrastim SD/01 (PEG-r-metHu G-CSF). Clin Cancer Res. 2001 Jul;7(7):2085-90.

138. Kuribayashi, T. Elimination half-lives of interleukin-6 and cytokine-induced neutrophil chemoattractant-1 synthesized in response to inflammatory stimulation in rats. Lab Anim Res. 2018 Jun;34(2):80-83. doi: 10.5625/lar.2018.34.2.80.

139. Handel TM, Johnson Z, Rodrigues DH, Dos Santos AC, Cirillo R, Muzio V, Riva S, Mack M, Déruaz M, Borlat F, Vitte PA, Wells TN, Teixeira MM, Proudfoot AE. An engineered monomer of CCL2 has anti-inflammatory properties emphasizing the importance of oligomerization for chemokine activity in vivo. J Leukoc Biol. 2008 Oct;84(4):1101-8. doi: 10.1189/jlb.0108061.

140. Hazuda DJ, Lee JC, Young PR. The kinetics of interleukin 1 secretion from activated monocytes. Differences between interleukin 1α and interleukin 1β. J Biol Chem. 1988 Jun 15;263(17):8473-9.

141. Huhn RD, Radwanski E, Gallo J, Affrime MB, Sabo R, Gonyo G, Monge A, Cutler DL. Pharmacodynamics of subcutaneous recombinant human interleukin-10 in healthy volunteers. Clin Pharmacol Ther. 1997 Aug;62(2):171-80. doi: 10.1016/S0009-9236(97)90065-5.

142. Nin N, Lorente JA, de Paula M, El Assar M, Vallejo S, Peñuelas O, Fernández-Segoviano P, Ferruelo A, Sánchez-Ferrer A, Esteban A. Rats surviving injurious mechanical ventilation show reversible pulmonary, vascular and inflammatory changes. Intensive Care Med. 2008 May;34(5):948-56. doi: 10.1007/s00134-007-0959-6.

143. Vlach KD, Boles JW, Stiles BG. Telemetric evaluation of body temperature and physical activity as predictors of mortality in a murine model of staphylococcal enterotoxic shock. Comp Med. 2000 Apr;50(2):160-6.

144. Stiles BG, Campbell YG, Castle RM, Grove SA. Correlation of temperature and toxicity in murine studies of staphylococcal enterotoxins and toxic shock syndrome toxin 1. Infect Immun. 1999 Mar;67(3):1521-5. doi: 10.1128/IAI.67.3.1521-1525.1999.

145. Ware LB, Matthay MA. The acute respiratory distress syndrome. N Engl J Med. 2000 May 4;342(18):1334-49. doi: 10.1056/NEJM200005043421806.

146. Matthay MA, Ware LB, Zimmerman GA. The acute respiratory distress syndrome. J Clin Invest. 2012 Aug;122(8):2731-40. doi: 10.1172/JCI60331.

147. Berger S, Goekeri C, Gupta SK, Vera J, Dietert K, Behrendt U, Lienau J, Wienhold SM, Gruber AD, Suttorp N, Witzenrath M, Nouailles G. Delay in antibiotic therapy results in fatal disease outcome in murine pneumococcal pneumonia. Crit Care. 2018 Nov 1;22(1):287. doi: 10.1186/s13054-018-2224-5.

148. Azghani, A. O. Pseudomonas aeruginosa and Epithelial Permeability: Role of Virulence Factors Elastase and Exotoxin A. Am J Respir Cell Mol Biol. 1996 Jul;15(1):132-40. doi: 10.1165/ajrcmb.15.1.8679217.

149. Ramírez P, Ferrer M, Gimeno R, Tormo S, Valencia M, Piñer R, Menendez R, Torres A. Systemic inflammatory response and increased risk for ventilator-associated pneumonia: A preliminary study. Crit Care Med. 2009 May;37(5):1691-5. doi: 10.1097/CCM.0b013e31819fec5f.

150. Conway Morris A, Kefala K, Wilkinson TS, Moncayo-Nieto OL, Dhaliwal K, Farrell L, Walsh TS, Mackenzie SJ, Swann DG, Andrews PJ, Anderson N, Govan JR, Laurenson IF, Reid H, Davidson DJ, Haslett C, Sallenave JM, Simpson AJ. Diagnostic importance of pulmonary interleukin-1β and interleukin-8 in ventilator-associated pneumonia. Thorax. 2010 Mar;65(3):201-7. doi: 10.1136/thx.2009.122291.

151. Amano H, Morimoto K, Senba M, Wang H, Ishida Y, Kumatori A, Yoshimine H, Oishi K, Mukaida N, Nagatake T. Essential Contribution of Monocyte Chemoattractant Protein-1/C-C Chemokine Ligand-2 to Resolution and Repair Processes in Acute Bacterial Pneumonia. J Immunol. 2004 Jan 1;172(1):398-409. doi: 10.4049/jimmunol.172.1.398.

152. Jeong ES, Won YS, Kim HC, Cho MH, Choi YK. Role of IL-10 deficiency in pneumonia induced by Corynebacterium kutscheri in mice. J Microbiol Biotechnol. 2009 Apr;19(4):424-30. doi: 10.4014/jmb.0807.436.

153. Peñaloza HF, Nieto PA, Muñoz-Durango N, Salazar-Echegarai FJ, Torres J, Parga MJ, Alvarez-Lobos M, Riedel CA, Kalergis AM, Bueno SM. Interleukin-10 plays a key role in the modulation of neutrophils recruitment and lung inflammation during infection by Streptococcus pneumoniae. Immunology. 2015 Sep;146(1):100-12. doi: 10.1111/imm.12486.

154. Martin-Loeches I, Bos LD, Povoa P, Ramirez P, Schultz MJ, Torres A, Artigas A. Tumor necrosis factor receptor 1 (TNFRI) for ventilator-associated pneumonia diagnosis by cytokine multiplex analysis. Intensive Care Med Exp. 2015 Dec;3(1):26. doi: 10.1186/s40635-015-0062-1.

155. Kellum JA, Kong L, Fink MP, Weissfeld LA, Yealy DM, Pinsky MR, Fine J, Krichevsky A, Delude RL, Angus DC; GenIMS Investigators. Understanding the inflammatory cytokine response in pneumonia and sepsis: Results of the genetic and inflammatory markers of sepsis (GenIMS) study. Arch Intern Med. 2007 Aug 13-27;167(15):1655-63. doi: 10.1001/archinte.167.15.1655.

156. Meduri GU, Kanangat S, Stefan J, Tolley E, Schaberg D. Cytokines IL-1β, IL-6, and TNF-a Enhance In Vitro Growth of Bacteria. Am J Respir Crit Care Med. 1999 Sep;160(3):961-7. doi: 10.1164/ajrccm.160.3.9807080.

157. Kirtland SH, Corley DE, Winterbauer RH, Springmeyer SC, Casey KR, Hampson NB, Dreis DF. The diagnosis of ventilator-associated pneumonia: A comparison of histologic, microbiologic, and clinical criteria. Chest. 1997 Aug;112(2):445-57. doi: 10.1378/chest.112.2.445.

158. Paudel S, Baral P, Ghimire L, Bergeron S, Jin L, DeCorte JA, Le JT, Cai S, Jeyaseelan S. CXCL1 regulates neutrophil homeostasis in pneumonia-derived sepsis caused by Streptococcus pneumoniae serotype 3. Blood. 2019 Mar 21;133(12):1335-1345. doi: 10.1182/blood-2018-10-878082.

159. Liu Y, Mei J, Gonzales L, Yang G, Dai N, Wang P, Zhang P, Favara M, Malcolm KC, Guttentag S, Worthen GS. IL-17A and TNF-α Exert Synergistic Effects on Expression of CXCL5 by Alveolar Type II Cells In Vivo and In Vitro. J Immunol. 2011 Mar 1;186(5):3197-205. doi: 10.4049/jimmunol.1002016.

160. Zeng X, Moore TA, Newstead MW, Hernandez-Alcoceba R, Tsai WC, Standiford TJ. Intrapulmonary expression of macrophage inflammatory protein 1α (CCL3) induces neutrophil and NK cell accumulation and stimulates innate immunity in murine bacterial pneumonia. Infect Immun. 2003 Mar;71(3):1306-15. doi: 10.1128/IAI.71.3.1306-1315.2003.

161. Gregory AD, Hogue LA, Ferkol TW, Link DC. Regulation of systemic and local neutrophil responses by G-CSF during pulmonary Pseudomonas aeruginosa infection. Blood. 2007 Apr 15;109(8):3235-43. doi: 10.1182/blood-2005-01-015081.

162. Tsai WC, Strieter RM, Mehrad B, Newstead MW, Zeng X, Standiford TJ. CXC chemokine receptor CXCR2 is essential for protective-innate host response in murine Pseudomonas aeruginosa pneumonia. Infect Immun. 2000 Jul;68(7):4289-96. doi: 10.1128/IAI.68.7.4289-4296.2000.

163. Koh AY, Priebe GP, Ray C, Van Rooijen N, Pier GB. Inescapable need for neutrophils as mediators of cellular innate immunity to acute Pseudomonas aeruginosa pneumonia. Infect Immun. 2009 Dec;77(12):5300-10. doi: 10.1128/IAI.00501-09.

164. Wilkinson TS, Conway Morris A, Kefala K, O'Kane CM, Moore NR, Booth NA, McAuley DF, Dhaliwal K, Walsh TS, Haslett C, Sallenave JM, Simpson AJ. Ventilator-associated pneumonia is characterized by excessive release of neutrophil proteases in the lung. Chest. 2012 Dec;142(6):1425-1432. doi: 10.1378/chest.11-3273.

165. Mikacenic C, Moore R, Dmyterko V, West TE, Altemeier WA, Liles WC, Lood C. Neutrophil extracellular traps (NETs) are increased in the alveolar spaces of patients with ventilator-associated pneumonia. Crit Care. 2018 Dec 27;22(1):358. doi: 10.1186/s13054-018-2290-8.

166. Cavalcanti M, Ferrer M, Ferrer R, Morforte R, Garnacho A, Torres A. Risk and prognostic factors of ventilator-associated pneumonia in trauma patients. Crit Care Med. 2006 Apr;34(4):1067-72. doi: 10.1097/01.CCM.0000206471.44161.A0.

167. Li YT, Wang YC, Lee HL, Tsao SC, Lu MC, Yang SF. Monocyte chemoattractant protein-1, a possible biomarker of multiorgan failure and mortality in ventilator-associated pneumonia. Int J Mol Sci. 2019 May 6;20(9):2218. doi: 10.3390/ijms20092218.

168. Gursel G, Demir N. Incidence and risk factors for the development of acute renal failure in patients with ventilator-associated pneumonia. Nephrology (Carlton). 2006 Jun;11(3):159-64. doi: 10.1111/j.1440-1797.2006.00567.x.

169. Moliva JI, Rajaram MV, Sidiki S, Sasindran SJ, Guirado E, Pan XJ, Wang SH, Ross P Jr, Lafuse WP, Schlesinger LS, Turner J, Torrelles JB. Age (Dordr). 2014 Jun;36(3):9633. doi: 10.1007/s11357-014-9633-4.

170. Berkebile AR, McCray PB Jr. Effects of airway surface liquid pH on host defense in cystic fibrosis. Int J Biochem Cell Biol. 2014 Jul;52:124-9. doi: 10.1016/j.biocel.2014.02.009.

171. Pezzulo AA, Tang XX, Hoegger MJ, Abou Alaiwa MH, Ramachandran S, Moninger TO, Karp PH, Wohlford-Lenane CL, Haagsman HP, van Eijk M, Bánfi B, Horswill AR, Stoltz DA, McCray PB Jr, Welsh MJ, Zabner J. Reduced airway surface pH impairs bacterial killing in the porcine cystic fibrosis lung. Nature. 2012 Jul 4;487(7405):109-13. doi: 10.1038/nature11130.

172. Abou Alaiwa MH, Reznikov LR, Gansemer ND, Sheets KA, Horswill AR, Stoltz DA, Zabner J, Welsh MJ. pH modulates the activity and synergism of the airway surface liquid antimicrobials β-defensin-3 and LL-37. Proc Natl Acad Sci U S A. 2014 Dec 30;111(52):18703-8. doi: 10.1073/pnas.1422091112.

173. Kostikas K, Papatheodorou G, Ganas K, Psathakis K, Panagou P, Loukides S. pH in expired breath condensate of patients with inflammatory airway diseases. Am J Respir Crit Care Med. 2002 May 15;165(10):1364-70. doi: 10.1164/rccm.200111-068OC.

174. Lewenza S, Johnson L, Charron-Mazenod L, Hong M, Mulcahy-O'Grady H. Extracellular DNA controls expression of Pseudomonas aeruginosa genes involved in nutrient utilization, metal homeostasis, acid pH tolerance and virulence. J Med Microbiol. 2020 Jun;69(6):895-905. doi: 10.1099/jmm.0.001184.

175. Wilton M, Charron-Mazenod L, Moore R, Lewenza S. Extracellular DNA acidifies biofilms and induces aminoglycoside resistance in Pseudomonas aeruginosa. Antimicrob Agents Chemother. 2015 Nov 9;60(1):544-53. doi: 10.1128/AAC.01650-15.

Statutory Declaration

“I, Chunjiang Tan, by personally signing this document in lieu of an oath, hereby affirm that I prepared the submitted dissertation on the topic " Ventilator-induced alveolar acidification increases the susceptibility and severity to Pseudomonas aeruginosa pneumonia " " Die beatmungsinduzierte alveoläre Übersäuerung erhöht die Suszeptibilität und den Schweregrad einer Pseudomonas aeruginosa Pneumonie ", independently and without the support of third parties, and that I used no other sources and aids than those stated.

All parts which are based on the publications or presentations of other authors, either in letter or in spirit, are specified as such in accordance with the citing guidelines. The sections on methodology (in particular regarding practical work, laboratory regulations, statistical processing) and results (in particular regarding figures, charts and tables) are exclusively my responsibility.

Furthermore, I declare that I have correctly marked all of the data, the analyses, and the conclusions generated from data obtained in collaboration with other persons, and that I have correctly marked my own contribution and the contributions of other persons (cf. declaration of contribution). I have correctly marked all texts or parts of texts that were generated in collaboration with other persons.

My contributions to any publications to this dissertation correspond to those stated in the below joint declaration made together with the supervisor. All publications created within the scope of the dissertation comply with the guidelines of the ICMJE (International Committee of Medical Journal Editors; www.icmje.org) on authorship. In addition, I declare that I shall comply with the regulations of Charité – Universitätsmedizin Berlin on ensuring good scientific practice.

I declare that I have not yet submitted this dissertation in identical or similar form to another Faculty.

The significance of this statutory declaration and the consequences of a false statutory declaration under criminal law (Sections 156, 161 of the German Criminal Code) are known to me.”

Date 28,09,2022 Signature Chunjiang Tan

Curriculum Vitae

My curriculum vitae does not appear in the electronic version of my paper for reasons of data protection.

Acknowledgements

As the end of my doctoral project approaches, the time of my stay in Berlin seems to be entering a countdown. Instinctively, I start to appreciate every person I meet, each scenery I see and every moment I experience. From the depth of my heart, I could never have imagined that I would be able to live and study abroad and, in the meantime, pursue my doctorate in Germany, a country almost 8000 km away from my home. I experienced a lot, learned a lot, laughed and cried a lot during this memorable time of three years. Most importantly, I would never have had the chance to overcome the difficulties and challenges if I had not received the gracious help and guidance from my great supervisors and colleagues. They are synonymous with Berlin in my life.

The immense and gracious supports from my great supervisors are indispensable for the successful accomplishment of my doctoral project. Thus, first of all, I would like to express most sincere gratitude for my senior supervisor - Prof. Dr. Martin Witzenrath. I am grateful that you have given me the opportunity to study and work in the Department of Infectious Diseases and Respiratory Medicine- a fascinating and inspiring laboratory. Without your invaluable advice, creative ideas, and constant support, my project would not have gone to smoothly. Thanks to the valuable opportunities you have given me, my horizons have broadened and my language skills have improved as a result of presenting my work at several international conferences and workshops. My special appreciation also goes to another supervisor of mine - Dr. Matthias Felten. You have always helped me with my project with endless patience and guided me, especially when I was a novice. I am also deeply impressed by your encouragement and motivation in difficult times. From my great supervisors, I not only acquired the knowledge of experimental techniques and developed a valuable scientific thinking, but also learned how to evaluate and analyze things from different angles and how to stay calm when facing challenges. These great experiences

will always stay in my memory and I will pass them on to others when I become a supervisor later on.

In addition, it is my honor to study and work in such a great laboratory with an inspiring and harmonious working atmosphere. I am grateful for the fruitful collaborations and incredible expertise from all my former and current colleagues: Prof. Dr. Wolfgang Kübler, Prof. Dr. Andreas Hocke, Dr. Birgitt Gutbier, Dr. Katrin Reppe, Dr. Geraldine Nouailles, Dr. Sandra-Maria Wienhold, Dr. Luiz Gustavo Teixeira Alves, Dr. Ling Yao, Sebastian, Qi Zhang, Ulrike, Diana, Katharina, Silke, Jingjing, Alex and Yadong. Many thanks to all of you for your selfless technical support and excellent working atmosphere.

Last but not least, I would like to offer my greatest appreciation for my beloved parents. The endless support and encouragement from you cannot be simply expressed by any words. Your deep trust, love and care always enable me to have the strength and confidence to overcome any challenges and to be able to live abroad independently as I always deem that you are my strongest backup wherever I am.

Statistician confirmation

CHARITÉ

CharitéCentrum für Human- und Gesundheitswissenschaften

Charité | Campus Charité Mitte | 10117 Berlin

Institut für Biometrie und klinische Epidemiologie (iBikE)
Direktor: Prof. Dr. Geraldine Rauch
Postanschrift:
Charitéplatz 1 | 10117 Berlin
Besucheranschrift:
Reinhardtstr. 58 | 10117 Berlin
Tel. +49 (0)30 450 562171
geraldine.rauch@charite.de
https://biometrie.charite.de/

Name, Vorname: Tan, Chunjiang
Emailadresse: chunjiang.tan@charite.de
Matrikelnummer:
PromotionsbetreuerIn: Prof. Dr. med. Martin Witzenrath
Dr. med. Matthias Felten
Promotionsinstitution / Klinik: Medizinische Klinik m. S. Infektiologie und Pneumologie

Bescheinigung

Hiermit bescheinige ich, dass Herr Chunjiang Tan innerhalb der Service Unit Biometrie des Instituts für Biometrie und klinische Epidemiologie (iBikE) bei mir eine statistische Beratung zu einem Promotionsvorhaben wahrgenommen hat. Folgende Beratungstermine wurden wahrgenommen:

- Termin 1: 28.06.2021

Folgende wesentliche Ratschläge hinsichtlich einer sinnvollen Auswertung und Interpretation der Daten wurden während der Beratung erteilt:

- Da es sich bei der Arbeit um eine explorative Studie mit vielen verschiedenen primären Endpunkten handelt, sollte zwischen den verschiedenen Endpunkten nicht für multiples Testen adjustiert werden. Zudem sollte der Fokus der Analyse nicht auf p-Werten liegen, sondern auf Effektstärken (z.B. mittlere Differenzen, Konfidenzintervalle).
- Ergebnisse, die auf sehr kleinen Fallzahlen (z.B. n = 5) beruhen sollten vorsichtig interpretiert werden.

Diese Bescheinigung garantiert nicht die richtige Umsetzung der in der Beratung gemachten Vorschläge, die korrekte Durchführung der empfohlenen statistischen Verfahren und die richtige Darstellung und Interpretation der Ergebnisse. Die Verantwortung hierfür obliegt allein dem Promovierenden. Das Institut für Biometrie und klinische Epidemiologie übernimmt hierfür keine Haftung.

Datum: 28.06.2021 Name des Beraters/ der Beraterin: Kerstin Rubarth